Uniform bathymetric zonation of marine benthos on a Pan-Arctic scale

Vedenin A.A.[1], Mironov A.N.[1], Bluhm B.A.[2], Käß M. [3,4], Degen R.[5], Galkin S.V.[1], Gebruk A.V.[1]

[1] – Shirshov Institute of Oceanology, Russian Academy of Sciences

[2] – UiT, The Arctic University of Norway

[3] – Alfred-Wegener-Institute for Polar and Marine Research

[4] – University of Oldenburg

[5] – University of Vienna

Corresponding author:

Vedenin A.A., urasterias@gmail.com

Abstract

While numerous regional studies of bathymetric zonation of benthic fauna globally have been done, few large-scale analyses exist, and no ocean-scale studies have focused on the Arctic Ocean to date. In the present work we, hence, examined bathymetric zonation of macro- and megabenthos over a depth range spanning from the shelf to the abyssal plain (14 – 5416 m) and regionally extending from the Fram Strait to the Beaufort Sea (as a whole hereafter called the Central Arctic). Based on 104 quantitative (box-corers and grabs) and 37 semi- quantitative (trawls) samples compiled from different studies we evaluated bathymetric zonation patterns in abundance, biomass and diversity, and also compared species composition among samples. Abundance and biomass decreased with depth from >3000 ind. m^{-2} and >40 g ww m^{-2} to ~130 ind. m^{-2} and <1 g ww m^{-2} corroborating previous studies. Diversity showed a parabolic pattern, peaking at ~100-600 m. Cluster analysis revealed four (macrofauna) and five (megafauna) groups of benthic assemblages, including three that covered the upper and lower continental slope and the abyssal plains with relatively little overlap (named the *Lower Shelf – Upper Slope 1*, the *Lower Slope* and the *Abyss*). Substantial changes in benthic community composition were observed at depths 650-950 m (between the *Lower Shelf – Upper Slope 1* and the *Lower Slope*) and 2600-3000 m (between the *Lower Slope* and the *Abyss*), so we interpreted these two depth horizons as major bathymetric boundaries. The first boundary (650-950 m) corresponds to the transition from sublittoral to bathyal fauna consistent with previous studies. The second boundary (2600-3000 m) reflects a decrease in benthic abundance, biomass and diversity within the Central Arctic abyssal plain. Bathymetric patterns and species overturn of benthos were relatively uniform throughout the entire Central Arctic continental slope and abyssal plain. For some regions of the Arctic Ocean, foremost for the area north from Greenland and Canadian Archipelago, benthic data are still unavailable and further research is needed.

Key Words: Central Arctic; Bathymetric zonation; Benthic assemblages; Biogeography

1. Introduction

Multiple lines of evidence suggest we can expect that on-going climate change and continuous decline of sea ice cover will lead to shifts in the Arctic marine ecosystem, eventually affecting benthic biota (Wassmann et al., 2011; Jansen et al., 2020). In particular, changes in species distributions, benthic abundance and biomass are expected due to sea ice losses followed by regionally enhanced algal blooms and subsequent increase of carbon uptake and storage (Meredith et al., 2019). To better understand possible changes, and perhaps predict them, a solid understanding of large-scale *current* patterns, derived from comparable and standardized data on benthic fauna, across all regions of the Arctic Ocean are required.

Bathymetric distribution of macro- and megabenthic communities was addressed by numerous studies worldwide (Hedgpeth, 1957; Grassle & Morse-Porteous, 1987; Golikov et al., 1990; Rex & Etter, 2010; Watling et al., 2013), but most consider small-scale basins or regions on scales of hundreds of kilometers at best. Past studies have examined depth-associated changes for specific seas (for example, Denisenko et al., 2003; Budaeva et al., 2008; Käß et al., 2019; Vedenin et al., 2015; Ravelo et al., 2020). Few investigations included the deep Central Arctic Ocean (e.g. Kröncke, 1994; Kröncke, 1998; Deubel, 2000), a still poorly sampled area. From the spotty data Sirenko et al. (1998) produced a schematic map of the types of benthic communities replacing one another with depth from coastal regions to the base of the continental slope along a wide band of Eurasian Arctic from the Barents Sea to the Chukchi Sea. More recently, Piepenburg et al. (2011) and Bluhm et al. (2011; 2020) demonstrated some degree of uniformity of bathymetric patterns of benthos distribution around the entire Arctic Ocean.

To date, however, few studies have attempted an integration of benthic fauna data from different Arctic regions and those that have gone beyond a single region showed somewhat differing results or focused on one benthic size fraction only. For example, from the Barents Sea to the Laptev Sea macrobenthic communities replaced one another relatively uniformly with depth in five main types of benthic communities corresponding to the shelf, upper slope, mid-slope, lower slope and abyssal plain (Vedenin et al., 2018). These same authors reported a peak in species richness at a depth of 100-300 m, which is shallower than the bathymetric richness peak reported in other bathymetric studies (e.g. Wlodarska-Kowalczuk et al., 2004 and a meta-analysis by Bluhm et al., 2011). Combining data from different regions processed by different authors into one data set can introduce bias owing to differences in sampling methods, protocols and taxonomy, as was summarized in Bluhm et al. (2011) and Vedenin et al. (2018). Yet, such integration must be the goal if we are to attempt to provide a comparable understanding of benthic bathymetric zonation based on quantitative taxonomical structure at the scale of the Arctic Ocean.

In this study, despite the difficulties mentioned, we pooled different data sets on benthic communities in the Arctic Ocean to analyze patterns of bathymetric distribution over a broad depth range

(from 14 to 5416 m). We hypothesize that the major patterns of bathymetric distributions of macro- and megabenthos remain relatively constant across all regions of the Central Arctic Ocean. We use the approximate position of bathymetric biogeographic boundaries as well as bathymetric trends in abundance, biomass, and diversity as metrics. Based on earlier findings we also hypothesize that bathymetric patterns in diversity differ from known patterns in other areas of the World Ocean. Our geographic scope is large-scale- including the Barents, Kara and Greenland Seas, the Yermak Plateau, the Beaufort Sea, and the entire Eurasian deep-sea basins.

Materials & Methods

2.1.Study Area

We focused on an extensive area of the Arctic Ocean extending across the continental shelf, continental slope, and abyssal plain. The sampled shelf areas vary in depth and size and include the broad and Barents Sea that extends down to ~500 m depth, the shallow and broad Kara and Laptev Seas, and the shallow and narrow Beaufort Sea. The continental slopes vary in steepness and the depth of the abyssal plains ranges from ~2500 to 4500 m. Several basins and a series of ridges, including the Gakkel, Lomonosov, Mendeleev and Alpha Ridges divide the abyssal Arctic Ocean north of Eurasia from that off of North America. The shallow waters of the focal areas differ markedly from one another, mainly because of differences in river run-off, which is especially prominent on the Siberian (Kara and Laptev Seas) shelf and in the Beaufort Sea. At ~100-700 m, warmer and more saline waters of Atlantic origin flow through the eastern Fram Strait into the central Arctic Ocean, thereby warming the water masses along the slopes of the Eurasian Arctic (Wassmann et al., 2019). The Atlantic layer gradually decreases in temperature as it travels eastward and into the Amerasian Basin (Bluhm et al., 2020). Below the Atlantic layer, cold Arctic deep-sea waters straddle the entire Arctic Ocean at depths ~>700-800 m (Bluhm et al., 2020; see Meltofte, 2013 for detailed hydrology of the Arctic Ocean). Sea ice covers vast areas of the deep-sea Arctic temporarily or permanently although mean sea ice extent is decreasing rapidly (Wassmann et al., 2011; Jansen et al., 2020).

In particular, our focal areas include Fram Strait, the Yermak Plateau, the Northern Barents Sea slope, the Kara Sea, the Laptev Sea, the Beaufort Sea and adjacent Canada Basin and the deep-sea Nansen and Amundsen basins (Fig. 1, 2). Water depths range from 10s of meters in the Kara and Laptev Seas to over 5000 meters (Molloy Deep in the Fram Strait as our deepest point at 5416 meters). Hereafter we refer to this focal area as the Central Arctic.

2.2.Material processing

The total pool of invertebrate macro- and megafauna samples included 141 stations taken during 13 expeditions. We divided all samples into quantitative and semi-quantitative based on the sampling gear used. Overall we obtained 106 quantitative stations using grabs and corers: the 'Okean' grab (0.1 or 0.25 m^2 sampling area), USNEL Box-corer and Multibox-corer (Lisitsyn & Udintsev, 1955; Hessler & Jumars, 1974; Gerdes, 1990) (Fig. 1). The sampling area per station varied from 0.023 m^2 to 0.75 m^2 depending on the number of subsamples taken from each gear (Table S1), the mesh sizes varied from 0.2 to 0.5 mm. The final quantitative dataset was compiled from 11 expeditions: the 1991 expedition, where extensive box-corer sampling was surveyed in the Central Arctic Ocean across the Nansen and Amundsen Basins (Kröncke, 1994; Kröncke, 1998); the 1995 expedition, where multiple box-corer transects were collected and published for the continental slope in the Kara and Laptev seas (Anisimova et al., 2003; Sirenko et

al., 2004); the 1997 expedition to the Yermak Plateau with box-corers presented by Degen et al. (2014); the 2002 and 2005 expeditions to the Beaufort Sea slope and abyssal plain, the results of macrobenthic surveys using box corers were published by Bluhm et al. (2005) and MacDonald et al. (2011); the 2007 and 2015 expeditions where a series of grab samples on the shelf and slope of the Kara and Laptev Seas was obtained (Vedenin et al. 2015; 2018); the 1993 and 2012 surveys in the Central Arctic were performed using Multibox-corer (Vedenin et al., 2018). the 2012 and 2016 surveys of macrobenthos using box-corers at the Long-Term Ecological Research observatory "HAUSGARTEN" in the Fram Strait (Vedenin et al., 2016; Käß et al., 2019).

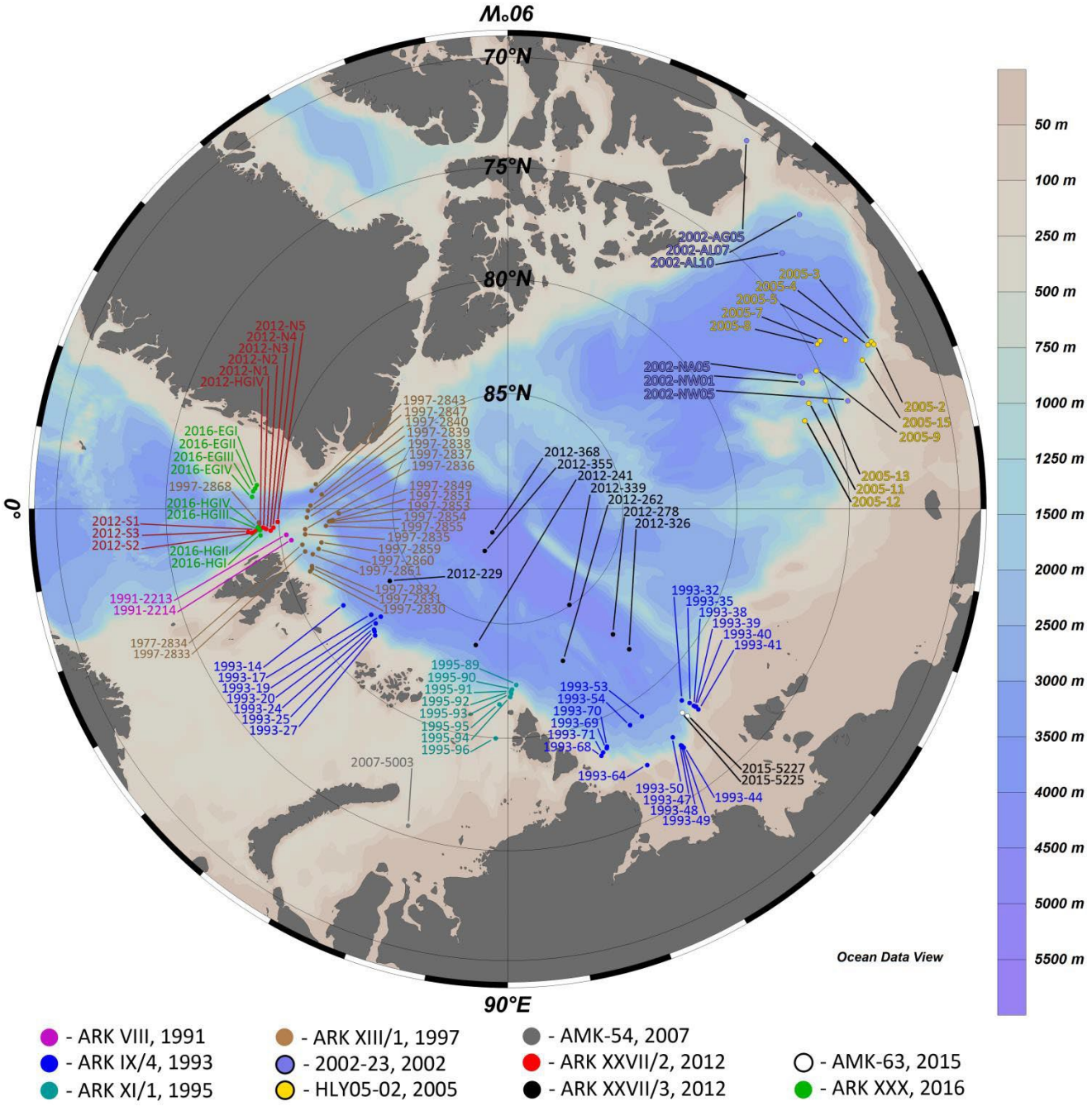

Fig. 1. Study area indicating the 104 quantitative stations across the Arctic. Specific expeditions are marked by colour. ARK – RV 'Polarstern'; 2002-23 – CCGS 'Louis S. St. Laurent'; HLY05-02 – USCGC 'Healy'; AMK – RV 'Akademik Mstislav Keldysh'.

The above listed publications provide species lists with abundance and biomass data (wet weight) standardized to square meter from these stations. The original samples were re-sorted and re-identified by a single pool of experts [except for samples in Anisimova et al. (2003), Bluhm et al. (2005) and Macdonald et al. (2010)] to avoid bias due to possible misidentification of benthic organisms. All taxa names were verified with use of the World Register of Marine Species database http://marinespecies.org/.

In addition, we obtained material from 37 semi-quantitative samples using Sigsbee and Agassiz trawls (Eleftheriou & McIntyre, 2005) (Fig. 2), samples were sieved through 1 mm mesh sized sieve, both total number of individuals and percentage values of abundance for each taxon was calculated. The expeditions included trawl surveys in the Kara and Laptev seas shelf and adjacent areas of the deep-sea Central Arctic; again, species lists from trawl samples were previously published (Kim et al., 2006; Vedenin et al., 2015; Vedenin et al., 2018; Rybakova et al., 2019; Vedenin et al., 2020; Udalov et al., 2020). A complete list of all stations with the expedition name, year, coordinates, depth and sampling area is given in Appendix Table S1.

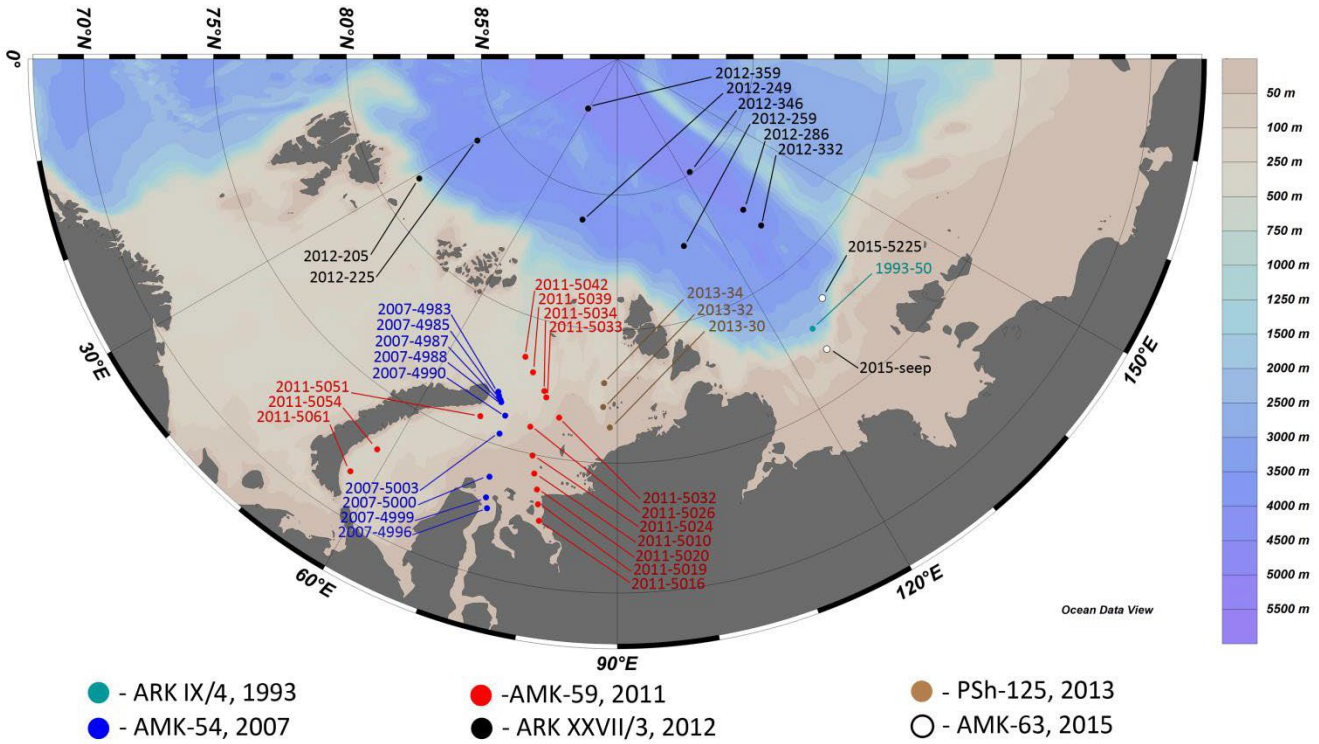

Fig. 2. Study area indicating the 37 semi-quantitative stations across the Eurasian Arctic. Specific expeditions are marked by colour. ARK – RV 'Polarstern'; AMK – RV 'Akademik Mstislav Keldysh'; PSh – RV 'Professor Shtokman'.

2.3. Statistics

We used abundance, biomass and diversity indices calculated for quantitative samples as summary metrics for each station. For semi-quantitative (trawl) samples we calculated diversity indices only because it is impossible to normalize the abundance and biomass per square area (Eleftheriou & McIntyre, 2005).

Diversity metrics included number of taxa per sample, Shannon index (Shannon & Weaver, 1963), Pielou's evenness (Pielou, 1966; McCune et al., 2002) and Hurlbert rarefaction per 100 individuals (ES-100) (Hurlbert, 1971) which is suited to compare different sample sizes (Magurran, 2004). In addition, because of the low macrobenthic abundance in some samples, we extrapolated diversity using Hill numbers (q = 0) for 50 individuals (further referred to as 'Hill 50 extrapolated'). Chao et al. (2014) introduced this method and provided the detailed algorithms for extrapolation (see Appendix Table S2). We calculated Hill numbers using original non-transformed number of individuals in each sample.

We estimated similarity between all quantitative and (separately) among all trawl samples using Bray-Curtis similarity based on sample abundances (macrofauna) and number of individuals in trawl haul (megafauna):

$$C_{BC} = 200\frac{\sum_1^{S_{12}} \min\{x_i, y_i\}}{\sum_1^{S_1} x_i + \sum_1^{S_2} y_i},$$

where C_{BC} is the similarity value, x_i and y_i are the abundances of i-th species in sample 1 and 2, S_1 and S_2 are the species richness of sample 1 and 2 and $\min\{x_i,y_i\}$ is the smaller abundance value of i-th species shared for samples 1 and 2 (Bray & Curtis, 1957; Clarke et al., 1996). Noting the sensitivity of Bray-Curtis to sample size differences (Chao et al., 2006) we also employed two other indices – the Morisita-Horn similarity index:

$$C_{MH} = 2\frac{\sum_1^{S_{12}}(\frac{x_i}{S_1}\frac{y_i}{S_2})}{\sum_1^{S_1}(\frac{x_i}{S_1})^2 + \sum_1^{S_2}(\frac{y_i}{S_2})^2},$$

and the quantitative Sørensen similarity index:

$$C_S = \frac{2UV}{U+V},$$

Where U and V are total relative abundances of those species in sample 1 and, respectively, sample 2, that are shared, i.e. present in both samples (Horn 1966; Chao et al., 2006).

Quantitative samples were analyzed untransformed and square-root transformed depending on specific metric used (Bray-Curtis similarity was calculated based on the untransformed data to accentuate the quantitative differences in species composition); semi-quantitative samples (data on simple number of individuals of each taxon) were fourth-root transformed to reduce the dominant taxa bias, as one-two taxa often contribute over 50% of the total abundance in the trawl samples (Galkin & Vedenin, 2015).

Hierarchical clusters were generated using the UPGMA-algorithm, i.e. group-average (Clarke et al., 1996). The similarity profile routine (SIMPROF) was used at the significance level of 0.01, to test for statistical significance of clusters (Clarke & Warwick, 2001). We identified different benthic assemblages based on quantitative faunal similarity in the dendrogram by slicing above the statistically insignificant nodes outlined with the SIMPROF routine. Identified assemblages were tested with Permutational multivariate analysis of variance (PERMANOVA) (Andersen, 2005). Hereafter we avoid the term

184 ‘benthic community’ because of the debate over the specific definition of this term, and replace it with
185 ‘benthic assemblage’. Non-parametric Kruskal-Wallis tests followed by Dunn’s post-hoc tests verified
186 differences between identified assemblages for abundance, biomass and diversity (Marshall, 2019).
187 Similarity percentages analysis based on the Bray-Curtis dissimilarity (SIMPER) was used for identifying
188 character species contributing most to cluster differences (Clarke & Warwick, 1994). We then plotted the
189 identified benthic assemblages along the depth axis to visualize bathymetric structure within the study
190 area.

191 Statistical analysis used PAST 3.0, Primer V6, IBM SPSS statistics and Microsoft Excel 2010
192 software (Clarke & Warwick, 2001; Hammer et al., 2001; Marshall, 2019). Hill numbers, Morisita-Horn
193 and quantitative Sørensen similarity indices were calculated using original Python 3.8 scripts using
194 NumPy, Pandas, Scipy, Scikit-bio, Scikit-learn, Math, and Matplotlib libraries
195 (https://www.python.org/downloads/release/python-380/). The scripts are available in Appendix S3.
196 Maps were built using Ocean Data View software (Schlitzer, 2020).
197

3. Results

3.1.Quantitative samples

Abundance and biomass values varied greatly, from 12 ind. m^{-2} (at st. 2012-229) to 8861 ind. m^{-2} (st. 1993-31) and, from 0.004 g ww m^{-2} (st. 2002-AL10) to 2316.500 g ww m^{-2} (st. 1995-93), respectively. The number of species per station varied from 2 (at several stations, including sts. 1997-2833, 1997-2847, 1997-2849-7, 1997-2868 and 2012-229) to 120 (st. 1995-93), recognizing taxon numbers are affected by area sampled. Sampling area was smallest at st. 1993-20 (0.023 m^2) and largest at sts. 2015-5225 and 2015-5227 (0.750 m^2), see Table S1 for details. Smaller variation characterized diversity indices: ES-100 differed from 2 (same stations as for lowest number of species per station) to 44 (st. 1993-40); Hill 50 extrapolated numbers varied from 2 (st. 2012-229) to 30 (st. 1997-2837); Pielou's evenness varied from 0.48 (st. 2005-5) to 1 (st. 2012-229) and Shannon index varied from 0.58 (st. 1997-2868) to 3.93 (st. 1993-40). For details, see Appendix Table S5. A complete list of individual taxa abundances per station is given in Appendix Table S6.

Cluster analysis with SIMPROF test based on Bray-Curtis similarity identified four distinct clusters (= benthic assemblages) at 6% similarity, including all but two stations (Fig. 3). We identified the clusters as the *Lower Shelf - Upper Slope 1*, *Lower Shelf - Upper Slope 2*, *Lower Slope* and *Abyss* assemblages. *Lower Shelf - Upper Slope* 2 was defined based on lower similarity level (4) due to taxonomical peculiarity (described in this subsection below) (Fig. 3). The names of the clusters were chosen according to the geographic and bathymetric position of the station, explained below (Fig. 4). PERMANOVA showed significant results with p-value < 0.001 (Fig. 3). Non-parametric Kruskal-Wallis test found significant differences between most clusters in terms of the community parameters, including abundance, biomass and diversity metrics (Table 1).

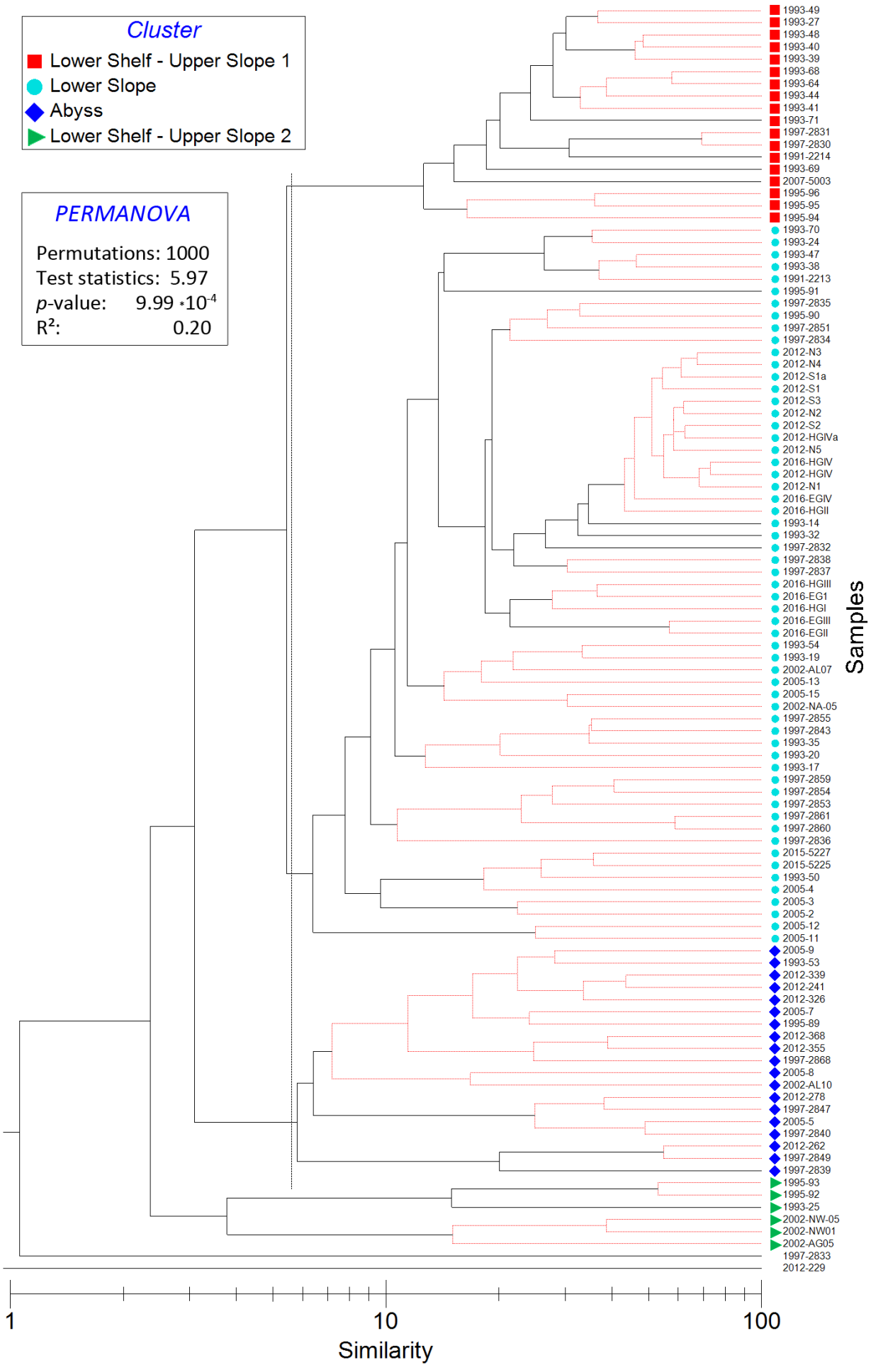
Cluster
Lower Shelf - Upper Slope 1
Lower Slope
Abyss
Lower Shelf - Upper Slope 2
PERMANOVA
Permutations: 1000
Test statistics: 5.97
p-value: 9.99 *10-4
R²: 0.20
1993-49
1993-27
1993-48
1993-40
1993-39
1993-68
1993-64
1993-44
1993-41
1993-71
1997-2831
1997-2830
1991-2214
1993-69
2007-5003
1995-96
1995-95
1995-94
1993-70
1993-24
1993-47
1993-38
1991-2213
1995-91
1997-2835
1995-90
1997-2851
1997-2834
2012-N3
2012-N4
2012-S1a
2012-S1
2012-S3
2012-N2
2012-S2
2012-HGIVa
2012-N5
2016-HGIV
2012-HGIV
2012-N1
2016-EGIV
2016-HGII
1993-14
1993-32
1997-2832
1997-2838
1997-2837
2016-HGIII
2016-EG1
2016-HGI
2016-EGIII
2016-EGII
1993-54
1993-19
2002-AL07
2005-13
2005-15
2002-NA-05
1997-2855
1997-2843
1993-35
1993-20
1993-17
1997-2859
1997-2854
1997-2853
1997-2861
1997-2860
1997-2836
2015-5227
2015-5225
1993-50
2005-4
2005-3
2005-2
2005-12
2005-11
2005-9
1993-53
2012-339
2012-241
2012-326
2005-7
1995-89
2012-368
2012-355
1997-2868
2005-8
2002-AL10
2012-278
1997-2847
2005-5
1997-2840
2012-262
1997-2849
1997-2839
1995-93
1995-92
1993-25
2002-NW-05
2002-NW01
2002-AG05
1997-2833
2012-229
Samples
1
10
100
Similarity

220

Fig. 3. Cluster analysis of quantitative stations using Bray-Curtis similarity index with SIMPROF results. Red lines indicate branches and nodes not statistically significant at $p<0.01$. Marker colour and shape indicate benthic assemblages, defined at a similarity level of 6 percent; similarity is plotted on a logarithmic scale. Enclosed the PERMANOVA results are shown.

Morisita-Horn or Sørensen similarity indices yielded similar results, with the *Lower Shelf - Upper Slope 1* assemblage containing almost identical stations to the Bray-Curtis dendrogram. However, compared to the Bray-Curtis dendrogram, several stations shifted between the *Lower Slope* and *Abyss* assemblages, whereas the *Lower Shelf - Upper Slope* 2 assemblage became indistinct (Supplementary 5, Fig. S-1, S-2). Given that all 3 indices yielded generally comparable results, and that some of the statistical methods work only with Bray-Curtis similarity, we based plots and figures in the main text on Bray-Curtis similarities.

The benthic assemblages were distributed within specific depth ranges, with three forming consistent depth bands that spanned the study area – the *Lower Shelf - Upper Slope 1*, the *Lower Slope* and the *Abyss* (Fig. 4).

Table 1. Mean values of benthic abundance, biomass and diversity of each assemblage and results of Kruskal-Wallis and Dunn's post-hoc tests for quantitative samples.

Group	**Mean values ± SD**				**Kruskal-Wallis**		**Dunn's post-hoc comparisons**
	(1) *Lower Shelf - Upper Slope 1*	(2) *Lower Slope*	(3) *Abyss*	(4) *Lower Shelf - Upper Slope 2*	Chi square	*p*	
Quantitative samples							
Number of samples	18	59	19	6	-	-	-
Abundance (ind m^{-2})	3845 ±2020	805 ±453	134 ±156	3694 ±2765	73.08	<0.001	1-2; 1-3; 1-4; 2-3; 2-4
Biomass (g ww m^{-2})	44 ±75	4 ±5	0.8 ±1.1	633 ±901	57.63	<0.001	1-2; 1-3; 2-3; 2-4
Species number	70 ±23	28 ±20	8 ±6	57 ±45	51.15	<0.001	1-2; 1-3; 2-3; 3-4
ES-100	34 ±8	20 ±10	8 ±6	24 ±12	45.61	<0.001	1-2; 1-3; 2-4; 3-4
Hill 50 extrapolated	24 ±5	18 ±6	11 ±8	17 ±7	29.66	<0.001	1-2; 1-3; 1-4; 2-3

Numbers in Dunn's post-hoc comparisons column indicate corresponding group of benthic assemblages, revealed with Bray-Curtis similarity.

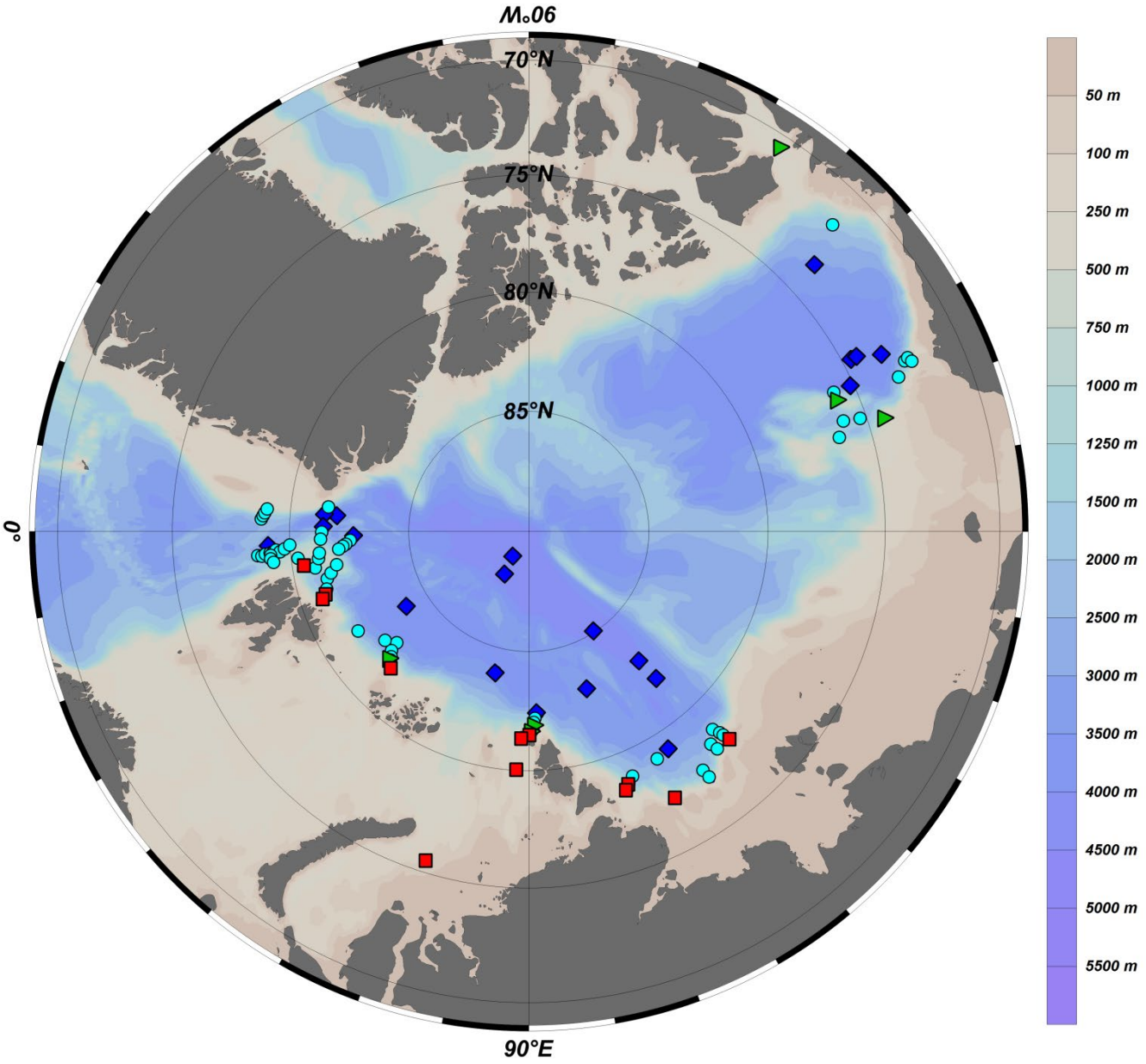

Fig. 4. Distribution of groups of benthic assemblages (color-shape-coded) based on quantitative samples (Bray-Curtis similarity). Colours and shapes of markers are the same as in Fig. 3.

Each of the identified assemblages was generally weakly structured within clusters on the dendrogram. One exception included station groups of high similarity (> 50%) in the Fram Strait area (2012 and 2016 stations on Fig. 1, e.g. HGIV, S1-S3, N1-N5) within the *Lower Slope* assemblage. Second exception were the Beaufort Sea stations (2002 and 2005 stations on Fig. 1) grouped separately within the *Lower Shelf – Upper Slope 2* group and, to a lesser extent, within the *Lower Slope* group (Fig. 3).

The SIMPER analysis based on Bray-Curtis similarity identified the most characteristic species according to their mean contribution to differences between the assemblages (taxa with cumulative contribution up to 70% are shown, Table 2). In the *Lower Shelf - Upper Slope 1* group the bivalve *Yoldiella solidula* was the most characteristic species, followed by the polychaetes *Prionospio cirrifera*, *Spiophanes kroyeri* and *Tharyx* sp. The polychaetes *Galathowenia fragilis*, *Myriochele heeri*, *Chaetozone jubata* and

256 *Prionospio* sp. contributed most to the *Lower Slope* cluster. The polychaetes *Anobothrus laubieri*,
257 *Ophelina opisthobranchiata*, *Aricidea* spp. and *Tharyx* sp. and sponge *Thenea abyssorum* were primarily
258 responsible for separating the *Abyss* group. In the *Lower Shelf - Upper Slope 2* assemblage, the
259 polychaetes *Bushiella* (*Jugaria*) *similis*, sponges Demospongiae gen. sp. and the bryozoans *Tubulipora*
260 *fruticosa* were of primary importance (Table 2).

261 Changes in the summary metrics with depth indicated several patterns. Abundance and biomass
262 gradually decreased with depth (Fig. 5 a,b) except for samples from the Lower Shelf - Upper Slope 2
263 assemblage. Exponential trend lines produced the best approximations. The species number and
264 extrapolated Hill 50 values changed parabolically with maximum values in the ~100-500 m depth range
265 (Fig. 5 c,d). For diversity values, polynomial trend lines provided the best approximations given by the
266 equations and R^2 values (Fig. 5). The Hill 50 values of *Lower Slope* and *Abyss* stations decreased with
267 depth more slowly than other diversity measures due to extrapolation of diversity considering the
268 potentially unsampled taxa (Fig. 5 d, Fig. 6). The 'true' rarefactions (Fig. 6) are denoted with continuous
269 lines ending with large circles, with dashed lines showing the extrapolated rarefaction with larger values
270 of expected number of species per 50 individuals (Fig. 6).
271

Table 2. Results of SIMPER analysis of quantitative samples with values of average abundance, average dissimilarity and percentage contribution of taxa within retrieved groups of assemblages individually and cumulatively. First several most significant taxa in each assemblage are marked in grey.

Group	Species	Average abundance (ind. m^{-2})				Average Dissimilarity	Dissimilarity/ SD	Contribution (%)	Cumulative (%)
		Lower Shelf - Upper Slope 1	*Lower Slope*	*Abyss*	*Lower Shelf - Upper Slope 2*				
Pol	*Bushiella (Jugaria) similis*	0	0	0	363.1	5.6	0.8	5.7	5.7
Pol	*Siboglinum hyperboreum*	0	12.3	1.1	338.9	4.5	0.5	4.6	11.4
Por	Demospongiae gen.sp.	0.1	0.4	3.6	203.1	2.7	0.5	2.8	16
Pol	*Prionospio cirrifera*	196.3	23	0	21.5	2.7	0.8	2.8	18.8
Cni	Stephanoscyphus	2	6.5	0	141.7	2.5	0.4	2.5	21.5
Pol	*Tharyx* sp.	173.4	26.6	4.3	15.3	2.4	1	2.5	24.1
Biv	*Yoldiella solidula*	255.6	0.7	0	3.3	2.2	0.6	2.2	26.6
Pol	*Chone duneri*	124.3	0.1	0	70.4	2	0.5	2.1	28.8
Pol	*Galathowenia fragilis*	0	65.9	0.8	0	1.8	0.5	1.8	30.8
Pol	Polychaeta gen.sp.	0.4	8	0	127.7	1.7	0.4	1.7	32.7
Pol	*Myriochele heeri*	61.7	43.9	0.3	0.3	1.6	0.6	1.6	34.4
Por	*Tetilla infrequens* (sensu Koltun)	0	0	0	114.3	1.4	0.7	1.5	36
Pol	*Anobothrus laubieri*	14.6	1.9	45.9	1.5	1.4	0.4	1.4	37.5
Pol	*Spiophanes kroyeri*	137.4	0.4	0	0	1.2	0.4	1.2	38.9
Biv	*Mendicula ferruginosa*	131.2	0.1	0	0	1.1	0.4	1.2	40.1
Pol	*Galathowenia oculata*	57.4	24.3	0.2	0.3	1.1	0.6	1.2	41.2
Sip	*Nephasoma* sp.	64.4	16.8	0	6.2	1.1	0.7	1.2	42.4
Cum	*Ectonodiastylis nimia*	89.7	0.5	0	0	1.1	0.3	1.1	43.5
Pol	*Chaetozone setosa*	94.4	0.5	0	29.2	1.1	0.7	1.1	44.6
Por	*Geodia* spp.	0	0	0	137	1.1	0.8	1.1	45.7
Pol	*Notoproctus oculatus*	89.6	1.1	0	22.9	1	0.6	1.1	46.8
Oph	*Ophiacantha bidentata*	9.7	0	0	77.5	1	0.7	1.1	47.9
Pol	*Pholoe* sp.	92.5	0.6	0	1.8	1	0.6	1	48.9
Pol	*Chaetozone jubata*	0	36.5	2.9	0	1	0.6	1	50
Bry	*Tubulipora fruticosa*	4.2	0.2	0	182.5	0.9	0.4	1	51
Pol	*Aricidea (Strelzovia) abranchiata*	10.2	31	3.9	0	0.9	0.4	1	51.9
Pol	*Prionospio* sp.	1	34.1	0	0	0.9	0.4	0.9	52.9
Pol	*Proclea graffi*	83.6	0.8	0	0.3	0.9	0.6	0.9	53.8
Pol	*Melinnopsis arctica*	40.4	18.7	0	0	0.9	0.4	0.9	54.7
Nem	Nemertea gen.sp.	64.7	9.7	2.3	2.1	0.9	0.8	0.9	55.6
Pol	*Maldane arctica*	67.5	5.9	1.2	0	0.8	0.4	0.9	56.5
Amp	*Harpinia mucronata*	55.7	4.6	0.3	0	0.8	0.6	0.8	57.3
Por	*Sycon* sp.	17.5	4.3	0	96.9	0.8	0.4	0.8	58.1
Por	Polymastiidae gen.spp.	12.8	14.1	0	10.1	0.7	0.5	0.7	58.9
Pol	*Terebellides atlantis*	20.6	11.2	5.6	0	0.6	0.6	0.7	59.6
Pol	*Scoletoma fragilis*	76.1	0.5	0	0.7	0.6	0.4	0.7	60.3
Por	*Craniella cranium*	2.1	0	0	95	0.6	0.6	0.6	60.9
Pol	*Ophelina opisthobranchiata*	0	21.5	3.7	0	0.6	0.4	0.6	61.6
Bry	*Exidmonea atlantica disticha*	0	0	0	119.6	0.6	0.5	0.6	62.2
Oph	*Ophiocten sericeum*	61.9	0.2	0	12.8	0.6	0.5	0.6	62.8
Pol	*Apomatus globifer*	0	0.1	0	59.1	0.6	0.4	0.6	63.4
Bry	*Diplosolen intricarium*	0	0	0	95.2	0.6	0.6	0.6	64
Pol	*Aricidea nolani* (tax. inquirend.)	14	1.5	2.3	20.8	0.5	0.5	0.6	64.6
Pol	*Ophelina cylindricaudata*	21.5	3.2	0	11.7	0.5	0.5	0.5	65.1
Tan	*Akanthophoreus gracilis*	59.3	1.3	0	4	0.5	0.6	0.5	65.7
Pol	*Euchone* sp.	23.3	1.7	0	44.6	0.5	0.6	0.5	66.2
Bry	Cyclostomatida gen.sp.	3.6	0.8	0.3	19.4	0.5	0.4	0.5	66.7
Biv	*Bathyarca frielei*	3.2	12.6	0	20.8	0.5	0.5	0.5	67.3
Por	*Thenea abyssorum*	0	8.7	8.6	0	0.5	0.5	0.5	67.8
Biv	*Yoldiella annenkovae*	8.9	15.5	0.8	0	0.5	0.4	0.5	68.3
Pol	*Clymenura polaris*	55.4	1.2	0	1.5	0.5	0.4	0.5	68.8
Pol	*Terebellides* sp.	17.6	0.4	0	12	0.5	0.6	0.5	69.3
Amp	*Byblis minuticornis*	41.4	1.4	0	0	0.5	0.3	0.5	69.8
Pol	*Praxillura longissima*	43.5	4.7	0	0	0.5	0.6	0.5	70.3

Taxa with cumulative contribution < 70% are shown. First several most significant taxa in each assemblage are marked in grey. Por – Porifera; Cni – Cnidaria; Pol – Polychaeta; Sip – Sipuncula; Nem – Nemertea; Biv – Bivalvia; Cum – Cumacea; Amp – Amphipoda; Tan – Tanaidacea; Bry – Bryozoa; Oph – Ophiuroidea.

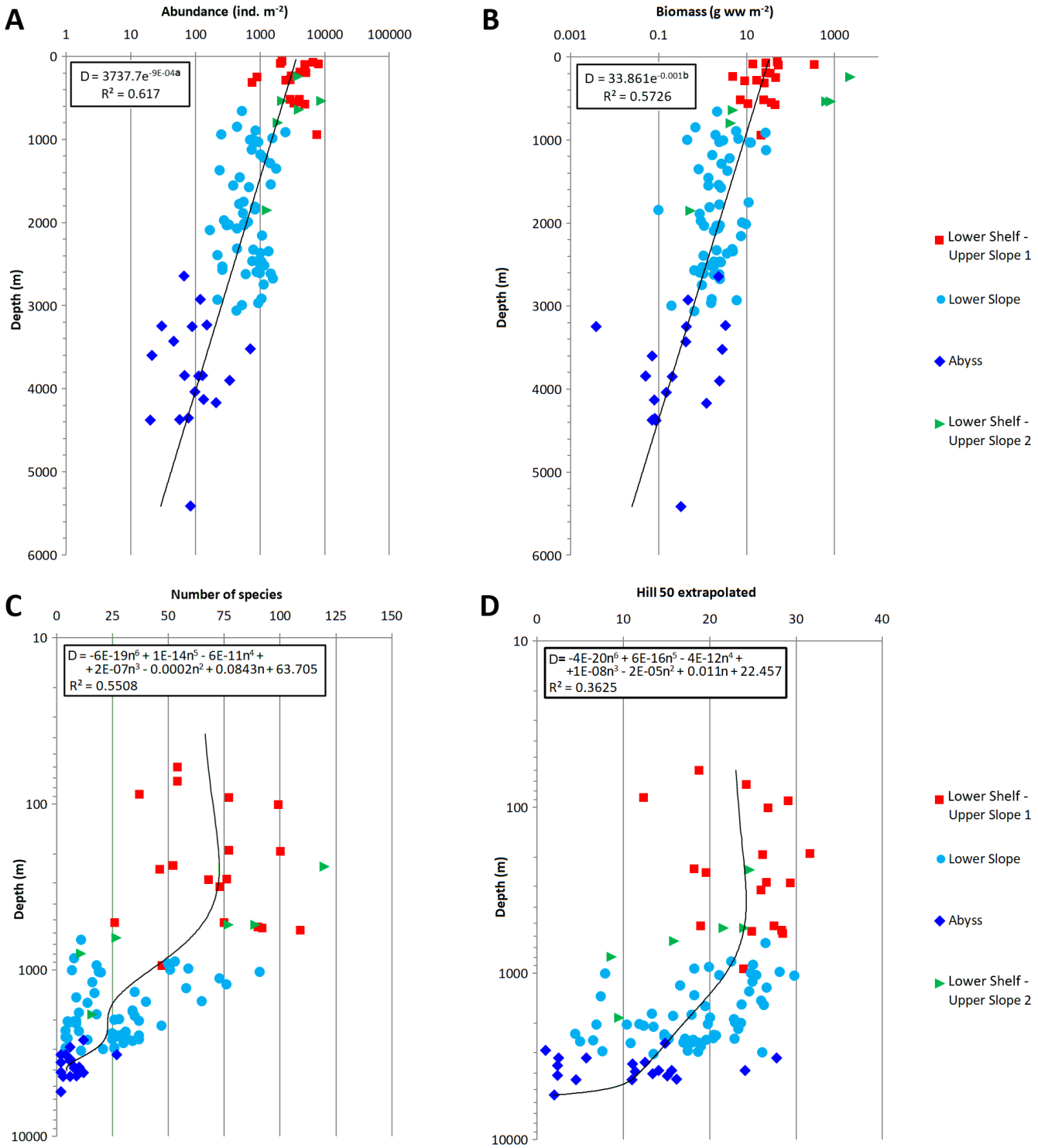

Fig. 5. Total abundance (ind. m^{-2}, a), biomass (g ww m^{-2}, b), species number (c) and Hill 50 extrapolated values (d) in quantitative Arctic benthic samples in relation to depth. Colour and shape of markers correspond to assemblages as in Figs. 3 and 4. Axes of abundance, biomass in upper plots and depth in lower plots are logarithmic. Trend line equations and R^2 values are shown in boxes (D – depth; a – abundance; b – biomass; n – species number or rarefaction per 50 individuals).

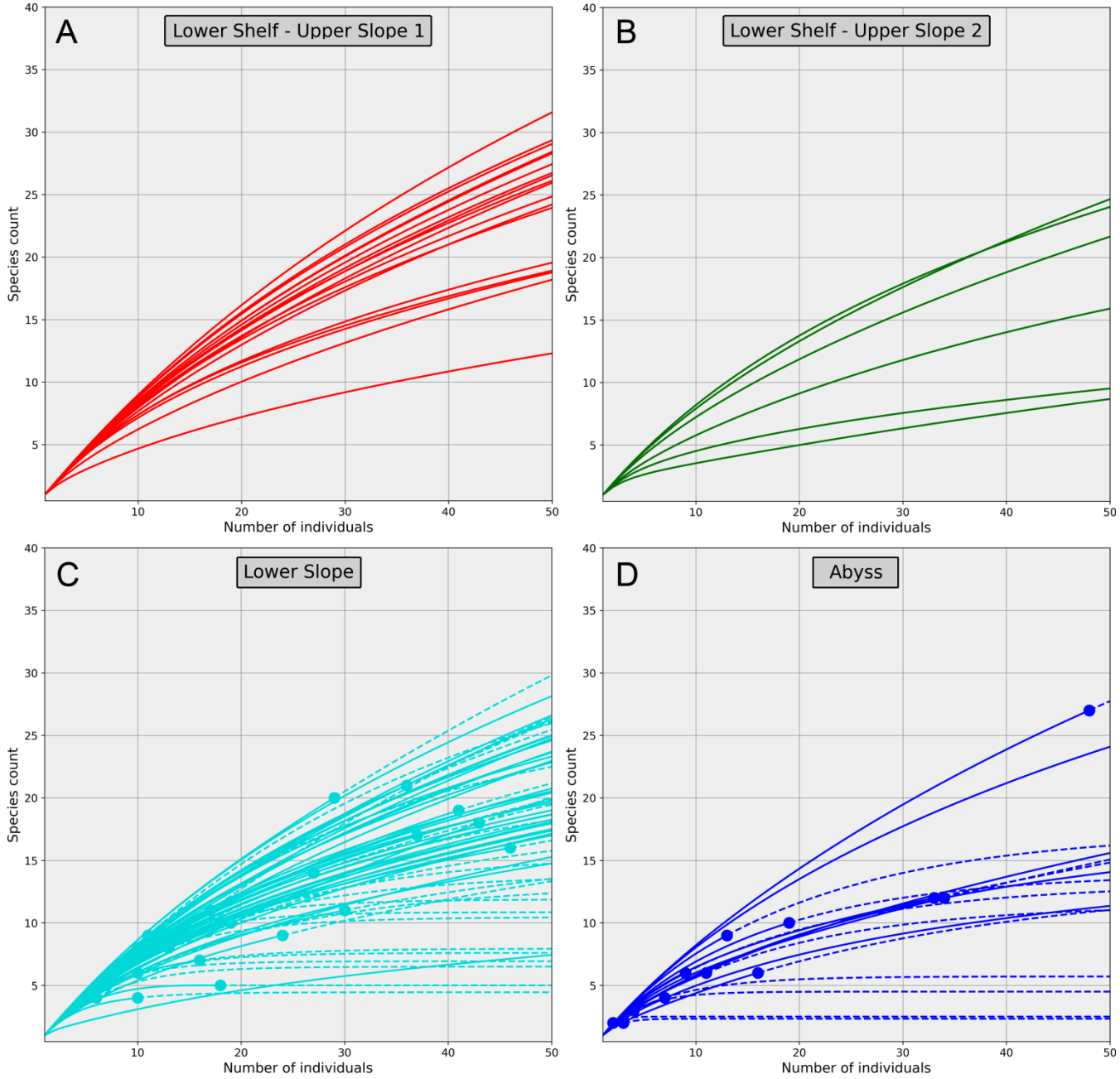

Fig. 6. Rarefaction curves for the quantitative samples up to 50 individuals with extrapolation based on the Hill numbers (q = 0). A – *Lower Shelf - Upper Slope 1* assemblage; B – *Lower Shelf - Upper Slope 2* assemblage; C – *Lower Slope* assemblage; D – *Abyss* assemblage. Colour corresponds to assemblages as in Figs. 3-5. Continuous lines indicate true (sample-sized) rarefaction; circles indicate the end of sample in case of <50 ind m^{-2}; dashed lines indicate the extrapolated rarefaction.

Benthic assemblages largely replaced one another with depth except the *Lower Shelf - Upper Slope 2* assemblage that sits within the depth range of the *Lower Shelf - Upper Slope 1* and *Lower Slope* assemblages (Fig. 7). The Bray-Curtis similarity dendrogram identified depth ranges of community clusters as follows: 60-942 m for the *Lower Shelf - Upper Slope 1* group; 239-1850 m for the *Lower Shelf - Upper Slope 2* group; 657-3054 m for the *Lower Slope* group and 2644-5416 m for the *Abyss* group (Fig. 7). The depth ranges differed some for the Morisita-Horn index: 60-1026 m for the *Lower Shelf - Upper Slope 1* group; 640-3848 m for the *Lower Slope* group and 3677-5416 m for the *Abyss* group; the *Lower*

Shelf - Upper Slope 2 group stations split into few clusters not forming a single assemblage (Fig 7, Supplementary 5, Fig. S-1). For the quantitative Sørensen similarity index the depth ranges were a bit more overlapping between assemblages: 60-1216 m for the *Lower Shelf - Upper Slope 1* group; 640-3848 m for the *Lower Slope* group and 2027-5416 m for the *Abyss* group; the *Lower Shelf - Upper Slope 2* stations overlapped the *Lower Shelf - Upper Slope 1* group and the *Lower Slope* group (Fig 7, Supplementary 5, Fig. S-2).

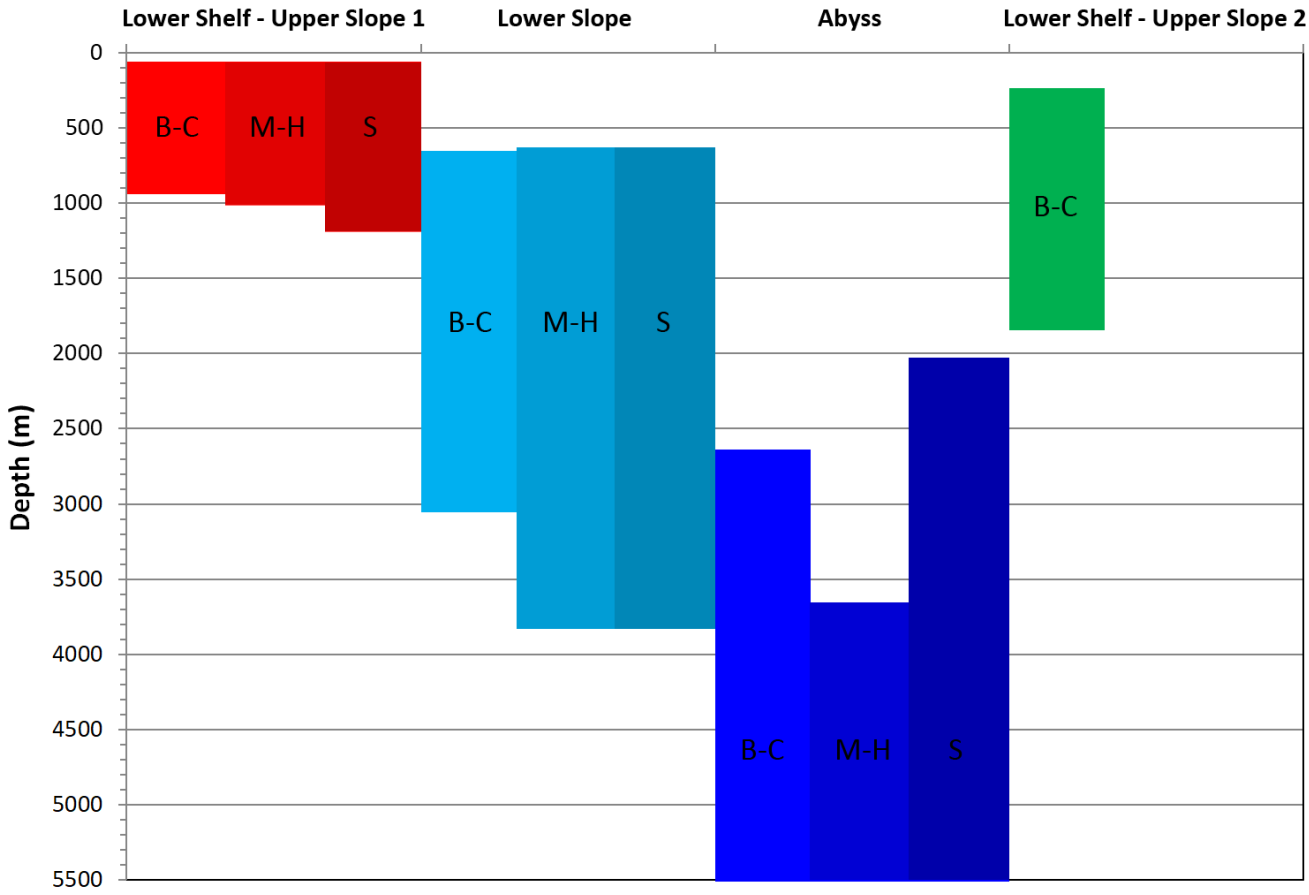

Fig. 7. Bathymetric distribution of groups of Arctic benthic assemblages based on quantitative samples (three different similarity indices). Colours as in Figs. 3-5. B-C – depth ranges from the Bray-Curtis similarity dendrogram; M-H – depth ranges from the Morisita-Horn similarity dendrogram; S – depth ranges from the quantitative Sørensen similarity dendrogram.

3.2.Semi-quantitative samples

The number of taxa per semi-quantitative sample varied from 8 (st. 2012-259) to 199 (st. 2015-seep), the diversity index values varied from 8 (st. 2012-259) to 39 (st. 2012-205) for ES-100, from 0.23 (st. 2007-4996) to 0.98 (st. 2012-359) for Pielou's evenness and from 0.8 (st. 2007-4996) to 3.5 (st. 2012-205) for Shannon diversity (Supplementary 3). A complete list of individual taxa with percentage abundance at each station appears in Supplementary 6.

The cluster analysis based on the Bray-Curtis similarity index with SIMPROF test identified five distinct clusters (= benthic assemblages), corresponding to the same cluster names introduced in the

previous section except the *Upper Shelf*, since no shelf stations were included in the quantitative data set (Fig. 8). PERMANOVA showed significant results with p-value < 0.001 (Fig. 8). Other similarity indices demonstrated similar dendrogram topology, except of the *Upper Shelf*, *Lower Shelf - Upper Slope 2* clustered within the *Upper Shelf*, *Lower Shelf - Upper Slope 1* assemblage (Morisita-Horn index – Supplementary 5, Fig. S-3). Furthermore, *Lower Slope* stations clustered together with the *Abyss* stations (Sørensen index – Supplementary 5, Fig. S-4).

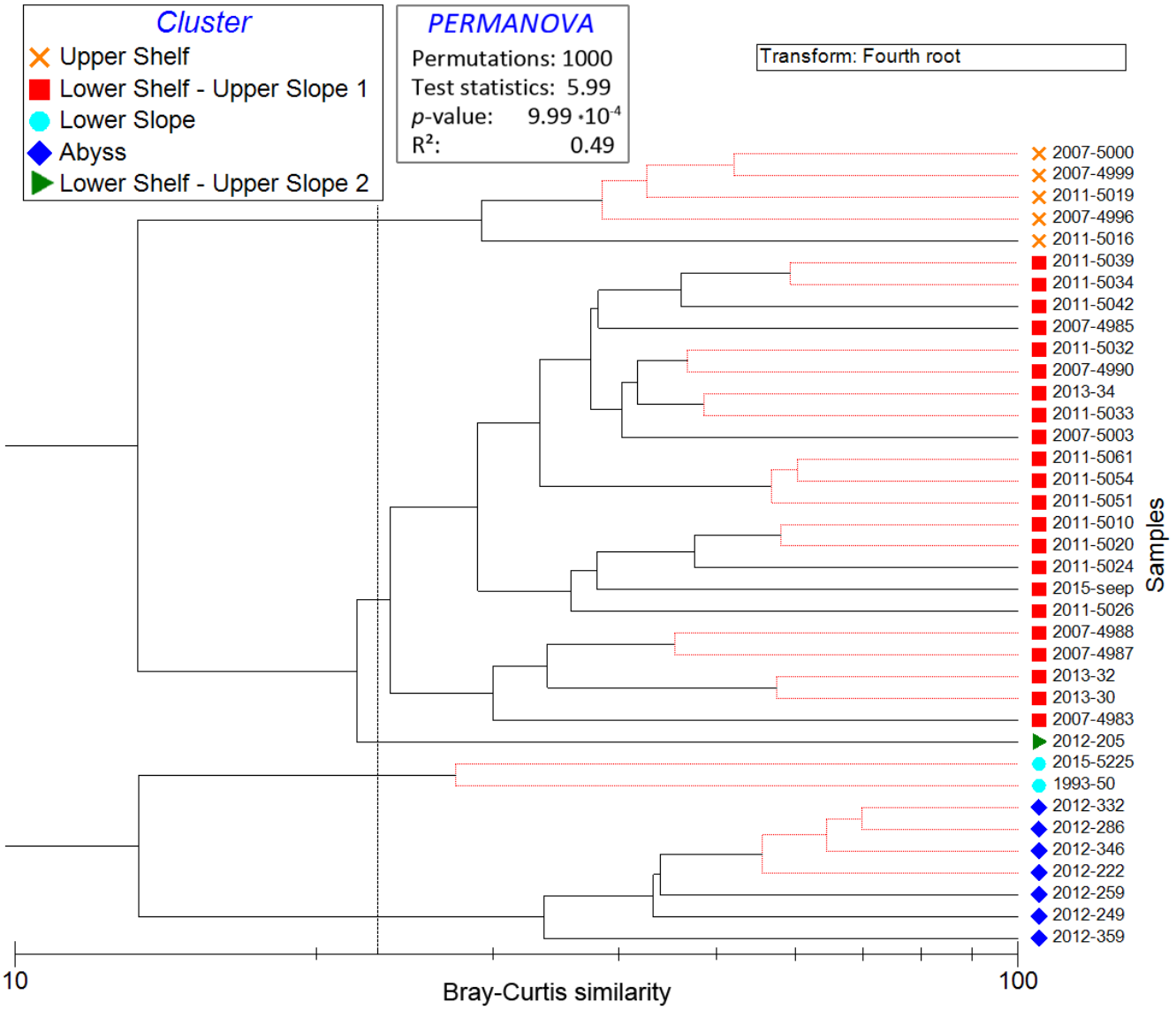

Fig. 8. Cluster analysis of semi-quantitative Arctic benthos samples using Bray-Curtis similarity index with SIMPROF results. Branches and nodes not statistically significant at p<0.01 are shown with red lines. Colour and shape indicate benthic assemblages, defined at the similarity level of 22 (vertical line); similarity axis is logarithmic. Enclosed the PERMANOVA results are shown.

Kruskal-Wallis tests indicated significant difference between benthic assemblages for diversity indices (Table 3), though with lower p-values compared to quantitative samples. The *Lower Shelf – Upper Slope 1* and the *Abyss* groups appeared widely distributed across the entire area. The *Upper Shelf*, *Lower*

Shelf - Upper Slope 2 and *Lower Slope* groups were more localized, resulting from the limited geographic spread of samples in those assemblages (Fig. 9).

Table 3. Mean values of benthic diversity of each assemblage and results of Kruskal-Wallis and Dunn's post-hoc tests for semi-quantitative samples.

Group	Mean values ± SD					Kruskal-Wallis		Dunn's post-hoc comparisons
	(1) *Upper Shelf*	(2) *Lower Shelf - Upper Slope 1*	(3) *Lower Slope*	(4) *Abyss*	(5) *Lower Shelf - Upper Slope 2*	Chi square	*p*	
Number of samples	7	20	2	7	1	-	-	-
Species number	55 ±36	98 ±34	50 ±33	19 ±6	133	22.82	<0.001	1-2; 2-4; 4-5
ES-100	16 ±7	24 ±8	22 ±6	11 ±2	39	17.46	0.0016	2-4; 4-5
Hill 50 extrapolated	10±3	15 ±5	16 ±3	11 ±6	24	11.24	0.0240	1-2; 1-5; 2-4; 4-5

Numbers in Dunn's post-hoc comparisons column indicate corresponding group of benthic assemblages, revealed with Bray-Curtis similarity.

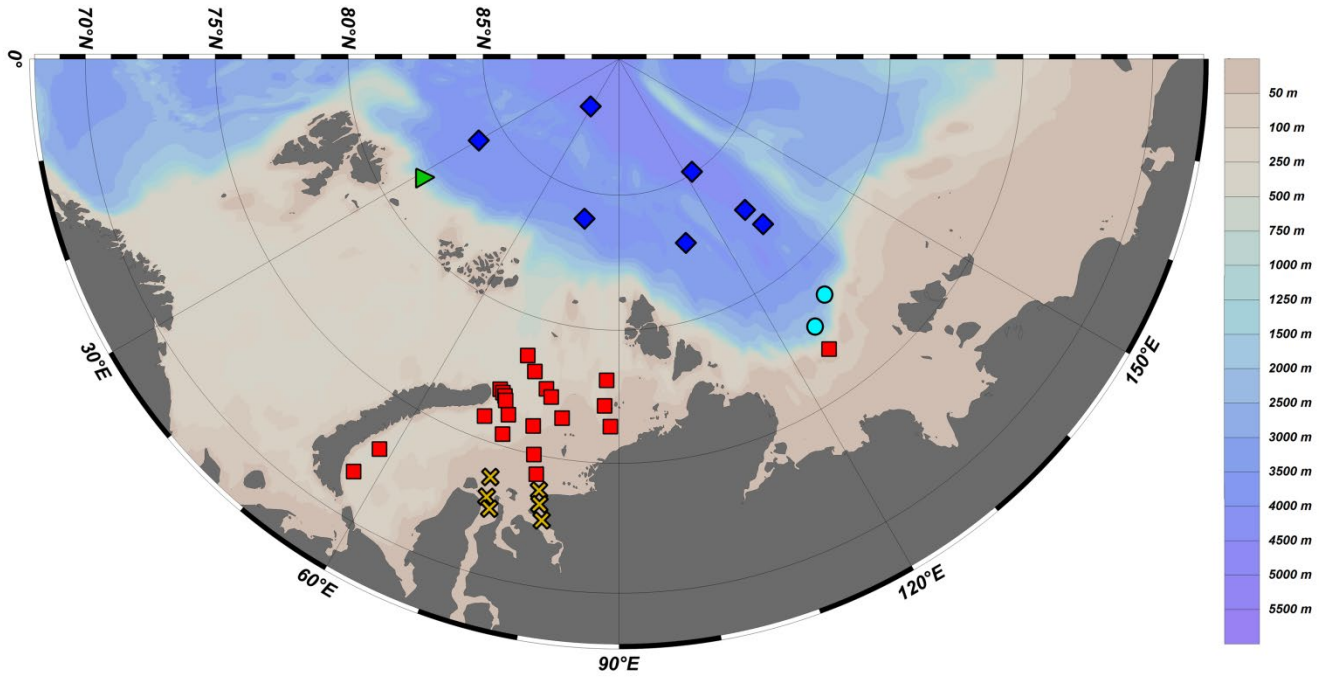

Fig. 9. Distribution of semi-quantitative samples coloured according to benthic assemblages. Colours and shapes of markers as in Fig. 3-7.

SIMPER analysis revealed a suite of taxa from different phyla and classes responsible for differences among assemblages (Table 4). As in Table 2, all taxa are listed according to their mean contribution to assemblage differences (only taxa with cumulative contribution up to 70% are shown). The bivalve *Portlandia arctica*, the mysid *Mysis oculata*, the polychaete *Spio* cf. *filicornis* and the ophiuroid *Stegophiura nodosa* were dominant in relative abundance and separated the *Upper Shelf* cluster. The *Lower Shelf - Upper Slope 1* group differed from other clusters by the high relative abundances of the ophiuroids *Ophiocten sericeum* and, to a lesser extent, *Ophiacantha bidentata* and *Ophiura robusta* and the bivalve *Yoldiella solidula*. The prevalence of the bivalve *Bathyarca frielei*, the isopod *Saduria sabini*, the gastropod *Mohnia danielsseni* and, to a lesser extent, the holothurian *Kolga hyalina* differentiated the *Lower Slope* group. The extreme dominance of *K. hyalina* and high relative abundances

of the actiniarian *Bathyphellia margaritacea*, the polychaete *Anobothrus laubieri* and, occasionally the ophiuroid *Ophiostriatus striatus* differentiated the *Abyss* group. The *Lower Shelf – Upper Slope 2* group, represented by a single station, contained high proportional abundances of the polychaete *Notoproctus oculatus*, the sipunculid *Nephasoma diaphanes*, the sponge *Geodia barretti* and Scyphozoa polyps (Stephanoscyphus) (Table 4).

Diversity parameters in semi-quantitative samples also yielded a parabolic relationship with depth with maximum species numbers and ES-100 at depths of ~100-600 m (Fig. 10).

Table 4. Results of SIMPER analysis of semi-quantitative Arctic benthos samples with values of average percentage abundance, average dissimilarity and percentage contribution within retrieved groups of assemblages.

Group	Species	Average Abundance (%)					Average Dissimilarity	Dissimilarity/ SD	Contribution (%)	Cumulative (%)
		Upper Shelf	*Lower Shelf - Upper Slope 1*	*Lower Slope*	*Abyss*	*Lower Shelf - Upper Slope 2*				
Biv	*Portlandia arctica*	59.1	6	0	0	0	11	0.6	11.2	11.2
Pol	*Notoproctus oculatus*	0	0.1	0	0	24.7	5.7	2	5.8	17
Oph	*Ophiocten sericeum*	0.01	14.4	3.6	0	0	4.7	0.8	4.9	21.9
Biv	*Bathyarca frielei*	0	0	33	0	0	4.7	0.8	4.9	26.8
Sip	*Nephasoma diaphanes*	0	8.1	0	0	11.3	4.2	1.9	4.3	31.1
Mys	*Mysis oculata*	11.2	0.1	0	0	0	3.6	0.7	3.6	34.7
Hol	*Kolga hyalina*	0	0	3.6	48.8	0	3.5	3.1	3.6	38.3
Oph	*Ophiacantha bidentata*	0	6.8	0	0	0.7	2.4	1.9	2.5	40.8
Biv	*Yoldiella solidula*	0	7.4	0	0	0.7	2.4	1.8	2.4	43.2
Pol	cf. *Spio filicornis*	5.5	0	0	0	0	2.4	0.5	2.4	45.6
Oph	*Ophiura robusta*	0	4.4	0	0	0.2	2.2	1.8	2.2	47.8
Cni	Stephanoscyphus	0	4.7	0	0.1	4.4	2.1	1.5	2.1	49.9
Por	*Geodia barretti*	0	0	0	0	8.4	1.9	3.3	2	51.9
Cni	*Bathyphellia margaritacea*	0	0	6.9	13.5	0	1.9	0.8	2	53.9
Oph	*Stegophiura nodosa*	3.4	0	0	0	0	1.9	0.5	1.9	55.8
Iso	*Saduria sabini*	2.0	0.3	2.7	0	0	1.6	1	1.6	57.4
Gas	*Mohnia danielsseni*	0	0	4.0	0.1	0	1.2	1	1.3	58.7
Biv	*Portlandia aestuariorum*	2.7	0	0	0	0	1.2	0.5	1.2	59.9
Pol	*Myriochele heeri*	0	0.9	1.3	0	3.5	1.1	1.9	1.2	61.1
Pol	*Anobothrus lauberi*	0	0	0	13.4	0.7	1.1	1.3	1.2	62.2
Hol	*Elpidia heckeri*	0	0	6.1	4.1	0	1.1	0.8	1.1	63.3
Biv	*Dacrydium vitreum*	0	5.1	0	0	0	0.9	0.3	1	64.3
Pol	*Siboglinum hyperboreum*	0	0	6.2	0	0	0.9	0.8	0.9	65.2
Iso	*Saduria sibirica*	1.8	0.1	0.6	0	0	0.8	0.8	0.9	66.1
Por	*Thenea muricata*	0	0	0	0	3.5	0.8	3.3	0.8	66.9
Pol	*Galathowenia oculata*	0	0.04	0	0	3.2	0.8	2	0.8	67.6
Hol	*Elpidia glacialis*	0	4	0	0	0	0.7	0.3	0.8	68.4
Hol	*Myriotrochus theeli*	0	0	4.9	0	0	0.7	0.8	0.7	69.1
Pol	*Notomastus* sp.	0	0	1.3	0	0.4	0.6	1.6	0.6	69.8
Biv	*Similipecten greenlandicus*	0	1.8	0	0	0	0.6	0.5	0.6	70.4

Taxa with cumulative contribution <70% are shown. First several most significant taxa in each assemblage are marked in grey. Por – Porifera; Cni – Cnidaria; Pol – Polychaeta; Sip – Sipuncula; Gas – Gastropoda; Biv – Bivalvia; Mys – Mysida; Iso – Isopoda; Hol – Holothuroidea; Oph – Ophiuroidea.

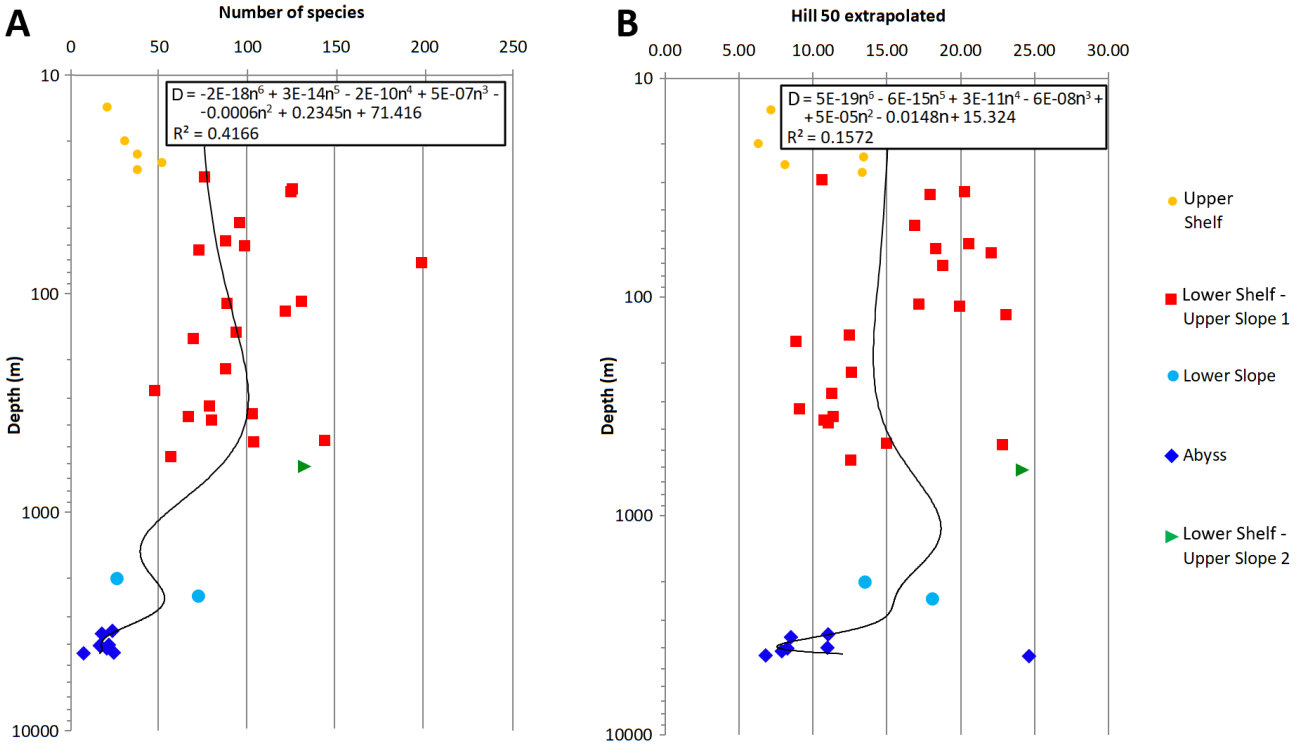

Fig. 10. Values of species number (a) and Hill 50 extrapolated (b) in semi-quantitative samples in relation to depth. Colour corresponds to clusters as in Figs. 3-8. Depth axis is logarithmic. Trend line equations and R^2 values are shown in rectangles (D – depth; n – species number or rarefaction per 50 individuals).

The benthic assemblages identified for semi-quantitative samples did not overlap by depth. The depth ranges of the benthic assemblages based on Bray-Curtis similarity were as follows: 14-27 m for the *Upper Shelf*; 29-553 m for the *Lower Shelf - Upper Slope 1* group; 615 m for the *Lower Shelf - Upper Slope 2* group; 1992-2390 m for the *Lower Slope* group and 3472-4380 m for the *Abyss* group. For the Morisita-Horn index identified depth ranges of 14-27 m for the *Upper Shelf* group; 29-615 m for the *Lower Shelf - Upper Slope 1* group; 1992-2390 m for the *Lower Slope* group and 3472-4380 m for the *Abyss* group; the *Lower Shelf - Upper Slope 2* assemblage fell within the *Lower Shelf - Upper Slope* 1 cluster. The depth ranges for the quantitative Sørensen similarity index were the same as for the Bray-Curtis index except that the *Lower Slope* and the *Abyss* assemblages shared a single cluster (Supplementary 5, Fig. S-3, S-4). Unlike groups based on quantitative samples, large depth gaps separated the groups of benthic assemblages based on semi-quantitative samples, likely reflecting the lower sample size and geographic coverage. Bathymetric distribution of clusters and rarefaction curves are available in Supplementary Figures S-5 and S-6.

4. Discussion

4.1. Benthic assemblages along a depth gradient

Our analysis done within the Central Arctic was the first one to analyse the bathymetric distribution of the benthic assemblages across a large geographic area (from the Fram Strait to the Beaufort Sea) and a large depth range (from 14 to 5416 m). We identified five groups of benthic assemblages, and all except the *Lower Shelf – Upper Slope 2* group replaced, rather than transitioned into, one another with depth. This is especially interesting considering the sampling area of each sample varied over 30-fold (from 0.023 to 0.750 m^2), apparently not decisively affecting the dendrogram structure (Figs. 3, 8). This zonation pattern spanned the entire analysed area, based either on quantitative (for macrofauna) or semi-quantitative (for megafauna) samples and based on three different quantitative similarity indices (Figs. 3-10). The five assemblages we identified largely aligned with those described in previous smaller-scale regional studies, (Deubel, 2000; Sirenko et al., 2004; Vedenin et al. 2018; Käß et al., 2019; Ravelo et al., 2020) with impressively little bathymetric or geographic structure and variation within each assemblage. The exceptions were the Fram Strait area, which resembled the *Lower Slope* group, and the Beaufort Sea stations that grouped separately within the *Lower Shelf - Upper Slope 2* and, to a lesser extent, within the *Lower Slope* groups (Fig. 3, Supplementary 5). Three of the described assemblages (the *Lower Shelf – Upper Slope 1*, the *Lower Slope* and the *Abyss*) formed consistent bands of zonation across entire study area. The distributional patterns of all five assemblages likely relate to environmental gradients at corresponding depths such as water masses, organic carbon fluxes, and near-bottom currents (Watling et al., 2013) which we discussed below, acknowledging that the exact factors remain hypothetical.

The *Upper Shelf* group identified from semi-quantitative trawl samples partly corresponds to the *Portlandia arctica* and *Ennucula tenuis* bivalve community previously described for the Kara, Laptev, and East-Siberian Seas (Filatova & Zenkevich 1957; Deubel, 2000; Petryashev et al. 2004; Sirenko & Denisenko 2010; Vedenin et al. 2018). A similar assemblage type was reported from the Beaufort Sea coastal areas (Carey & Ruff, 1977). The low overall diversity of this assemblage corresponds with high values of abundance and biomass (Petryashev et al., 2004; Vedenin et al., 2018). The *Upper Shelf* group distribution likely relates to high sedimentation rate from the freshwater inflow over the wide and shallow Siberian shelves (Weber, 1989; Fütterer & Galimov, 2003; Flint et al., 2019; Vedenin et al., 2021). The shallow Chukchi Sea inflow shelf (of which we did not include samples) experiences little of this freshwater influence, and higher diversity (Blanchard et al., 2013; Schonberg et al., 2014; Grebmeier et al., 2015), so the pattern is not pan-Arctic but rather characteristic for interior shelves (Williams & Carmack 2015).

The *Lower Shelf – Upper Slope 1* group partly corresponds to two communities dominated by the ophiuroids *Ophiocten sericeum* and *Ophiopleura borealis*, both widely distributed across the Siberian and Beaufort shelves (Filatova & Zenkevich 1957; Petryashev et al., 2004; Ravelo et al., 2020). Near Franz-

Joseph Land, Svalbard and in the Chukchi Sea, *Ophiura robusta* ophiuroids and/or *Yoldiella solidula* bivalves (Dahle et al., 2009) dominate communities at similar depths, along with the ophiuroids *Ophiacantha bidentata* and *Ophiura sarsi* (Piepenburg et al., 1996; Bluhm et al., 2009). Vedenin et al. (2018) and Deubel (2000) delineated this benthic assemblage as the UPPER SLOPE and HANG (= 'slope') groups, respectively, for the Barents, Laptev and East-Siberian Seas shelf edge and slope. Assemblages similar in taxonomic composition were described for the Beaufort Sea by Ravelo et al. (2020). The quantitative and semi-quantitative samples used in this study identified *Y. solidula* and *O. sericeum* as the dominant species in this area, and an assemblage of higher diversity than the *Upper Shelf* group. This distribution likely relates to the higher number of ecological niches at the shelf edge and upper slope and less stress from turbidity and low salinity associated with river discharge (Carney, 2005; Flint et al., 2019). In addition, its lower limit roughly corresponds with the lower boundary of the Atlantic water layer (Wassman et al., 2019; Bluhm et al., 2020). Hydrobiochemical connectivity of the entire Arctic upper continental slope is given through boundary currents, cross-slope upwelling of nutrient rich water, and down-welling particulate organic matter from upper waters (summarized in Bluhm et al., 2020). Previous studies report faunal changes coinciding with the transition between the Atlantic layer and other water masses for polychaetes, isopods, gastropods and fishes in the Norwegian Sea, where a particularly steep hydrological gradient occurs (Svavarsson et al., 1990; Bergstad et al., 1999; Høisæter, 2010; Oug et al., 2017).

The *Lower Slope* group in our study extended from the continental slope in the Fram Strait (at both Eastern and Western sides) to the Beaufort Sea and corresponds to benthic communities described in smaller-scale studies: *Galathowenia fragilis - Myriochele heeri* polychaete community in the Fram Strait (Budaeva et al., 2008; Vedenin et al., 2016; Käß et al., 2019); Polychaeta-dominated community in the Laptev Sea (Fütterer, 1993; Sirenko, 1998; Sirenko et al., 2004); the MID-SLOPE and LOWER SLOPE (Vedenin et al., 2018) and RAND and RÜCKEN (= 'margin' and 'ridge'; Deubel, 2000) communities within the Barents and Laptev Seas and on Lomonosov Ridge. Oweniidae polychaetes and *Bathyarca frielei* bivalves dominated our quantitative and semi-quantitative samples, respectively. The *Lower Slope* group apparently spans a huge area around the Central Arctic Basin perimeter and including slopes of the Greenland and Norwegian Seas at depths of ~700-3000 m (Nilsen & Holthe, 1985; Schnack, 1998; Vedenin et al., 2016). Bluhm et al. (2020) suggested faunistic similarity along the entire continental slope in the Arctic Ocean based on a smaller data set. Our data set supports this assertion, along with occasional reports of communities dominated by polychaetes, for example Paraonidae and Cirratulidae (Paul & Menzies, 1974) or *Prionospio* sp. and unidentified polychaetes (Bluhm et al., 2005) from the Canada Basin continental slope. Environmental conditions defining the *Lower Slope* group distribution may include weaker currents compared to the *Lower Shelf – Upper Slope 1* group and similar hydrographic properties related to Arctic Deep Water (synthesized in Bluhm et al., 2020). Interestingly, the mentioned

462 *Galathowenia* and *Myriochele* polychaetes are strict deposit-feeders that build their tubes out of fragments
463 of plankton foraminifers and sponge spicules, depending therefore indirectly on the higher organic matter
464 supply from upper water layers (Nilsen & Holthe, 1985; Parapar, 2006). This factor might be the reason
465 for preventing Oweniidae distribution down to the abyssal plain.

466 The holothurians *Kolga hyalina* and *Elpidia heckeri* and the actiniarian *Bathyphellia margaritacea*
467 dominated the *Abyss* group, that apparently occupies the entire Central Arctic at depths >~3000 m, as
468 shown in numerous publications based on data from the Greenland, Nansen, Amundsen and Canada basins
469 (Gorbunov, 1946; Kröncke, 1992; Kröncke, 1994; Deubel, 2000; Sirenko et al., 2004; Soltwedel et al.,
470 2009; Vedenin et al., 2018; Rybakova et al., 2019). These dominants also often appear in bottom images
471 and in semi-quantitative samples such as in trawls (Macdonald et al., 2010; Rybakova et al., 2019; Zhulay
472 et al., 2019). Smaller quantitative gears demonstrate also high abundances of smaller polychaete species,
473 such as *Anobothrus laubieri*, *Ymerana pteropoda* and *Ophelina opisthobranchiata* (Table 2). The poor
474 trophic conditions likely resulted in the lowest values of abundance, biomass and diversity within the
475 *Abyss* group (described in Bluhm et al. 2011; Bluhm et al., 2015; Vedenin et al., 2018; Rybakova et al.,
476 2019). For megafauna, including the holothurians *K. hyalina* and *E. heckeri*, falls of *Melosira arctica*
477 algae colonies torn off the sea ice were shown to be important (if not primary) food source, that possibly
478 drives the distribution of these taxa across the Central Arctic abyssal plains (Boetius et al., 2013).

479 The *Lower Shelf – Upper Slope 2* group overlapped the *Lower Shelf – Upper Slope 1* and *Lower*
480 *Slope* groups in depth. The former differed from other clusters in our study by its greater biomass and
481 species number and the prevalence of filter-feeders, such as sponges (mostly *Geodia* spp. and *Thenea*
482 *muricata*), polychaetes (*Bushiella similis*) and bryozoans (*Tubulipora* spp.). This benthic assemblage
483 corresponds to the community of filter-feeders described by Sirenko et al. (2004) from a few areas around
484 the Severnaya Zemlya archipelago. Furthermore, the taxonomic composition of this group resembled the
485 benthic ecosystems in several areas in the northern Barents Sea and around Svalbard (Sswat et al., 2015).
486 The similarity within this assemblage was lower than for the other assemblages because of some
487 taxonomic differences between the Eurasian samples (northern slopes of Barents and Kara seas) and the
488 Amerasian samples (northern slopes of Beaufort Sea and Northwind Ridge / Chukchi Plateau, see Fig. 3).
489 However, we decided to retain the *Lower Shelf – Upper Slope 2* as a separate assemblage because of
490 similarity in filter-feeders composition. Strong near-bottom currents enriched with suspended food
491 particles usually favour the development of communities dominated by filter-feeders, as shown for
492 communities on the shelf edge of the North-Eastern Beaufort Sea (Pisareva et al., 2015; Rand et al., 2018).
493 This type of benthic assemblages may occur widely across the Arctic continental slope, though with
494 uneven distribution given its strong dependence on near-bottom hydrodynamics (Thomson, 1982).
495
496 *4.2. Benthic abundance, biomass and taxon richness*

Previous studies have documented gradual decrease of abundance and biomass of macrobenthos with depth for different areas of the Arctic Ocean (Rex & Etter, 2010; Macdonald et al., 2010; Bluhm et al., 2011; Bluhm et al., 2015; Bluhm et al., 2020; Vedenin et al., 2018). Our study extends earlier work by Vedenin et al. (2018) with three times more stations and several fold extension of the study region, however, we find similar patterns of depth-related changes (Fig. 5). One notable difference links to different diversity patterns using extrapolated rarefactions based on Hill numbers, which indicated higher diversity values for the *Lower Slope* and for the *Abyss* assemblages (Fig. 6, Supplementary 3). We also identified a cluster of *Lower Shelf – Upper Slope 2* stations, absent in Vedenin et al. (2018). Decreases in abundance and biomass with depth likely relate to decreased food availability at the seabed with increasing ocean depth, a trend common for the global ocean and especially prominent in the Arctic Ocean largely covered with seasonal sea-ice (Wei et al., 2010 a; Degen et al., 2015; Vedenin et al., 2018; Käß et al., 2019; Górska et al., 2020; Oleszczuk et al., 2021). Exceptions to this depth-related decline are rare and probable exist only where oceanographic anomalies disrupt typical patterns of food supply and oxygen concentrations, such as the East Pacific off Peru where biomass peaks at mid-depths of 800-1000 m (Rowe, 1971).

Trends in diversity with depth in the ocean differ from trends in abundance and biomass. Maximum values of species richness and diversity often occur at mid- and low-bathyal depths from 2000 m to 4000 m (Rex, 1981; Flach & de Bruin, 1999; Gage et al., 2000; Gebruk et al., 2010; Brown & Tatje, 2014). However, in some locations, gradual decrease in diversity with depth (similar to the abundance and biomass trends) occur (Rex & Etter, 2010). Such a pattern may relate to the biogeographic history of a basin. For example, in basins with limited deep-water exchange such as those with shallow straits or sills where geologically recent impoverishment or extinction of the benthic ecosystem occurred, recolonization could follow from shallow waters or more slowly from adjacent deep-sea areas (Rex & Etter, 2010). The Mediterranean Sea and Arctic Ocean illustrate this process. The former was recolonized through the Gibraltar Strait after complete fauna extinction during the Messinian salinity crisis (Krijgsman et al., 1999). In the Eastern Mediterranean, maximum benthic diversity occurs in shallow waters and decreases with depth (Tselepides & Eleftheriou, 1992; Tselepides et al., 2000). Several lines of evidence point to depletion (and possible extinction) of the benthic fauna of the Arctic Ocean during the Pleistocene glaciations, given that primary production dropped dramatically or even ceased beneath the ice shield (Menzies, 1962; Dunbar, 1968; Menzies, 1973; Renaud et al., 2008; Kędra et al., 2015). Following glaciation, recolonization took place from the Atlantic through the Fram Strait and from the Pacific through the Bering Strait, involving mostly shallow-water species (Vermeij, 1991; Nesis, 2001; Mironov, 2013). Therefore species numbers (and biodiversity) decrease with depth in the high Arctic, as shown by Wlodarska-Kowalczuk et al. (2004), Bluhm et al. (2011) and Käß et al. (2019). However, recent analysis of a subset of the samples used in the present study identified a diversity peak at depths 100-300 m

(Vedenin et al., 2018), a depth range not included in these previous deep-sea studies. Our study extended the sampling area westward to the Yermak Plateau and Fram Strait (Fig. 4), and we found a similar parabolic pattern of diversity change with depth. Based on semi-quantitative trawl samples on the Siberian shelf and slope (Fig. 9), diversity peaked at 100-600 m. Vedenin et al. (2018) linked the diversity maximum at 100-300 m on the Laptev Sea shelf and slope to river run-off that impacts ocean stratification and primary productivity above the shallow shelf. However, this explanation cannot apply to the Svalbard area. A possible reason for peak diversity values can be the warmer Atlantic waters inflowing at ~100-800 m, enriching this area with organic carbon as well as Atlantic boreal species (Wassmann et al., 2019; Bluhm et al., 2020). For example, the inflow of zooplankton biomass contributed by *Calanus* spp. alone might exceed a million tons C $year^{-1}$ (Wassmann et al., 2015; Basedow et al., 2018). Our dataset lacks samples from <100 m depth near Svalbard, so the local diversity trends could be different.

4.3.Bathymetric boundaries in the Arctic benthic fauna

Different researchers have used different approaches to describe biogeographic zonation, including bathymetric patterns. Mironov (2013) distinguished three main types: based on the distribution of species (1), communities (2) and environmental parameters (3). Multiple studies show major bathymetric boundaries in the global ocean, based on species distributions near 200 m, corresponding to the boundary between sublittoral and bathyal faunas, and near 3000 m at the boundary between bathyal and abyssal faunas (Carney, 2005; Howell et al., 2002; Krayushkina, 2000; Mironov, 1986; Vinogradova, 1962). The 200-m boundary roughly corresponds to the lower limit of the photic zone and to the shelf break (Carney, 2005; Wei et al., 2010 b), whereas the 3000-m boundary likely reflects decreasing food availability and significant changes in bottom topography, such as the transition from continental slope to continental rise and abyssal plain (Thistle, 2003; Wei et al., 2010 b; Watling et al., 2013). Many studies also identify a boundary at 800-1200 m depth (Gage, 1986; Svavarsson, 1990; Howell et al., 2002), explaining this boundary by peculiarities of bottom topography, near-bottom currents and sediment changes, that affect the distribution of benthos in case of isopods (Svavarsson, 1990) and distributional paths of plankton larvae in case of echinoderms (Gage, 1986). Most of these publications were based on data from the Pacific, Atlantic and the Norwegian Sea. In the high Arctic, only Vedenin et al. (2021) used a species-based approach to bathymetric zonation. Based on data on three macrofaunal taxa - Polychaeta, Crustacea and Echinodermata, we identified two main boundaries, the first at 450-800 m between the sublittoral and bathyal faunas and at 1800-2000 m between the bathyal and abyssal faunas. Our study, based on the distribution of groups of benthic assemblages rather than species, identified the boundary between sublittoral and bathyal faunas at depths of ~650-950 m (between the *Lower Shelf – Upper Slope 1* and *Lower Slope* groups) based on Bray-Curtis similarity or at ~650-1200 m based on Sørensen similarity. Thus, two different methods support a strong boundary around ~450-1200 m. We refrained from defining

a boundary between the *Upper Shelf* and *Lower Shelf – Upper Slope 1* groups because of the small sample set, and because previously published data suggest a deeper position for biogeographic boundaries in the Arctic (Mironov, 2013; Vedenin et al., 2021). As we already mentioned, a possible environmental driver for this boundary is the transition from the warm Atlantic layer to the deep and cold Arctic waters that lies at approximately 700-800 m (Wassman et al., 2019; Bluhm et al., 2020).

Species distributions indicated a boundary at ~2000 m (Vedenin et al., 2021). When considering the distribution of benthic assemblages based on quantitative samples from our study, similar species appeared to dominate within a depth range of 650-3000 m (based on Bray-Curtis similarity) or 650-3800 m (based on Morisita-Horn and Sørensen indices) for the *Lower Slope* assemblage. The semi-quantitative (trawl) material we have is relatively scarce, with large depth gaps. However, Sirenko et al. (2004) reported a boundary at ~1900-2000 m between the slope 'polychaete community' and the deeper community dominated mainly by the holothurians *Kolga hyalina* and *Elipida heckeri*. Deubel (2000) reported boundaries at ~530-990 m and at 1740-2100 m based on quantitative macrofaunal data. For the Beaufort Sea and Canada Basin stations in this study, we identified a transition between the different deep-sea communities at ~1850-3200 m (Bluhm et al., 2005) and at ~2700-3500 m (MacDonald et al., 2010). We lack any bathymetric transects on the slope north of Ellesmere Island and Greenland but identify different bathymetric boundaries in the Arctic Ocean based on our own data and on previous studies (Fig. 11).

For the Barents and Laptev Seas previous work showed that benthic communities replace one another with depth with little bathymetric overlap (Vedenin et al., 2018). Unlike these results, we found significant depth overlap at ~650-950 m (or 650-1200 m by different similarity indices) between two groups of benthic assemblages – the *Lower Shelf – Upper Slope 1* and *Lower Slope*. This overlap may reflect regional differences in the depth ranges of the eurybathic species that dominated their corresponding assemblages (discussed in Vermeij, 1991; Nesis, 2001; Vedenin et al., 2021). At greater depths we found overlap between the *Lower Slope* and *Abyss* groups (2644-3054 m based on Bray-Curtis similarity; 3677-3848 m based on Morisita-Horn similarity; 2027-3848 m based on Sørensen similarity). No published evidence suggests any boundary at these depths in the Arctic, except for Vedenin et al. (2018) and, possibly, MacDonald et al. (2010) (both data sets integrated in this study). Based on the present and earlier studies we think that the boundary at this depth reflects abrupt changes in major community characteristics, including abundance and diversity (Table 1, 3; Figs. 5, 10) at the continental rise to abyssal seafloor transition, rather than significant changes in taxonomic composition (Boetius et al., 1996; Klages et al., 2004; Degen et al., 2015). Therefore, reduced sensitivity of the Morisita-Horn and Sørensen similarity indices to sample size (Chao et al., 2006), elucidated a markedly different depth range of the *Lower Slope* / *Abyss* transition compared to the Bray-Curtis index.

Environmental gradients, briefly discussed earlier and in previous publications (Mironov, 2013; Watling et al., 2013; Vedenin et al., 2021) drive the boundaries elucidated by these different approaches. In particular, the boundary between the *Lower Shelf – Upper Slope 1* and the *Lower Slope* assemblages roughly corresponds to the lower boundary of the warm Atlantic water masses, while the boundary between the *Lower Slope* and the *Abyss* matches the transition from the continental rise to abyssal plain. However, the exact mechanisms remain unknown and require further studies.

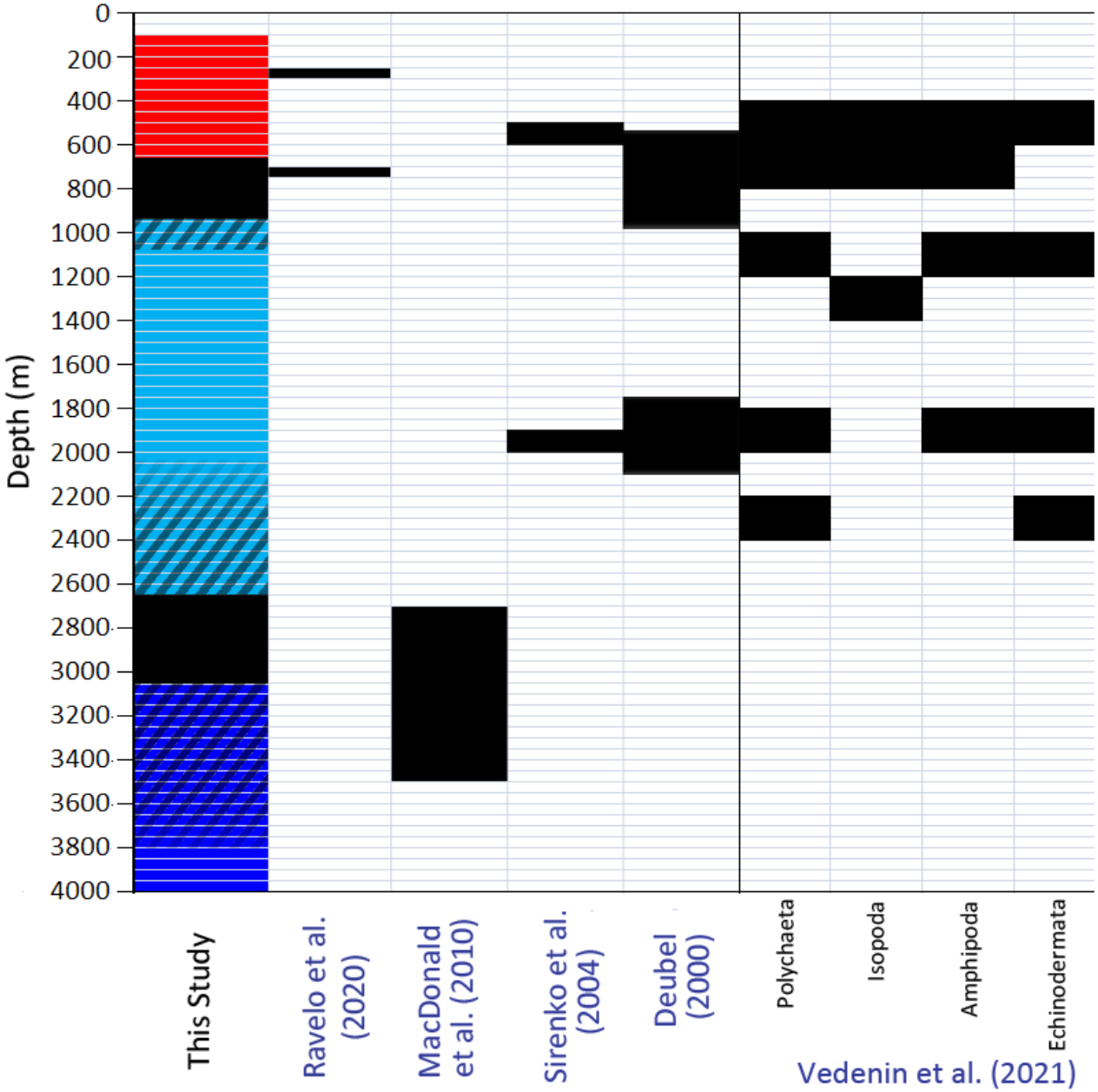

Fig. 11. Bathymetric boundaries between the sublittoral and bathyal (black rectangles within ~450-900 m) and between the bathyal and abyssal (black rectangles within ~1700-2100 and ~2000 m) faunas identified in the Arctic in the present study (based on Bray-Curtis similarity) and in published research. Diagonal pattern indicate boundaries at different depth ranges revealed by different similarity indices (either Morisita-Horn or Sørensen). Colours in the left column are the same as in Fig. 3-10. MacDonald et al. (2010) did not sample shallower than 800 m and Ravelo et al. (2020) sampled to 1000 m.

4.4. Pan-arctic extrapolation

Based on combined data on bathymetric benthic fauna zonation across the Central Arctic slope and abyssal zone, our study confirms major boundaries at ~450-900 m (Deubel, 2000; Sirenko et al., 2004; Bluhm et al., 2020; Vedenin et al., 2021; this study) and at ~1700-2100 m (Deubel, 2000; Sirenko et al., 2004; Vedenin et al., 2021). The entire macrofauna essentially changes at these pronounced biogeographic boundaries. The less universal deeper boundary at ~2600-3000 m (MacDonald et al., 2010; present study) can be distinguished based on cluster analysis and corresponds to the depth of a steep decrease in abundance, biomass, and diversity within the Central Arctic rather than a taxonomic turnover (Klages et al., 2004; Degen et al., 2015; Vedenin et al., 2018). The shelf benthic assemblages documented in our study are unlikely to be Pan-arctic, given quite marked differences in species composition between the Barents Sea, the Siberian seas and the Chukchi Sea within the Arctic (Sirenko et al., 1998; Grebmeier et al., 2006; Mironov, 2013).

The bathymetric overlap between the deeper benthic assemblages increases when extending the area from the smaller Barents and Laptev Sea area to almost the entire Arctic (Vedenin et al., 2018; this study). Apparently, higher environmental variability (e.g. varying freshwater discharge, sea ice volume or Atlantic/Pacific waters influence, Bluhm et al., 2020) over the broader study area contributes to this overlap. However, general trends of replacement of benthic communities and their composition remain similar at similar depths. Therefore, we suggest potential extrapolation of these bathymetric patterns across the continental slope and abyssal plain around the entire Central Arctic Ocean. Similar bathymetric patterns occur on both sides of the continental slope of the Fram Strait, despite the influence of different water masses: The warm Norwegian Current bathes the eastern slope, whereas the western slope sits beneath the cold East Greenland Current (Käß et al., 2019). Faunal composition deviates in the Beaufort Sea where the upper slope differs slightly as a result of the admixture of species of Pacific origin with those that disappear rapidly with the transition to the Atlantic layer (Bluhm et al., 2005; MacDonald et al., 2010; Conlan et al. 2013; Zhulay et al., 2019; Ravelo et al., 2020). In addition, a significant data gap remains on benthic communities from the continental slope of a large area north of Greenland and the Canadian Arctic Archipelago (Bluhm et al., 2020). A comprehensive test of the hypothesis of the pan-arctic uniformity of benthic bathymetric zonation will require adding data from this area, where remaining multi-year sea ice has hindered access to date.

We propose a visualization of the benthic bathymetric boundaries in the Central Arctic (Fig. 12), averaging the bathymetric profile for the Arctic Ocean and setting the shelf boundary at ~200 m (see Jakobsson et al., 2012; Hay, 2016). Within the study area we propose relatively uniform patterns including: (1) a parabolic change in species diversity that peaks at ~100-600 m, (2) bathymetric zonation of benthic assemblages (based on cluster analysis), that changes with increasing depth, (3) major biogeographic boundaries at ~450-900 m (or 450-1200 m depending on similarity indices) and ~1700-

2100 m, and a less universal boundary (recognised by community summary characteristics such as biomass and species richness) at around ~2600-3000 m (Fig. 12).

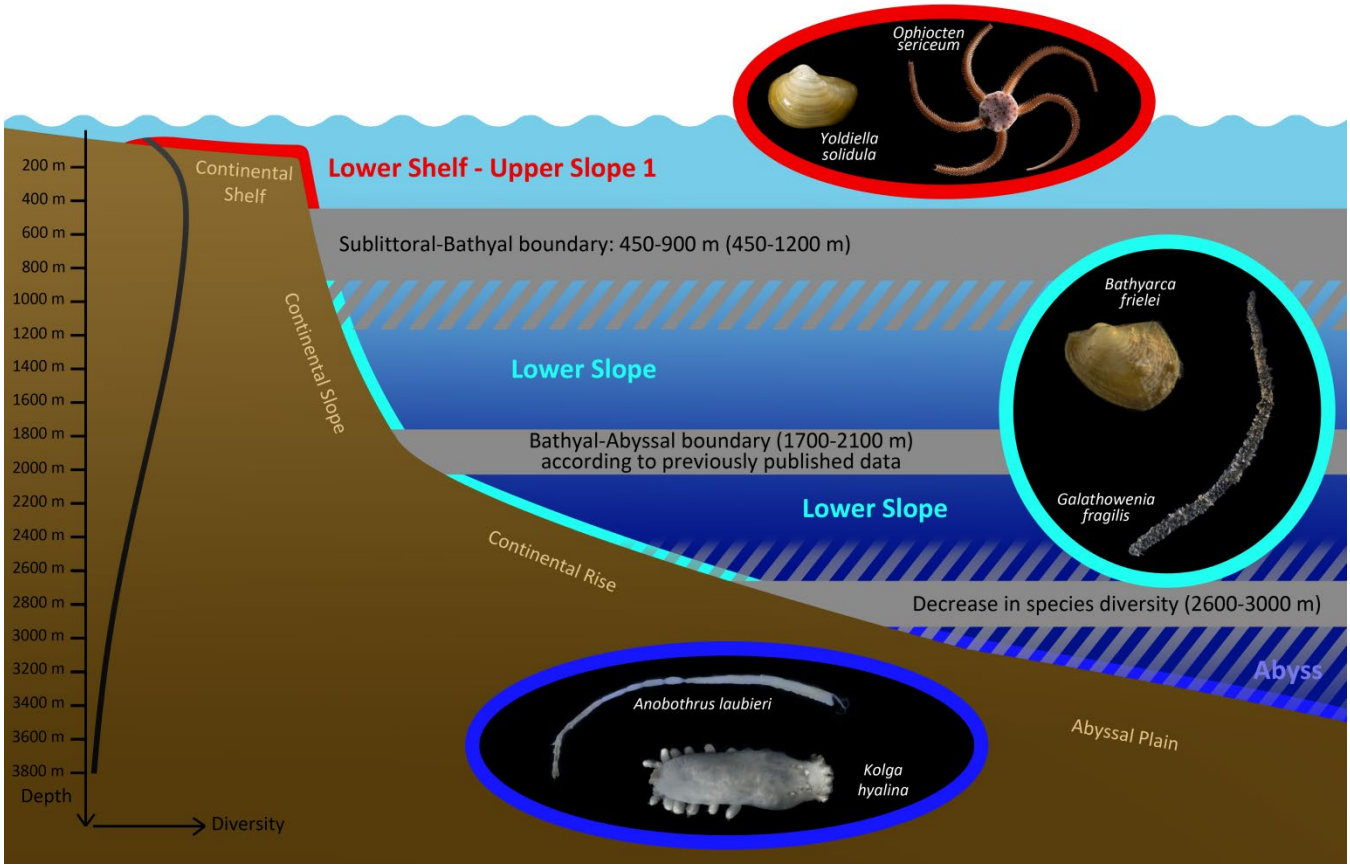

Fig. 12. Schematic of the benthic faunal bathymetric zonation in the Central Arctic based on the present study and published data. Upper and lower solid gray horizontal lines indicate boundaries at different depth ranges revealed by Bray-Curtis similarity index; diagonal pattern indicate boundaries revealed by different similarity indices (Morisita-Horn and Sørensen). Diversity trend is shown in the left. The seafloor contour and the outline of ellipses are coloured according to the benthic assemblages as in Figs. 3-11. Species characterizing the community clusters are shown in the corresponding ellipses (photos by A. Vedenin).

Acknowledgments

We thank Dr. Natalya Budaeva, Dr. Kirill Minin, Dr. Alexey Udalov, Dr. Vadim Mokievsky, Dr. Thomas Soltwedel and Dr. Vassily Spiridonov for their help with the literature search. Many thanks are due to Dr. Antje Boetius and Dr. Ingrid Krönke for providing original macrobenthic data from earlier expeditions. We are grateful to all the specialists who identified benthic organisms in the original samples – Dr. Nataliya Anisimova, Dr. Manuela Gusky, Dr. Hendrik Deubel. We acknowledge support from NOAA's office of Ocean Exploration and Research for the original work conducted in the Beaufort Sea/Canada Basin, and from the Arctic SIZE project co-funded by UiT The Arctic University of Norway and the Tromsø Research Foundation. This research was supported by the Russian Foundation for Basic Research (RFBR) project #18-05-60228.

References

1. Anderson, M. J. (2005). Permutational multivariate analysis of variance. Department of Statistics, University of Auckland, Auckland, 26, 32-46.
2. Anisimova, N.V., Frolova, E.A., Lubin, P.A., Frolova, A.A., Denisenko, N.V., Panteleeva, N.N., Lubina, O.S. (2003). Species composition and quantitative distribution of macrobenthos in the Voronin trench and on the adjacent continental slope. In: Fauna of invertebrates of Kara, Barents and White Seas (ecology, biogeography), p. 79-92. [In Russian]
3. Basedow, S. L., Sundfjord, A., von Appen, W. J., Halvorsen, E., Kwasniewski, S., & Reigstad, M. (2018). Seasonal variation in transport of zooplankton into the Arctic basin through the Atlantic gateway, Fram Strait. Frontiers in Marine Science, 5, 194 p. https://doi.org/10.3389/fmars.2018.00194
4. Bergstad, O. A., Bjelland, O., Gordon, J. D. (1999). Fish communities on the slope of the eastern Norwegian Sea. Sarsia, 84(1), 67-78. https://doi.org/10.1080/00364827.1999.10420452
5. Blanchard, A. L., Parris, C. L., Knowlton, A. L., & Wade, N. R. (2013). Benthic ecology of the northeastern Chukchi Sea. Part I. Environmental characteristics and macrofaunal community structure, 2008–2010. Continental Shelf Research, 67, 52-66. https://doi.org/10.1016/j.csr.2013.04.021
6. Bluhm, B. A., MacDonald, I. R., Debenham, C., & Iken, K. (2005). Macro-and megabenthic communities in the high Arctic Canada Basin: initial findings. Polar Biology, 28(3), 218-231. https://doi.org/10.1007/s00300-004-0675-4
7. Bluhm, B. A., Iken, K., Hardy, S. M., Sirenko, B. I., & Holladay, B. A. (2009). Community structure of epibenthic megafauna in the Chukchi Sea. Aquatic Biology, 7(3), 269-293. https://doi.org/10.3354/ab00198
8. Bluhm, B. A., Ambrose, W. G. Jr., Bergmann, M., Clough, L. M., Gebruk, A. V., Hasemann, C., et al. (2011). Diversity of the Arctic deep-sea benthos. Marine Biodiversity 41, 87–107. https://doi.org/10.1007/s12526-010-0078-4
9. Bluhm, B. A., Kosobokova, K. N., & Carmack, E. C. (2015). A tale of two basins: An integrated physical and biological perspective of the deep Arctic Ocean. Progress in Oceanography, 139, 89-121. https://doi.org/10.1016/j.pocean.2015.07.011
10. Bluhm, B. A., Janout, M. A., Danielson, S. L., Ellingsen, I., Gavrilo, M., Grebmeier, J. M., ... & Carmack, E. C. (2020). The pan-Arctic continental slope: sharp gradients of physical processes affect pelagic and benthic ecosystems. Frontiers in Marine Science. https://doi.org/10.3389/fmars.2020.544386
11. Boetius, A., Grahl, C., Kröncke, I., Liebezeit, G., & Nöthig, E. M. (1996). Distribution of plant pigments in surface sediments of the Eastern Arctic. Reports of Polar Research, 212, 213-218.
12. Boetius, A., Albrecht, S., Bakker, K., Bienhold, C., Felden, J., Fernández-Méndez, M., ... & ARK27, R. P. (2013). Export of algal biomass from the melting Arctic sea ice. Science, 339(6126), 1430-1432. https://doi.org/ 10.1126/science.1231346
13. Bray, J. R., Curtis, J. T., (1957). An ordination of the upland forest communities of southern Wisconsin. Ecological monographs, 27(4), 325-349. https://doi.org/10.2307/1942268
14. Brown, A., & Thatje, S. (2014). Explaining bathymetric diversity patterns in marine benthic invertebrates and demersal fishes: physiological contributions to adaptation of life at depth. Biological Reviews, 89(2), 406-426. https://doi.org/10.1111/brv.12061
15. Budaeva, N. E., Mokievsky, V. O., Soltwedel, T., & Gebruk, A. V. (2008). Horizontal distribution patterns in Arctic deep-sea macrobenthic communities. Deep-Sea Research Part I: Oceanographic Research Papers, 55(9), 1167-1178. https://doi.org/10.1016/j.dsr.2008.05.002
16. Carey Jr, A. G., Ruff, R. E. (1977). Ecological studies of the benthos in the western Beaufort Sea with special reference to bivalve molluscs. Polar oceans. Arctic Institute of North America, Calgary, 505-530.
17. Carney, R.S. (2005). Zonation of deep biota on continental margins. In: (Gibson, R.N., Atkinson, R.J.A., Gordon, J.D.M. (Eds.) Oceanography and Marine Biology: an annual review, 43, p. 211-278.
18. Chao, A., Chazdon, R. L., Colwell, R. K., & Shen, T. J. (2006). Abundance-based similarity indices and their estimation when there are unseen species in samples. Biometrics, 62(2), 361-371.
19. Chao, A., Gotelli, N. J., Hsieh, T. C., Sander, E. L., Ma, K. H., Colwell, R. K., & Ellison, A. M. (2014). Rarefaction and extrapolation with Hill numbers: a framework for sampling and estimation in species diversity studies. Ecological monographs, 84(1), 45-67.
20. Clarke, K., Warwick, R., (1994). An Approach to Statistical Analysis and Interpretation. PRIMER-E, Plymouth.
21. Clarke, K.R., Warwick, R.M. (2001). Changes in Marine Communities: An Approach to Statistical Analysis and Interpretation (2nd ed.). PRIMER-E, Plymouth.
22. Clarke, K. R., Somerfield, P. J., & Chapman, M. G., (2006). On resemblance measures for ecological studies, including taxonomic dissimilarities and a zero-adjusted Bray–Curtis coefficient for denuded assemblages. Journal of Experimental Marine Biology and Ecology, 330(1), 55-80. https://doi.org/10.1016/j.jembe.2005.12.017
23. Cochrane, S. K., Denisenko, S. G., Renaud, P. E., Emblow, C. S., Ambrose Jr, W. G., Ellingsen, I. H., & Skarðhamar, J. (2009). Benthic macrofauna and productivity regimes in the Barents Sea—ecological implications in a changing Arctic. Journal of Sea Research, 61(4), 222-233. https://doi.org/10.1016/j.seares.2009.01.003
24. Conlan, K., Hendrycks, E., Aitken, A., Williams, B., Blasco, S., & Crawford, E. (2013). Macrofaunal biomass distribution on the Canadian Beaufort Shelf. Journal of Marine Systems, 127, 76-87. https://doi.org/10.1016/j.jmarsys.2013.07.013
25. Dahle, S., Anisimova, N. A., Palerud, R., Renaud, P. E., Pearson, T. H., & Matishov, G. G. (2009). Macrobenthic fauna of the Franz Josef Land archipelago. Polar Biology, 32(2), 169-180. https://doi.org/10.1007/s00300-008-0516-y

26. Degen, R., Vedenin, A., Gusky, M., Boetius, A., Brey, T. (2014): Macrobenthic abundance, biomass, productivity and production during POLARSTERN cruise ARK-VIII/3. PANGAEA, https://doi.org/10.1594/PANGAEA.828340.
27. Degen, R., Vedenin, A., Gusky, M., Boetius, A., & Brey, T. (2015). Patterns and trends of macrobenthic abundance, biomass and production in the deep Arctic Ocean. Polar Research, 34(1), 24008. https://doi.org/10.3402/polar.v34.24008
28. Denisenko, S. G., Denisenko, N. V., Lehtonen, K. K., Andersin, A. B., & Laine, A. O. (2003). Macrozoobenthos of the Pechora Sea (SE Barents Sea): community structure and spatial distribution in relation to environmental conditions. Marine Ecology Progress Series, 258, 109-123. https://doi.org/10.3354/meps258109
29. Deubel, H. (2000). Struktureigenschaften und Nahrungsbedarf der Zoobenthosgemeinschaften im Bereich des Lomonossowrückens im Arktischen Ozean. Berichte zur Polarforschung (Reports on Polar Research), 370.
30. Deubel H., Engel M., Fetzer I., Gagaev S., Hirche H.J., Klages M., Larionov V., Lubin P., Lubina O., Nothig E.M., Okolodkov Y., Rachor E. (2003) The southern Kara Sea ecosystem: Phytoplankton, zooplankton and benthos communities influenced by river run-off. In: Ruediger S. (ed.) Siberian River Runoff in the Kara Sea: characterization, quantification variability and environmental significance. Proceedings in Marine Science, 6, Elsevier, Amsterdam, pp 237–275.
31. Dunbar, M.J. (1968). Ecological development in polar regions. A study in evolution. Englewood Cliffs, N. J., Prentice Hall, VIII, 119 p.
32. Eleftheriou, A., McIntyre, A. (2005). Methods for the study of marine benthos. Blackwell Science, Oxford, UK, 418 p.
33. Filatova, Z. A., Zenkevich, L. A. (1957). The quantitative distribution of the bottom fauna of the Kara Sea. Trudy Vsesoyuznogo Gidrobiologicheskogo Obshchestva, 8, 3-67. [In Russian]
34. Flach, E., & de Bruin, W. (1999). Diversity patterns in macrobenthos across a continental slope in the NE Atlantic. Journal of Sea Research, 42(4), 303-323. https://doi.org/10.1016/S1385-1101(99)00034-9
35. Flint, M. V., Poyarkov, S. G., Rimskii-Korsakov, N. A., Miroshnikov, A. Y. (2019). Ecosystems of the Siberian Arctic Seas 2018 (Cruise 72 of the R/V Akademik Mstislav Keldysh). Oceanology, 59(3), 460-463. https://doi.org/10.1134/S0001437019030056
36. Fredriksen, R., Christiansen, J. S., Bonsdorff, E., Larsen, L. H., Nordström, M. C., Zhulay, I., & Bluhm, B. A. (2020). Epibenthic megafauna communities in Northeast Greenland vary across coastal, continental shelf and slope habitats. Polar Biology, 43(10), 1623-1642. https://doi.org/10.1007/s00300-020-02733-z
37. Fütterer, D. (1993). The expedition ARCTIC'93: Leg ARK-IX/4 of RV "Polarstern" 1993. Reports for Polar Research, 149.
38. Fütterer, D., Galimov, E.M. (2003). Siberian river run-off into the Kara Sea: Characterization, quantification, variability and environmental significance – An introduction. In: Stein R., Fahl K., Fütterer, D., Stepanets O. (Eds.) Siberian river run-off in the Kara Sea. Amsterdam: Elsevier Science B.V., pp. 1-9.
39. Gage J. (1986). The benthic fauna of the Rockall Trough: regional distribution and bathymetric zonation. Proceedings of Royal Society of Edinburgh, 88b: 159–174. https://doi.org/10.1017/S026972700000453X
40. Gage, J. D., Lamont, P. A., Kroeger, K., Paterson, G. L., & Vecino, J. L. G. (2000). Patterns in deep-sea macrobenthos at the continental margin: standing crop, diversity and faunal change on the continental slope off Scotland. In Island, Ocean and Deep-Sea Biology (pp. 261-271). Springer, Dordrecht.
41. Galkin, S. V., & Vedenin, A. A. (2015). Macrobenthos of Yenisei Bay and the adjacent Kara Sea shelf. Oceanology, 55(4), 606-613. https://doi.org/10.1134/S0001437015040086
42. Gebruk, A. V., Budaeva, N. E., & King, N. J. (2010). Bathyal benthic fauna of the Mid-Atlantic Ridge between the Azores and the Reykjanes Ridge. Journal of the Marine Biological Association of the United Kingdom, 90(1), 1-14. https://doi.org/10.1017/S0025315409991111
43. Gerdes, D. (1990). Antarctic trials with the multibox corer, a new device for benthos sampling. Polar Records, 26, 35–38.
44. Golikov, A. N., Dolgolenko, M. A., Maximovich, N. V., & Scarlato, O. A. (1990). Theoretical approaches to marine biogeography. Marine Ecology Progress Series., 63(2), 289-301.
45. Gorbunov G.P. (1946). Bottom life of the Novosiberian shoalwaters and the central part of the Arctic Ocean. In: Gorbunov G.P., Uschakov P.V. (Eds.) Proceedings of the drifting expedition of Glavsevmorput on ice-breaker "G. Sedov" in 1937-1940. Glavsevmorput, Moscow-Leningrad, pp. 30-138. [In Russian]
46. Górska, B., Soltwedel, T., Schewe, I., Włodarska-Kowalczuk, M., 2020. Bathymetric trends in biomass size spectra, carbon demand, and production of Arctic benthos (76-5561 m, Fram Strait). Progress in Oceanography 102370. https://doi.org/10.1016/j.pocean.2020.102370
47. Grassle, J. F., & Morse-Porteous, L. S. (1987). Macrofaunal colonization of disturbed deep-sea environments and the structure of deep-sea benthic communities. Deep-Sea Research Part A. Oceanographic Research Papers, 34(12), 1911-1950. https://doi.org/10.1016/0198-0149(87)90091-4
48. Grebmeier, J. M., Cooper, L. W., Feder, H. M., Sirenko, B. I. (2006). Ecosystem dynamics of the Pacific-influenced Northern Bering and Chukchi Seas in the Amerasian Arctic. Progress in Oceanography, 71, 331–361. http://dx.doi.org/10.1016/j.pocean.2006.10.001
49. Grebmeier, J. M., Bluhm, B. A., Cooper, L. W., Denisenko, S. G., Iken, K., Kędra, M., & Serratos, C. (2015). Time-series benthic community composition and biomass and associated environmental characteristics in the Chukchi Sea during the RUSALCA 2004–2012 Program. Oceanography, 28(3), 116-133. http://dx.doi.org/10.5670/oceanog.2015.61

50. Hammer, Ø., Harper, D.A.T., Ryan, P.D. (2001). PAST: Paleontological Statistics Software Package for Education and Data Analysis. Palaeontologia Electronica, 4(1), 9pp., 178kb. http://palaeo-electronica.org/2001_1/past/issue1_01.htm.
51. Hay, W. W. (2016). "Continental slope," in Encyclopedia of Marine Geosciences, eds J. Harff, M. Meschede, S. Petersen, and J. Thiede (Berlin: Springer). https://doi.org/10.1007/978-94-007-6644-0_156-3
52. Hedgpeth, J. W. (1957). Marine biogeography. Treatise on marine ecology and paleoecology, 1, 359-382.
53. Hessler, R. R., & Jumars, P. A. (1974). Abyssal community analysis from replicate box cores in the central North Pacific. Deep-Sea Research, 21(18), 209. https://doi.org/10.1016/0011-7471(74)90058-8
54. Høisæter, T. (2010). The shell-bearing, benthic gastropods on the southern part of the continental slope off Norway. Journal of Molluscan Studies, 76(3), 234-244. https://doi.org/10.1093/mollus/eyq003
55. Horn, H. S. (1966). Measurement of "overlap" in comparative ecological studies. The American Naturalist, 100(914), 419-424.
56. Howell K. L., Billett D. S. M., Tyler P. A. (2002). Depth-related distribution and abundance of seastars (Echinodermata: Asteroidea) in the Porcupine Seabight and Porcupine Abyssal Plain, N.E. Atlantic. Deep-Sea Research. Part I, 49: 1901–1920. https://doi.org/10.1016/S0967-0637(02)00090-0
57. Hurlbert, S.H., (1971). The nonconcept of species diversity: a critique and alternative parameters. Ecology 52 (4), 577–586. https://doi.org/10.2307/1934145
58. Jakobsson, M., Mayer, L., Coakley, B., Dowdeswell, J. A., Forbes, S., Fridman, B., et al. (2012). The international bathymetric chart of the Arctic Ocean (IBCAO) version 3.0. Geophysical Research Letters, 39, L12609. https://doi.org/10.1029/2012GL052219
59. Jansen, E., Christensen, J. H., Dokken, T., Nisancioglu, K. H., Vinther, B. M., Capron, E., ... & Stendel, M. (2020). Past perspectives on the present era of abrupt Arctic climate change. Nature Climate Change, 10(8), 714-721. https://doi.org/10.1038/s41558-020-0860-7
60. Jørgensen, L. L., Pearson, T. H., Anisimova, N. A., Gulliksen, B., Dahle, S., Denisenko, S. G., & Matishov, G. G. (1999). Environmental influences on benthic fauna associations of the Kara Sea (Arctic Russia). Polar Biology, 22(6), 395-416. https://doi.org/10.1007/s003000050435
61. Käß, M., Vedenin, A., Hasemann, C., Brandt, A., & Soltwedel, T. (2019). Community structure of macrofauna in the deep Fram Strait: A comparison between two bathymetric gradients in ice-covered and ice-free areas. Deep-Sea Research Part I: Oceanographic Research Papers, 152, 103102. https://doi.org/10.1016/j.dsr.2019.103102
62. Kędra, M., Renaud, P. E., Andrade, H., Goszczko, I., & Ambrose, W. G. (2013). Benthic community structure, diversity, and productivity in the shallow Barents Sea bank (Svalbard Bank). Marine Biology, 160(4), 805-819. https://doi.org/10.1007/s00227-012-2135-y
63. Kędra, M., Moritz, C., Choy, E. S., David, C., Degen, R., Duerksen, S., ... & Węsławski, J. M. (2015). Status and trends in the structure of Arctic benthic food webs. Polar Research, 34(1), 23775. https://doi.org/10.3402/polar.v34.23775
64. Klages, M., Boetius, A., Christensen, J. P., Deubel, H., Piepenburg, D., Schewe, I., & Soltwedel, T. (2004). The benthos of Arctic seas and its role for the organic carbon cycle at the seafloor. In: The organic carbon cycle in the Arctic Ocean (pp. 139-167). Springer, Berlin, Heidelberg.
65. Krayushkina, A. B. (2000). Geography of the asteroids and holothurians of the Norwegian Sea. Benthos of the Russian Seas and the Northern Atlantic. Moscow: VNIRO Publishing House, 41. [In Russian]
66. Krijgsman, W., Hilgen, F. J., Raffi, I., Sierro, F. J., & Wilson, D. S. (1999). Chronology, causes and progression of the Messinian salinity crisis. Nature, 400(6745), 652-655. https://doi.org/10.1038/23231
67. Kröncke, I. (1994). Macrobenthos composition, abundance and biomass in the Arctic Ocean along a transect between Svalbard and the Makarov Basin. Polar Biology, 14(8), 519-529. https://doi.org/10.1007/BF00238221
68. Kröncke, I. (1998). Macrofauna communities in the Amundsen Basin, at the Morris Jesup Rise and at the Yermak Plateau (Eurasian Arctic Ocean). Polar Biology, 19(6), 383-392. https://doi.org/10.1007/s003000050263
69. Lisitsyn, A.P., Udintsev, G.B. (1955). A new model of a bottom grab. Trudy Vsesoyuznogo Gidrobiologicheskogo Obshchestva, 6, 217–222. [In Russian]
70. MacDonald, I. R., Bluhm, B. A., Iken, K., Gagaev, S., & Strong, S. (2010). Benthic macrofauna and megafauna assemblages in the Arctic deep-sea Canada Basin. Deep-Sea Research Part II: Topical Studies in Oceanography, 57(1-2), 136-152. https://doi.org/10.1016/j.dsr2.2009.08.012
71. Magurran, A. E. (2004). Measuring biological diversity. MA, USA: Blackwell Science Ltd.
72. Marshall, E. (2019). Kruskal-Wallis in SPSS. Community project encouraging academics to share statistics support resources. Available at: https://www.studocu.com/row/document/bahcesehir-ueniversitesi/managerial-skills-and-strategic-management/lecture-notes/kruskal-wallis-test-manual/6221473/view.
73. McCune, B., Grace, J.B., Urban, D.L. (2002). Analysis of ecological communities. Mjm software design. Oregon: Gleneden Beach, 28.
74. Meltofte, H., Barry, T., Berteaux, D., Bültmann, H., Christiansen, J. S., Cook, J. A., Dahlberg, A., Daniëls, F., Ehrich, D., Fjeldså, J., Friðriksson, F., Ganter, B., Gaston A.J., Gillespie, L.J., Grenoble, L., Hoberg, E.P., Kodkinson, I.D., Huntington, H.P., Ims, R.A., Josefson, A.B., Kutz, S.J., Kuzmin, S.L., Laidre K.L., Lassuy, D.R., Lewis, P.N., Lovejoy, C., Michel, C., Mokievsky, V., Mustonen, T., Payer, D.C., Poulin, M., Reid, D.G., Reist, J.D., Tessler, D.F., Wrona, F.J. (2013). Arctic Biodiversity Assesment. Synthesis. Conservation of Arctic Flora and Fauna (CAFF).
75. Menzies, R.J. (1963). The abyssal fauna of the sea floor of the Arctic Ocean. Proceedings of Arctic Symposium, Arctic Institute of North America, Hershey, Penn., pp. 46-66.

76. Menzies, R. J. (1973). Biological history of the Mediterranean Sea with reference to the abyssal benthos. Rapports de la Commission Internationale pour l'Exploration Scientifique de la Mer Méditerranée, 1, 717-723.
77. Meredith, M., Sommerkorn, M., Cassotta, S., Derksen, C., Ekaykin, A., Hollowed, A., & Kofinas, G. (2019). Polar Regions: IPCC Special Report on the Ocean and Cryosphere in a Changing Climate. IPCC. https://www.ipcc.ch/srocc/#home-chapter-3.
78. Mironov, A. N. (1986). Vertical zonation of the sea urchins. Zoological Journal, 65(9): 1341-1349. [In Russian]
79. Mironov, A. N. (2013). Biotic complexes of the Arctic Ocean. Invertebrate Zoology, 10(1), 3-48.
80. Nesis, K. N. (2001). West-Arctic and East-Arctic distributional ranges of cephalopods. Sarsia, 86(1), 1-11. https://doi.org/10.1080/00364827.2001.10420456
81. Nilsen, R., & Holthe, T. (1985). Arctic and Scandinavian Oweniidae (Polychaeta) with a description of *Myriochele fragilis* sp. n., and comments on the phylogeny of the family. Sarsia, 70(1), 17-32. https://doi.org/10.1080/00364827.1985.10420615
82. Oleszczuk, B., Grzelak, K., Kędra, M. (2021). Community structure and productivity of Arctic benthic fauna across depth gradients during springtime. Deep-Sea Research Part I: Oceanographic Research Papers 170: 103457. https://doi.org/10.1016/j.dsr.2020.103457
83. Oug, E., Bakken, T., Kongsrud, J. A., Alvestad, T. (2017). Polychaetous annelids in the deep Nordic Seas: Strong bathymetric gradients, low diversity and underdeveloped taxonomy. Deep Sea Research Part II: Topical Studies in Oceanography, 137, 102-112. https://doi.org/10.1016/j.dsr2.2016.06.016
84. Parapar, J. (2006). The genera *Myriochele* and *Myrioglobula* (Polychaeta, Oweniidae) in Icelandic waters with the revision of type material of *Myriochele heeri* Malmgren, 1867, and the description of a new species. Journal of Natural History, 40(9-10), 523-547. https://doi.org/10.1080/00222930600711758
85. Paul, A. Z., & Menzies, R. J. (1974). Benthic ecology of the high Arctic deep sea. Marine Biology, 27(3), 251-262. https://doi.org/10.1007/BF00391950
86. Petryashov, V. V., Golikov, A. A., Schmid, M., Rachor, E. (2004). Macrobenthos of the Laptev Sea shelf. Explorations of the fauna of the seas, 54(63), 9-27. [In Russian]
87. Pielou, E.C., (1966). The measurement of diversity in different types of biological collections. J. Theor. Biol. 13, 131–144. https://doi.org/10.1016/0022-5193(66)90013-0.
88. Piepenburg, D., Chernova, N. V., Von Dorrien, C. F., Gutt, J., Neyelov, A. V., Rachor, E., ... & Schmid, M. K. (1996). Megabenthic communities in the waters around Svalbard. Polar Biology, 16(6), 431-446. https://doi.org/10.1007/s003000050074
89. Piepenburg, D., Archambault, P., Ambrose, W. G., Blanchard, A. L., Bluhm, B. A., Carroll, M. L., ... & Włodarska-Kowalczuk, M. (2011). Towards a pan-Arctic inventory of the species diversity of the macro-and megabenthic fauna of the Arctic shelf seas. Marine Biodiversity, 41(1), 51-70.
90. Pisareva, M. N., Pickart, R. S., Spall, M. A., Nobre, C., Torres, D. J., Moore, G. W. K., & Whitledge, T. E. (2015). Flow of Pacific water in the western Chukchi Sea: Results from the 2009 RUSALCA expedition. Deep Sea Research Part I: Oceanographic Research Papers, 105, 53-73. https://doi.org/10.1016/j.dsr.2015.08.011
91. Rand, K., Logerwell, E., Bluhm, B., Chenelot, H., Danielson, S., Iken, K., & Sousa, L. (2018). Using biological traits and environmental variables to characterize two Arctic epibenthic invertebrate communities in and adjacent to Barrow Canyon. Deep Sea Research Part II: Topical Studies in Oceanography, 152, 154-169. https://doi.org/10.1016/j.dsr2.2017.07.015
92. Ravelo, A. M., Bluhm, B. A., Foster, N., & Iken, K. (2020). Biogeography of epibenthic assemblages in the central Beaufort Sea. Marine Biodiversity, 50(1), 1-19. https://doi.org/10.1007/s12526-019-01036-9
93. Renaud P.E., Carroll M.L., Ambrose W.G., Jr. Duarte C.M. (2008). Effects of global warming on Arctic sea-floor communities and its consequences for higher trophic levels. Impacts of global warming on polar ecosystems. Bilbao: Fundación BBVA. pp. 139–175.
94. Rex, M. A. (1981). Community structure in the deep-sea benthos. Annual Review of Ecology and Systematics, 12(1), 331-353. https://doi.org/10.1146/annurev.es.12.110181.001555
95. Rex, M. A., & Etter, R. J. (2010). Deep-sea biodiversity: pattern and scale. Harvard University Press.
96. Rowe, G. T. (1971). Benthic biomass in the Pisco, Peru upwelling. Investigacion Pesquera, 35(1), 127-135.
97. Rybakova, E., Kremenetskaia, A., Vedenin, A., Boetius, A., & Gebruk, A. (2019). Deep-sea megabenthos communities of the Eurasian Central Arctic are influenced by ice-cover and sea-ice algal falls. PloS one, 14(7), e0211009. https://doi.org/10.1371/journal.pone.0211009
98. Schlitzer, R. (2020). Ocean Data View. https://odv.awi.de/.
99. Schonberg, S. V., Clarke, J. T., & Dunton, K. H. (2014). Distribution, abundance, biomass and diversity of benthic infauna in the Northeast Chukchi Sea, Alaska: Relation to environmental variables and marine mammals. Deep-Sea Research Part II: Topical Studies in Oceanography, 102, 144-163. https://doi.org/10.1016/j.dsr2.2013.11.004
100. Shannon, C., Weaver, W., (1963). The Measurement Theory of Communication. University of Illinois Press, Urbana, IL.
101. Sirenko, B. I. (1998). Marine fauna of the Arctic (after the expeditions of the Zoological Institute, Russian Academy of Sciences). Russian Journal of Marine Biology, 24(6), 353-364. [In Russian]
102. Sirenko, B., Denisenko, S., Deubel, H., & Rachor, E. (2004). Deep water communities of the Laptev Sea and adjacent parts of the Arctic Ocean. Fauna and the ecosystems of the Laptev Sea and adjacent deep waters of the Arctic Ocean. Explorations of the fauna of sea. St. Petersburg: Zoological Institute of Russian Academy of Sciences, 54(62), 28-73.

103. Sirenko B.I., Denisenko S.G. (2010). Fauna of the East-Siberian Sea, distribution patterns and structure of bottom communities. Explorations of the fauna of the Seas, 66. Zoological Institute RAS, Saint-Petersburg, pp. 248 [In Russian]
104. Soltwedel, T., Jaeckisch, N., Ritter, N., Hasemann, C., Bergmann, M., & Klages, M. (2009). Bathymetric patterns of megafaunal assemblages from the arctic deep-sea observatory HAUSGARTEN. Deep-Sea Research Part I: Oceanographic Research Papers, 56(10), 1856-1872. https://doi.org/10.1016/j.dsr.2009.05.012
105. Sswat, M., Gulliksen, B., Menn, I., Sweetman, A. K., & Piepenburg, D. (2015). Distribution and composition of the epibenthic megafauna north of Svalbard (Arctic). Polar Biology, 38(6), 861-877. https://doi.org/10.1007/s00300-015-1645-8
106. Svavarsson J., Brattegard T. and Strömberg J.-O. (1990). Distribution and diversity pattern of asellote isopods (Crustacea) in the deep Norwegian and Greenland Seas. Progress in Oceanography, 24: 297-310. https://doi.org/10.1016/0079-6611(90)90039-5
107. Thistle, D. (2003). The deep-sea floor: an overview. In: Tyler, P. (ed.) Ecosystems of the deep oceans. Elsevier, Amsterdam, pp. 5-37
108. Thomson, D. H. (1982). Marine benthos in the eastern Canadian High Arctic: multivariate analyses of standing crop and community structure. Arctic, 61-74.
109. Tselepides, A., & Eleftheriou, A. (1992). South Aegean (Eastern Mediterranean) Continental Slope Benthos: Macroinfaunal—Environmental Relationships. In Deep-sea food chains and the global carbon cycle (pp. 139-156). Springer, Dordrecht. https://doi.org/10.1007/978-94-011-2452-2_9
110. Tselepides, A., Papadopoulou, K. N., Podaras, D., Plaiti, W., & Koutsoubas, D. (2000). Macrobenthic community structure over the continental margin of Crete (South Aegean Sea, NE Mediterranean). Progress in Oceanography, 46(2-4), 401-428. https://doi.org/10.1016/S0079-6611(00)00027-6
111. Udalov, A., Chikina, M., Azovsky, A., Basin, A., Galkin, S., Garlitska, L., ... & Mokievsky, V. (2020). Integrity of benthic assemblages along the arctic estuarine-coastal system. Ecological Indicators, 107115. https://doi.org/10.1016/j.ecolind.2020.107115
112. Vedenin, A. A., Galkin, S. V., & Kozlovskiy, V. V. (2015). Macrobenthos of the Ob Bay and adjacent Kara Sea shelf. Polar Biology, 38(6), 829-844. https://doi.org/10.1007/s00300-014-1642-3
113. Vedenin, A., Budaeva, N., Mokievsky, V., Pantke, C., Soltwedel, T., & Gebruk, A. (2016). Spatial distribution patterns in macrobenthos along a latitudinal transect at the deep-sea observatory HAUSGARTEN. Deep-Sea Research Part I: Oceanographic Research Papers, 114, 90-98. https://doi.org/10.1016/j.dsr.2016.04.015
114. Vedenin, A., Gusky, M., Gebruk, A., Kremenetskaia, A., Rybakova, E., & Boetius, A. (2018). Spatial distribution of benthic macrofauna in the Central Arctic Ocean. PloS one, 13(10), e0200121. https://doi.org/10.1371/journal.pone.0200121
115. Vedenin, A. A., Kokarev, V. N., Chikina, M. V., Basin, A. B., Galkin, S. V., & Gebruk, A. V. (2020). Fauna associated with shallow-water methane seeps in the Laptev Sea. PeerJ, 8, e9018. https://doi.org/10.7717/peerj.9018
116. Vedenin, A., Galkin, S., Mironov, A. N., & Gebruk, A. (2021). Vertical zonation of the Siberian Arctic benthos: bathymetric boundaries from coastal shoals to deep-sea Central Arctic. PeerJ, 9, e11640. https://doi.org/10.7717/peerj.11640
117. Vermeij G.J. 1991. Anatomy of an invasion: the trans-Arctic interchange. Paleobiology 17:281-307.
118. Vinogradova N.G., (1962). Vertical zonation in the distribution of deep-sea benthic fauna in the ocean. Deep-Sea Research, 8: 245-250. https://doi.org/10.1016/0146-6313(61)90025-9
119. Wassmann, P., Duarte, C. M., Agusti, S., & Sejr, M. K. (2011). Footprints of climate change in the Arctic marine ecosystem. Global Change Biology, 17(2), 1235-1249. https://doi.org/10.1111/j.1365-2486.2010.02311.x
120. Wassmann, P., Kosobokova, K. N., Slagstad, D., Drinkwater, K. F., Hopcroft, R. R., Moore, S. E., ... & Berge, J. (2015). The contiguous domains of Arctic Ocean advection: trails of life and death. Progress in Oceanography, 139, 42-65. https://doi.org/10.1016/j.pocean.2015.06.011
121. Wassmann, P. F., Slagstad, D., & Ellingsen, I. (2019). Advection of mesozooplankton into the northern Svalbard shelf region. Frontiers in Marine Science, 6, 458. https://doi.org/10.3389/fmars.2019.00458
122. Watling, L., Guinotte, J., Clark, M. R., & Smith, C. R. (2013). A proposed biogeography of the deep ocean floor. Progress in Oceanography, 111, 91-112. https://doi.org/10.1016/j.pocean.2012.11.003
123. Weber J.R. (1989). Physiography and bathymetry of the Arctic Ocean seafloor. In: Herman Y. (ed.). The Arctic Seas. Clymatology, Oceanography, Geology, and Biology. New York: Van Nostrand Reinhold Company, pp. 797-828
124. Wei, C. L., Rowe, G. T., Escobar-Briones, E., Boetius, A., Soltwedel, T., Caley, M. J., ... & Narayanaswamy, B. E. (2010 a). Global patterns and predictions of seafloor biomass using random forests. PloS one, 5(12), e15323. https://doi.org/10.1371/journal.pone.0015323
125. Wei, C. L., Rowe, G. T., Hubbard, G. F., Scheltema, A. H., Wilson, G. D., Petrescu, I., ... & Wang, Y. (2010 b). Bathymetric zonation of deep-sea macrofauna in relation to export of surface phytoplankton production. Marine Ecology Progress Series, 399, 1-14. https://doi.org/10.3354/meps08388
126. Williams, W. J., & Carmack, E. C. (2015). The 'interior'shelves of the Arctic Ocean: Physical oceanographic setting, climatology and effects of sea-ice retreat on cross-shelf exchange. Progress in Oceanography, 139, 24-41. http://doi.org/10.1016/j.pocean.2015.07.008
127. Wlodarska-Kowalczuk, M., Kendall, M. A., Weslawski, J. M., Klages, M., & Soltwedel, T. (2004). Depth gradients of benthic standing stock and diversity on the continental margin at a high-latitude ice-free site (off Spitsbergen, 79 N). Deep-Sea Research Part I: Oceanographic Research Papers, 51(12), 1903-1914. https://doi.org/10.1016/j.dsr.2004.07.013

128. Zhulay, I., Iken, K., Renaud, P. E., & Bluhm, B. A. (2019). Epifaunal communities across marine landscapes of the deep Chukchi Borderland (Pacific Arctic). Deep-Sea Research Part I: Oceanographic Research Papers, 151, 103065. https://doi.org/10.1016/j.dsr.2019.06.011

Supplementary captions

Supplementary 1. Station data used in this study with the information about expedition names, geographic regions, dates, station names, latitude, longitude, depths and sampling gears.

Supplementary 2. Python 3.8 script for calculating Hill numbers, the Morisita-Horn and quantitative Sørensen similarity indices.

Supplementary 3. The values of abundance, biomass, number of species, Pielou's evenness, ES-100 and Shannon index for each station.

Supplementary 4. List of individual taxa abundances per station for quantitative samples.

Supplementary 5. Non-metric multidimensional scaling based on Bray-Curtis similarity index and dendrogram plots based on Morisita-Horn and quantitative Sørensen similarity indices for quantitative and semi-quantitative samples.

Supplementary 6. List of individual taxa abundances per station for semi-quantitative samples.

Vedenin_etal_Arctic slope benthos_acc MS - Supplementary

Table S1

Expedition	Region	Date	Event	Station	Latitude	Longitude	Depth (m)	Gear	Sampling area (m^2)
ARK VIII	Yermak Plateau	30.09.1991	PS2213-2	1991-2213	80.4710	8.1817	888	USNEL Box-corer	0.2500
ARK VIII	Yermak Plateau	01.10.1991	PS2214-2	1991-2214	80.2742	6.6102	560	USNEL Box-corer	0.2500
ARK IX/4	Barents Sea	14.08.1993	PS2242	1993-14	81.7050	30.3300	2915	Multibox-corer	0.1380
ARK IX/4	Barents Sea	16.08.1993	PS2444	1993-17	82.4870	37.7400	2566	USNEL Box-corer	0.0690
ARK IX/4	Barents Sea	18.08.1993	PS2445	1993-19	82.7630	40.2430	2993	Multibox-corer	0.0690
ARK IX/4	Barents Sea	19.08.1993	PS2446	1993-20	82.4000	40.8930	2027	Multibox-corer	0.0230
ARK IX/4	Barents Sea	21.08.1993	PS2447	1993-24	82.1600	42.0450	1021	Multibox-corer	0.0460
ARK IX/4	Barents Sea	21.08.1993	PS2448	1993-25	82.1230	42.5380	534	Multibox-corer	0.1150
ARK IX/4	Barents Sea	21.08.1993	PS2449	1993-27	82.0230	43.5770	286	Multibox-corer	0.1150
ARK IX/4	Laptev Sea	02.09.1993	PS2454	1993-32	78.7100	132.2920	2962	Multibox-corer	0.1150
ARK IX/4	Laptev Sea	04.09.1993	PS2457	1993-35	78.3920	133.1600	2151	Multibox-corer	0.2990
ARK IX/4	Laptev Sea	05.09.1993	PS2458	1993-38	78.1670	133.3950	981	Multibox-corer	0.1380
ARK IX/4	Laptev Sea	05.09.1993	PS2459	1993-39	78.0980	133.5130	517	Multibox-corer	0.1380
ARK IX/4	Laptev Sea	06.09.1993	PS2460	1993-40	78.0720	133.6080	191	Multibox-corer	0.0690
ARK IX/4	Laptev Sea	06.09.1993	PS2461	1993-41	77.9100	133.5550	73	USNEL Box-corer	0.0460
ARK IX/4	Laptev Sea	07.09.1993	PS2463	1993-44	77.0300	126.4130	92	USNEL Box-corer	0.0460
ARK IX/4	Laptev Sea	09.09.1993	PS2465	1993-47	77.1830	126.2230	1026	USNEL Box-corer	0.0460
ARK IX/4	Laptev Sea	09.09.1993	PS2466	1993-48	77.1350	126.3530	552	Multibox-corer	0.1150
ARK IX/4	Laptev Sea	09.09.1993	PS2467	1993-49	77.0830	126.2230	284	Multibox-corer	0.1150
ARK IX/4	Laptev Sea	10.09.1993	PS2468	1993-50	77.6930	125.8930	1991	Multibox-corer	0.0910
ARK IX/4	Laptev Sea	12.09.1993	PS2470	1993-53	79.2283	122.8617	3234	Multibox-corer	0.3220
ARK IX/4	Laptev Sea	13.09.1993	PS2471	1993-54	79.1658	119.8205	3054	Multibox-corer	0.0690
ARK IX/4	Laptev Sea	18.09.1993	PS2477	1993-64	77.2470	118.5530	193	USNEL Box-corer	0.1610
ARK IX/4	Laptev Sea	20.09.1993	PS2481	1993-68	78.4730	110.7880	101	Multibox-corer	0.1610
ARK IX/4	Laptev Sea	21.09.1993	PS2482	1993-69	78.7020	112.5120	577	Multibox-corer	0.1380
ARK IX/4	Laptev Sea	21.09.1993	PS2483	1993-70	78.7620	112.7030	1216	USNEL Box-corer	0.3450
ARK IX/4	Laptev Sea	22.09.1993	PS2484	1993-71	78.5820	111.3870	235	Multibox-corer	0.1380
ARK XI/1	Kara Sea	09.09.1995	PS2785	1995-89	82.3383	92.7717	2644	USNEL Box-corer	0.5000
ARK XI/1	Kara Sea	09.09.1995	PS2786	1995-90	82.1408	91.3508	1771	USNEL Box-corer	0.5000
ARK XI/1	Kara Sea	10.09.1995	PS2787	1995-91	82.0763	91.0213	1117	USNEL Box-corer	0.5000
ARK XI/1	Kara Sea	10.09.1995	PS2788	1995-92	82.0375	90.9658	535	USNEL Box-corer	0.5000
ARK XI/1	Kara Sea	10.09.1995	PS2789	1995-93	81.9608	91.0767	239	USNEL Box-corer	0.5000
ARK XI/1	Kara Sea	10.09.1995	PS2790	1995-94	81.8105	90.7780	88	USNEL Box-corer	0.5000
ARK XI/1	Kara Sea	11.09.1995	PS2791	1995-95	81.4883	87.4883	315	USNEL Box-corer	0.5000
ARK XI/1	Kara Sea	11.09.1995	PS2792	1995-96	79.9842	86.9842	248	USNEL Box-corer	0.5000
ARK XIII/2	Barents Sea	04.07.1997	PS2830	1997-2830	80.9757	17.4945	517	USNEL Box-corer	0.2500
ARK XIII/2	Barents Sea	04.07.1997	PS2831	1997-2831	81.0943	16.9660	942	USNEL Box-corer	0.2500
ARK XIII/2	Barents Sea	05.07.1997	PS2823	1997-2832	81.1117	16.2183	2065	USNEL Box-corer	0.2500
ARK XIII/2	Yermak Plateau	06.07.1997	PS2833	1997-2833	80.9717	11.8333	1964	USNEL Box-corer	0.2500
ARK XIII/2	Yermak Plateau	08.07.1997	PS2834	1997-2834	80.9150	9.8233	1001	USNEL Box-corer	0.2500
ARK XIII/2	Yermak Plateau	10.07.1997	PS2835	1997-2835	81.1017	7.0667	847	USNEL Box-corer	0.2500
ARK XIII/2	Yermak Plateau	11.07.1997	PS2836	1997-2836	81.1310	5.6477	657	USNEL Box-corer	0.2500
ARK XIII/2	Yermak Plateau	12.07.1997	PS2837	1997-2837	81.2332	2.4178	1028	USNEL Box-corer	0.2500
ARK XIII/2	Yermak Plateau	13.07.1997	PS2838	1997-2838	81.2943	0.4433	2325	USNEL Box-corer	0.2500
ARK XIII/2	Yermak Plateau	14.07.1997	PS2839	1997-2839	81.4033	-0.9717	2926	USNEL Box-corer	0.2500
ARK XIII/2	Greenland Sea	15.07.1997	PS2840	1997-2840	81.4217	-5.3083	3524	USNEL Box-corer	0.2500
ARK XIII/2	Greenland Sea	17.07.1997	PS2843	1997-2843	81.5670	-7.3495	2526	USNEL Box-corer	0.2500
ARK XIII/2	Central Arctic	18.07.1997	PS2847	1997-2847	81.8717	-4.5383	4130	USNEL Box-corer	0.2500
ARK XIII/2	Central Arctic	21.07.1997	PS2849	1997-2849	82.6517	1.4967	3247	USNEL Box-corer	0.2500
ARK XIII/2	Central Arctic	23.07.1997	PS2851	1997-2851	82.3750	3.6150	2927	USNEL Box-corer	0.2500
ARK XIII/2	Central Arctic	24.07.1997	PS2853	1997-2853	82.3183	3.7083	2008	USNEL Box-corer	0.2500
ARK XIII/2	Central Arctic	25.07.1997	PS2854	1997-2854	82.2003	3.9015	1805	USNEL Box-corer	0.2500
ARK XIII/2	Yermak Plateau	26.07.1997	PS2855	1997-2855	82.0453	5.2848	1454	USNEL Box-corer	0.2500
ARK XIII/2	Yermak Plateau	29.07.1997	PS2859	1997-2859	81.7517	10.1900	1180	USNEL Box-corer	0.2500
ARK XIII/2	Yermak Plateau	30.07.1997	PS2860	1997-2860	81.5813	11.8523	2032	USNEL Box-corer	0.2500
ARK XIII/2	Yermak Plateau	31.07.1997	PS2861	1997-2861	81.2725	13.0503	2309	USNEL Box-corer	0.2500
ARK XIII/2	Fram Strait	04.08.1997	PS2868	1997-2868	79.1083	3.0950	5416	USNEL Box-corer	0.2500
AMK-54	Kara Sea	30.09.2007	AMK-5003	2007-5003	75.4430	72.5155	60	Okean grab	0.3000
ARK XXVII/3	Central Arctic	10.08.2012	PS80/229	2012-229	83.9970	31.3180	4008	Multibox-corer	0.1610
ARK XXVII/3	Central Arctic	15.08.2012	PS80/241	2012-241	83.9320	76.7110	3432	Multibox-corer	0.1840
ARK XXVII/3	Central Arctic	21.08.2012	PS80/262	2012-262	82.9760	109.9190	3601	Multibox-corer	0.1380
ARK XXVII/3	Central Arctic	25.08.2012	PS80/278	2012-278	82.8830	129.9550	4167	Multibox-corer	0.1610
ARK XXVII/3	Central Arctic	04.09.2012	PS80/326	2012-326	81.9270	130.9170	4038	Multibox-corer	0.1840
ARK XXVII/3	Central Arctic	08.09.2012	PS80/339	2012-339	85.0570	122.7360	4352	Multibox-corer	0.1610
ARK XXVII/3	Central Arctic	19.09.2012	PS80/355	2012-355	87.9270	61.0120	4381	Multibox-corer	0.1840
ARK XXVII/3	Central Arctic	23.09.2012	PS80/368	2012-368	88.7870	56.3720	4374	Multibox-corer	0.1840
ARK-XXVII/2	Fram Strait	24.07.2012	PS80/0186-4	2012-N5	79.9405	3.1728	2513	USNEL Box-corer	0.1250
ARK-XXVII/2	Fram Strait	23.07.2012	PS80/0185-5	2012-N4	79.7393	4.5052	2668	USNEL Box-corer	0.1250
ARK-XXVII/2	Fram Strait	25.07.2012	PS80/0188-3	2012-N3	79.6043	5.1723	2742	USNEL Box-corer	0.1250
ARK-XXVII/2	Fram Strait	26.07.2012	PS80/0191-3	2012-N2	79.4100	4.6930	2506	USNEL Box-corer	0.1250
ARK-XXVII/2	Fram Strait	26.07.2012	PS80/0194-3	2012-N1	79.2835	4.3265	2364	USNEL Box-corer	0.1250
ARK-XXVII/2	Fram Strait	27.07.2012	PS80/0195-3	2012-HGIVa	79.0822	4.0983	2458	USNEL Box-corer	0.1250
ARK-XXVII/2	Fram Strait	16.07.2012	PS80/0165-9	2012-HGIV	79.0652	4.1788	2466	USNEL Box-corer	0.1250
ARK-XXVII/2	Fram Strait	19.07.2012	PS80/0174-1	2012-S1a	78.9335	4.9930	2609	USNEL Box-corer	0.1250
ARK-XXVII/2	Fram Strait	27.07.2012	PS80/0197-1	2012-S1	78.9180	5.0017	2594	USNEL Box-corer	0.1250
ARK-XXVII/2	Fram Strait	20.07.2012	PS80/0177-1	2012-S2	78.7805	5.3320	2470	USNEL Box-corer	0.1250
ARK-XXVII/2	Fram Strait	20.07.2012	PS80/0176-1	2012-S3	78.6100	5.0663	2340	USNEL Box-corer	0.1250
AMK-63	Laptev Sea	12.09.2015	AMK-5225	2015-5225	78.3750	130.6590	2390	Okean grab	0.7500
AMK-63	Laptev Sea	13.09.2015	AMK-5227	2015-5227	78.0910	130.5210	2020	Okean grab	0.7500
ARK-XXX	Fram Strait	02.08.2016	PS99/0051-8	2016-EG1	78.9900	-5.4300	995	USNEL Box-corer	0.2500
ARK-XXX	Fram Strait	01.07.2016	PS99/0050-3	2016-EGII	78.9300	-4.6400	1548	USNEL Box-corer	0.2500
ARK-XXX	Fram Strait	01.07.2016	PS99/0049-3	2016-EGIII	78.8500	-3.9600	1971	USNEL Box-corer	0.2500
ARK-XXX	Fram Strait	30.06.2016	PS99/0048-1	2016-EGIV	78.8200	-2.7300	2603	USNEL Box-corer	0.2500
ARK-XXX	Fram Strait	10.08.2016	PS99/0066-4	2016-HGI	79.1400	6.0800	1282	USNEL Box-corer	0.2500
ARK-XXX	Fram Strait	06.07.2016	PS99/0057-3	2016-HGII	79.1400	4.9100	1540	USNEL Box-corer	0.2500
ARK-XXX	Fram Strait	11.08.2016	PS99/0069-6	2016-HGIII	79.1100	4.6000	1887	USNEL Box-corer	0.2500
ARK-XXX	Fram Strait	27.06.2016	PS99/0042-1	2016-HGIV	79.0600	4.1800	2462	USNEL Box-corer	0.2500
2002–23	Beaufort Sea	16.08.2002	AG05	2002-AG05	70.5833	-122.9833	640	USNEL Box-corer	0.0400
2002–23	Beaufort Sea	18.08.2002	AL07	2002-AL07	71.7000	-134.7000	1570	USNEL Box-corer	0.0400
2002–23	Beaufort Sea	20.08.2002	AL10	2002-AL10	73.5000	-137.0000	3250	USNEL Box-corer	0.0800
2002–23	Beaufort Sea	05.09.2002	NA05	2002-NA05	75.9333	-155.6500	1350	USNEL Box-corer	0.1200
2002–23	Beaufort Sea	02.09.2002	NW01	2002-NW01	75.9667	-156.8167	800	USNEL Box-corer	0.0400
2002–23	Beaufort Sea	31.08.2002	NW05	2002-NW05	74.3333	-162.3167	1850	USNEL Box-corer	0.1200
HLY05-02	Beaufort Sea	28.06.2005	HLY0502-2	2005-2	72.3220	-155.7566	910	USNEL Box-corer	0.1800
HLY05-02	Beaufort Sea	01.07.2005	HLY0502-3	2005-3	72.3560	-155.3248	1840	USNEL Box-corer	0.1800
HLY05-02	Beaufort Sea	03.07.2005	HLY0502-4	2005-4	72.5481	-155.5493	1750	USNEL Box-corer	0.1800
HLY05-02	Beaufort Sea	06.07.2005	HLY0502-5	2005-5	73.3710	-153.4192	3900	USNEL Box-corer	0.1500
HLY05-02	Beaufort Sea	10.07.2005	HLY0502-7	2005-7	74.4253	-151.7138	3841	USNEL Box-corer	0.1800
HLY05-02	Beaufort Sea	11.07.2005	HLY0502-8	2005-8	74.5865	-151.9773	3845	USNEL Box-corer	0.1500
HLY05-02	Beaufort Sea	13.07.2005	HLY0502-9	2005-9	75.1698	-155.9039	3848	USNEL Box-corer	0.1500
HLY05-02	Beaufort Sea	16.07.2005	HLY0502-11	2005-11	76.0215	-160.6869	1370	USNEL Box-corer	0.1500
HLY05-02	Beaufort Sea	17.07.2005	HLY0502-12	2005-12	76.4280	-163.4817	937	USNEL Box-corer	0.1500
HLY05-02	Beaufort Sea	21.07.2005	HLY0502-13	2005-13	75.2680	-161.2250	2090	USNEL Box-corer	0.1500
HLY05-02	Beaufort Sea	24.07.2005	HLY0502-15	2005-15	73.0727	-157.1896	2620	USNEL Box-corer	0.1500

Table S1, continued

Expedition	Region	Date	Event	Station	Latitude	Longitude	Depth (m)	Gear	Sampling area (m^2)
ARK IX/4	Laptev Sea	1993	PS2468	1993-50	77.6900	125.9183	1992	Agassiz trawl	-
AMK-54	Kara Sea	2007	AMK-4983	2007-4983	76.9200	70.2700	555	Sigsbee trawl	-
AMK-54	Kara Sea	2007	AMK-4985	2007-4985	76.7833	70.6167	465	Sigsbee trawl	-
AMK-54	Kara Sea	2007	AMK-4987	2007-4987	76.6583	71.0483	275	Sigsbee trawl	-
AMK-54	Kara Sea	2007	AMK-4988	2007-4988	76.5883	71.2567	160	Sigsbee trawl	-
AMK-54	Kara Sea	2007	AMK-4990	2007-4990	76.1533	72.4967	110	Sigsbee trawl	-
AMK-54	Kara Sea	2007	AMK-4996	2007-4996	72.5718	73.7862	20	Sigsbee trawl	-
AMK-54	Kara Sea	2007	AMK-4999	2007-4999	72.9565	73.2947	27	Sigsbee trawl	-
AMK-54	Kara Sea	2007	AMK-5000	2007-5000	73.7530	72.9423	23	Sigsbee trawl	-
AMK-54	Kara Sea	2007	AMK-5003	2007-5003	75.4430	72.5155	60	Sigsbee trawl	-
AMK-59	Kara Sea	2011	AMK-5016	2011-5016	72.5503	80.3420	14	Sigsbee trawl	-
AMK-59	Kara Sea	2011	AMK-5019	2011-5019	73.1699	79.8608	25	Sigsbee trawl	-
AMK-59	Kara Sea	2011	AMK-5020	2011-5020	73.7176	79.3896	29	Sigsbee trawl	-
AMK-59	Kara Sea	2011	AMK-5010	2011-5010	74.2930	78.6251	33	Sigsbee trawl	-
AMK-59	Kara Sea	2011	AMK-5024	2011-5024	74.9486	77.9020	34	Sigsbee trawl	-
AMK-59	Kara Sea	2011	AMK-5026	2011-5026	75.9970	76.6741	63	Sigsbee trawl	-
AMK-59	Kara Sea	2011	AMK-5032	2011-5032	76.5498	80.7481	57	Sigsbee trawl	-
AMK-59	Kara Sea	2011	AMK-5033	2011-5033	77.2100	78.1277	120	Sigsbee trawl	-
AMK-59	Kara Sea	2011	AMK-5034	2011-5034	77.4263	77.5674	220	Sigsbee trawl	-
AMK-59	Kara Sea	2011	AMK-5039	2011-5039	78.0074	74.8968	364	Sigsbee trawl	-
AMK-59	Kara Sea	2011	AMK-5042	2011-5042	78.4915	72.8047	472	Sigsbee trawl	-
AMK-59	Kara Sea	2011	AMK-5051	2011-5051	75.8272	68.9850	351	Sigsbee trawl	-
AMK-59	Kara Sea	2011	AMK-5054	2011-5054	72.9301	58.3447	376	Sigsbee trawl	-
AMK-59	Kara Sea	2011	AMK-5061	2011-5061	71.6692	57.0368	325	Sigsbee trawl	-
ARK XXVII/3	Central Arctic	2012	PS80/205	2012-205	81.4802	31.0252	615	Agassiz trawl	-
ARK XXVII/3	Central Arctic	2012	PS80/222	2012-222	84.0377	30.1620	4012	Agassiz trawl	-
ARK XXVII/3	Central Arctic	2012	PS80/249	2012-249	83.9673	77.6813	3470	Agassiz trawl	-
ARK XXVII/3	Central Arctic	2012	PS80/259	2012-259	82.7090	109.5777	3575	Agassiz trawl	-
ARK XXVII/3	Central Arctic	2012	PS80/286	2012-286	82.7780	129.8467	4159	Agassiz trawl	-
ARK XXVII/3	Central Arctic	2012	PS80/332	2012-332	81.9062	130.8432	4039	Agassiz trawl	-
ARK XXVII/3	Central Arctic	2012	PS80/346	2012-346	85.0688	122.6915	4354	Agassiz trawl	-
ARK XXVII/3	Central Arctic	2012	PS80/359	2012-359	87.8922	59.3887	4380	Agassiz trawl	-
PSh-125	Kara Sea	2013	125-30	2013-30	76.3533	88.8250	47	Sigsbee trawl	-
PSh-125	Kara Sea	2013	125-32	2013-32	77.1187	87.6292	149	Sigsbee trawl	-
PSh-125	Kara Sea	2013	125-34	2013-34	78.0150	87.6317	108	Sigsbee trawl	-
AMK-63	Laptev Sea	2015	AMK-5230	2015-seep	76.7715	125.8418	72	Sigsbee trawl	-
AMK-63	Laptev Sea	2015	AMK-5225	2015-5225	78.3747	130.6585	2390	Sigsbee trawl	-

Suppl 2

```
#################################################################
''' Defenition of functions for diversity measurements.
Input - np.array of list of species abundances in one sample'''

import sys
import numpy as np
import scipy.stats
from math import comb
import random

def SpRich(x): #Number of species
    a = np.count_nonzero(x)
    return a

def sdi(x): #Shannon-Wiener index
    from math import log as ln
    def p(n, N):
        if n == 0:
            return 0
        else:
            return (float(n)/N) * ln(float(n)/N)
    N = sum(x)
    return -sum(p(n, N) for n in x)

def Hill(x,q): #Simple Hill number
    N = sum(x)
    def p(i):
        if i == 0:
```

```
        return 0
    else:
        return (i/N)**q
if 1 !=0:
    return sum(p(i) for i in x)**(1/(1-q))
else: return sdi(x)


def Dm_0 (x): #Observed interpolated species rarefaction, q = 0, see Chao et al. 2014 for equations
    n = round(sum(x))
    S = SpRich(x)
    l = []
    noz = np.array([a for a in x if a != 0])
    for m in range(1,n+1):
        a_list = []
        for i in range(len(noz)):
            a = comb((n-int(noz[i])),m)/comb(n,m)
            a_list.append(a)
            z = (sum(a_list))
        Dm = S - z
        l.append(Dm)
    return np.array(l)


def Cind_0 (x): #Observed interpolated species sample coverage, q = 0
    n = round(sum(x))
    l = []
    noz = np.array([a for a in x if a != 0])
    for m in range(1,n-1):
        a_list = []
        for i in range(len(noz)):
```

```
            a = (int(noz[i])/n)*comb((n-int(noz[i])),m)/comb((n-1),m)
            a_list.append(a)
            z = (sum(a_list))
        Dm = 1 - z
        l.append(Dm)
    return np.array(l)


def Dm_1(x,y): #Observed extrapolated species rarefaction, q = 0; y (individuals) - the upper limit of the extrapolation
    n = round(sum(x))
    S = SpRich(x)
    f1 = np.count_nonzero(x == 1)
    f2 = np.count_nonzero(x == 2)
    if f1 == 0:
        f0 = 0
    elif f1 != 0 and f2 == 0:
        f0 = ((n-1)/n)*f1*(f1-1)/2
    else:
        f0 = ((n-1)/n)*f1**2/(2*f2)
    l = []
    for m in range (0,y):
        if f0 ==0:
            z = 0
        else:
            z = f1/(n*f0+f1)
        Dnm = S + f0*(1-(1-z)**m)
        l.append(Dnm)
    return np.array(l)


def Cind_1(x): #Observed extrapolated species sample coverage, q = 0
```

```
    n = round(sum(x))
    f1 = np.count_nonzero(x == 1)
    f2 = np.count_nonzero(x == 2)
    l = []
    for m in range (0,n+1):
        Ci = 1-(f1/n)*(((n-1)*f1/(2*f2+f1*(n-1)))**m)
        l.append(Ci)
    return np.array(l)


def pi_tuned(x): #Tuned probabilities of species occurence in sample x
    n = round(sum(x))
    f1 = np.count_nonzero(x == 1)
    f2 = np.count_nonzero(x == 2)
    if f2 == 0:
        f0 = ((n-1)/n)*f1*(f1-1)/2
    else:
        f0 = ((n-1)/n)*f1**2/(2*f2)
    CindN = 1-(f1/n)*((n-1)*f1/(2*f2+f1*(n-1)))
    a_list = []
    for i in range(len(x)):
        denom1 = (x[i]/n)*(1-x[i]/n)**n
        a_list.append(denom1)
    denom = (sum(a_list))
    l=[]
    for i in range(len(x)):
        if x[i] != 0:
            lamb = (1-CindN)/denom
            p_i = (x[i]/n)*(1-lamb*((1-x[i]/n)**n))
        else:
```

```
        p_i = ((1-CindN)/(round(f0)))**2
    l.append(p_i)
  return l

def pi_tuned_rev(x): #Reversed tuned probabilities for further randomization
  n = round(sum(x))
  f1 = np.count_nonzero(x == 1)
  f2 = np.count_nonzero(x == 2)
  if f2 == 0:
    f0 = ((n-1)/n)*f1*(f1-1)/2
  else:
    f0 = ((n-1)/n)*f1**2/(2*f2)
  CindN = 1-(f1/n)*((n-1)*f1/(2*f2+f1*(n-1)))
  a_list = []
  for i in range(len(x)):
    denom1 = (x[i]/n)*(1-x[i]/n)**n
    a_list.append(denom1)
  denom = (sum(a_list))
  l=[]
  for i in range(len(x)):
    if x[i] != 0:
      lamb = (1-CindN)/denom
      p_i = 1-(x[i]/n)*(1-lamb*((1-x[i]/n)**n))
    else:
      p_i = 1-((1-CindN)/(round(f0)))**2
    l.append(p_i)
  return l

def rand_gen(x,y): #Creates DataFrame with randomly generated samples of y replicates
```

```
    population = x
    sp_list = len(x)
    prob_distr = pi_tuned_rev(x)
    columns = np.array(range(1,len(x)))
    rand_frame = pd.DataFrame({0: np.array(random.choices(population, weights=prob_distr, k=sp_list))})
    for i in range (1,y):
        rand_frame[i] = np.array(random.choices(population, weights=prob_distr, k=sp_list))
    return rand_frame


def rand_df_curve(x,y,z): #Creates DataFrame with generated rarefactions up to y individuals of z random replicates
    col_0 = rand_gen(x,z)[0]
    N_0 = (round(sum(col_0)))
    if N_0 >= y:
        curve_frame = pd.DataFrame({0: Dm_0(col_0)[:y]})
    elif N_0 < y:
        curve_frame = pd.DataFrame({0: np.concatenate((Dm_0(col_0),Dm_1(col_0, y-N_0)[1:]),axis=None)})
    for i in range (1,z):
        col_i = rand_gen(x,z)[i]
        N_i = (round(sum(col_i)))
        if N_i >= y:
            curve_frame[i] = Dm_0(col_i)[:y]
        elif N_i < y:
            new_col1 = Dm_0(col_i)
            new_col2 = Dm_1(col_i, y-N_i)[1:]
            curve_frame[i] = np.concatenate((new_col1, new_col2), axis=None)
    return curve_frame


def confidence_interval(data, confidence): # To calculate Confidence interval
```

```
    a = 1.0 * np.array(data)
    n = len(a)
    m, se = np.mean(a), scipy.stats.sem(a)
    h = se * scipy.stats.t.ppf((1 + confidence) / 2., n-1)
    return h


def mean_interval(data, confidence): # To calculate mean
    a = 1.0 * np.array(data)
    n = len(a)
    m, se = np.mean(a), scipy.stats.sem(a)
    h = se * scipy.stats.t.ppf((1 + confidence) / 2., n-1)
    return m


def mean(x,y): # mean curve up to y individuals, concatenated Dm_0 and Dm_1 in case you deal with large samples
    N = (round(sum(x)))
    if N >= y:
        return Dm_0(x)[:y]
    else:
        return np.concatenate((Dm_0(x), Dm_1(x, y-N)[1:]), axis=None)


def CI_rarefaction_minus(x,y, confidence): # Lower confidence inderval of rarefaction curve
    fr = rand_df_curve(x,y)
    N = (round(sum(x)))
    mean = np.concatenate((Dm_0(x), Dm_1(x, 100-N)[1:]), axis=None)
    y_graph = mean - confidence_interval(fr.T, confidence)
    return y_graph


def CI_rarefaction_plus(x,y, confidence): # Upper confidence inderval of rarefaction curve
    fr = rand_df_curve(x,y)
```

```
    N = (round(sum(x)))
    mean = np.concatenate((Dm_0(x), Dm_1(x, 100-N)[1:]), axis=None)
    y_graph = mean + confidence_interval(fr.T, confidence)
    return y_graph


'''An example of the rarefaction curve for one of the stations (1995-89) used in this study'''
_1995_89_ = array([0, 0, 0, 0, 0, 0, 0, 0, 0, 0, 0, 0, 0, 0, 0, 0, 0, 0, 0, 0, 0, 4,
       0, 0, 0, 0, 0, 0, 0, 0, 0, 0, 0, 0, 0, 0, 0, 0, 0, 0, 0, 0, 0, 0,
       0, 0, 0, 0, 0, 0, 0, 0, 0, 0, 0, 0, 0, 0, 0, 0, 0, 0, 0, 0, 0, 0,
       0, 0, 0, 0, 0, 0, 0, 0, 0, 0, 0, 0, 0, 0, 0, 0, 0, 0, 0, 7, 0, 0,
       0, 0, 0, 0, 0, 0, 0, 0, 0, 0, 0, 0, 0, 0, 0, 0, 0, 0, 0, 0, 0, 0,
       0, 0, 1, 0, 0, 0, 0, 0, 0, 0, 0, 0, 0, 7, 0, 0, 0, 0, 0, 0, 0, 0,
       0, 0, 0, 0, 0, 0, 0, 0, 0, 0, 0, 0, 0, 0, 0, 0, 0, 0, 0, 0, 0, 0,
       0, 0, 0, 0, 0, 0, 0, 0, 0, 0, 0, 0, 0, 0, 0, 0, 0, 0, 0, 0, 0, 0,
       0, 0, 0, 0, 0, 0, 0, 0, 0, 0, 0, 0, 0, 0, 0, 0, 0, 0, 0, 0, 0, 0,
       0, 0, 0, 0, 0, 0, 0, 0, 0, 0, 0, 0, 0, 0, 0, 0, 0, 0, 0, 0, 0, 0,
       0, 0, 0, 0, 0, 0, 0, 0, 0, 0, 0, 0, 0, 0, 0, 0, 0, 0, 0, 0, 0, 0,
       0, 0, 0, 0, 0, 0, 0, 0, 0, 0, 0, 0, 0, 0, 0, 0, 0, 0, 0, 0, 0, 0,
       0, 0, 0, 0, 0, 0, 0, 0, 0, 0, 0, 0, 0, 0, 0, 0, 0, 0, 0, 0, 0, 0,
       0, 0, 0, 0, 0, 0, 0, 0, 0, 0, 0, 0, 0, 0, 0, 1, 0, 0, 0, 0, 0, 0,
       0, 0, 1, 0, 0, 0, 0, 0, 0, 0, 0, 0, 0, 0, 0, 0, 0, 0, 0, 0, 0, 0,
       0, 0, 0, 0, 0, 0, 0, 0, 0, 1, 0, 0, 0, 0, 0, 0, 0, 0, 0, 0, 0, 0,
       0, 0, 0, 0, 0, 0, 0, 0, 0, 0, 0, 0, 0, 0, 0, 1, 0, 0, 0, 0, 0, 0,
       0, 0, 0, 0, 0, 0, 0, 0, 0, 0, 0, 0, 0, 0, 0, 0, 0, 0, 0, 0, 0, 0,
       0, 0, 0, 0, 0, 0, 0, 0, 0, 0, 0, 0, 0, 0, 0, 0, 0, 0, 0, 0, 0, 0,
       0, 1, 0, 0, 0, 0, 0, 0, 0, 0, 0, 0, 0, 0, 0, 0, 0, 4, 0, 0, 0, 0,
       0, 0, 0, 0, 0, 0, 0, 0, 0, 0, 0, 0, 0, 0, 0, 0, 0, 0, 0, 0, 0, 0,
       0, 0, 0, 0, 0, 0, 0, 0, 0, 0, 0, 2, 0, 0, 0, 0, 0, 0, 0, 0, 0, 0,
```

```
    0, 0, 0, 0, 0, 0, 0, 0, 0, 0, 0, 0, 0, 0, 0, 0, 0, 0, 0, 0, 0,
    0, 0, 0, 0, 0, 0, 0, 0, 0, 0, 0, 0, 0, 0, 0, 0, 0, 0, 0, 0, 0,
    0, 0, 0, 0, 0, 0, 0, 0, 0, 0, 0, 0, 0, 0, 0, 0, 0, 0, 0, 0, 0,
    0, 0, 0, 0, 0, 0, 0, 0, 0, 0, 0, 0, 0, 0, 0, 0, 0, 0, 0, 0, 0,
    0, 0, 0, 0, 0, 0, 0, 0, 0, 0, 0, 0, 0, 0, 0, 0, 0, 0, 0, 3, 0])


N = (round(sum(_1995_89_)))
S = SpRich(_1995_89_)
x1 = np.array(list(range(1,N+1)))
y1 = Dm_0(_1995_89_)
x2 = np.array(list(range(N,100)))
y2 = Dm_1(_1995_89_, 100-N)
x3 = N
y3 = S


fr = rand_df_curve(_1995_89_,100,10)
mean = np.concatenate((Dm_0(_1995_89_), Dm_1(_1995_89_, 100-N)[1:]), axis=None)
ci = confidence_interval(fr.T, 0.99)


x4 = np.array(list(range(1,100)))
y4 = mean-ci
y5 = mean+ci


#
'''
Or, in case of large samples when the sum of individuals exceeds usual values of 50 or 100, use this:
ci = confidence_interval(fr.T, 0.99)
mean_f = mean(_1995_89_, 100)
x4 = np.array(list(range(1,101)))
```

```
y4 = mean_f-ci
y5 = mean_f+ci
'''
#

fig = plt.figure(figsize =(15, 7))

plt.plot(x4,y4, color='orange', linewidth=2)
plt.plot(x4,y5, color='orange', linewidth=2)
plt.fill_between(x4, y4, y5, color='navajowhite')

plt.plot(x1,y1, color='darkorange', linewidth=4)
plt.plot(x2,y2, color='darkorange', linewidth=4, linestyle='dashed')
plt.plot(x3,y3, color='darkorange', marker='o', markersize=12)

plt.title('Rarefaction curve and extrapolation')
plt.ylim(0.5,25)
plt.xlim(1,50)
plt.grid(True)
plt.xlabel('Number of individuals')
plt.ylabel('Species count')
plt.show


##################################################################
''' Defenition of similarity indices for cluster dendrograms.
Input - np.array of list of species abundances in each sample or pandas DataFrame'''

import pandas as pd
```

```
import numpy as np

import seaborn as sns

import matplotlib

import matplotlib.pyplot as plt

import scipy

import sklearn

import math

import os, re, sys

from math import log


def Br_Cur(data1, data2): #Bray-Curtis similarity index

   if len(data1) != len(data2):

      raise ValueError("Error while calculating Bray-Curtis similarity index. The two input data lists must have the same length!\n")

   if sum(data1) == 0 or sum(data2) == 0:

      return -1

   A = sum(data1)

   B = sum(data2)

   z = 0

   for i, (x,y) in enumerate(zip(data1, data2)):

      if x!=0 and x<=y:

         z+=x

      elif y!=0 and x>=y:

         z+=y

   minAB = z

   if float(A+B) == 0:

      return 0

   else:

      return (2*minAB)/(A+B)
```

```
def rev_Br_Cur(data1, data2): #Bray-Curtis dissimilarity
    return (1-Br_Cur(data1, data2))


'''
the script partly taken from https://github.com/ngannguyen/immunoseq/blob/master/src/similarity.py
Jun 13 2012
'''


def morisitaHorn(data1, data2): #Morisita-Horn similarity index
    S1 = sum(data1)
    S2 = sum(data2)
    if len(data1) != len(data2):
        raise ValueError("Error while calculating MorisitaHorn similarity index. The two input data lists must have the same length!\n")
    if S1 == 0 or S2 == 0:
        return -1
    sum_xy = 0
    sum_x_sq = 0
    sum_y_sq = 0
    for i, x in enumerate(data1):
        y = data2[i]
        sum_xy += x*y
        sum_x_sq += x*x
        sum_y_sq += y*y
    n = 2*sum_xy/(S1*S2)
    d = (float(sum_x_sq)/(S1**2) + float(sum_y_sq)/(S2**2))
    return float(n)/d


def reversed_morisitaHorn(data1,data2): #Morisita-Horn dissimilarity
```

```
    return (1-morisitaHorn(data1, data2))


def SoerAbIn(data1, data2): #Quantitative Soerensen similarity index
    if len(data1) != len(data2):
        raise ValueError("Error while calculating Soerensen similarity index. The two input data lists must have the same length!\n")
    if sum(data1) == 0 or sum(data2) == 0:
        return -1
    A = sum(data1)
    a = 0
    for i, (x,y) in enumerate(zip(data1, data2)):
        if y!=0:
            a+=x
    U = a/A
    B = sum(data2)
    b = 0
    for i, (x,y) in enumerate(zip(data1, data2)):
        if x!=0:
            b+=y
    V = b/B
    if float(U+V) == 0:
        return 0
    else:
        return float(2*U*V)/float(U+V)


def rev_SoerAbIn(data1, data2): #Quantitative Soerensen dissimilarity index
    return (1-SoerAbIn(data1, data2))


# Example of the dendrogram using Morisita-Horn similarity index.
```

```
#Input - DataFrame (named here as 'frame') with species as index names and stations as columns names



from scipy.spatial.distance import pdist, squareform


station_list = list(frame.columns)


sim_matr = pd.DataFrame(squareform(pdist(frame.T, morisitaHorn)), columns=station_list, index=station_list) #non-transformed data

sim_matr2 = pd.DataFrame(squareform(pdist(frame_trans.T, lambda u, v: morisitaHorn(u,v))), columns=station_list, index=station_list) #square-root transformed data


from scipy.cluster import hierarchy


ytdist = np.array(sim_matr2)


Z = hierarchy.linkage(ytdist, 'average', metric=reversed_morisitaHorn, optimal_ordering=True)


plt.figure(figsize=(15, 20))

matplotlib.rcParams['lines.linewidth'] = 1


dn = hierarchy.dendrogram(Z,

        p=100,

        truncate_mode='level',

        orientation='left',

        labels=stations,

        count_sort='ascending',

        distance_sort='ascending',
```

```
        show_leaf_counts=True,
        leaf_rotation=0,
        leaf_font_size=10,
        above_threshold_color='black')

plt.title('Cluster Analysis, Morisita-Horn index, sq-root transform, group average', fontdict={'fontsize':20}, pad=12);
plt.xlim()
plt.xticks(fontsize=12)
plt.xlabel('Morisita-Horn dissimilarity', fontsize=15)
plt.axvline(x=0.435, c='grey', lw=2, linestyle='dashed')

plt.savefig('Morisita_Horn_sq-root_average_stations.png', dpi=300, bbox_inches='tight')
```

Suppl. 3

Station	Abundance (ind. m^{-2})	Biomass (g ww m^{-2})	Species number	Pielou's evenness	ES(100)	Estimated diversity of 50 individuals	Shannon-Wiener index
			Quantitative samples				
1991-2213	856	5.785	53	0.85	33.60	25.02	3.36
1991-2214	3292	10.701	92	0.78	35.91	24.84	3.52
1993-14	1051	1.633	26	0.80	20.88	17.50	2.60
1993-17	261	0.647	5	0.97	5.00	5.00	1.56
1993-19	522	0.196	21	0.93	20.31	26.13	2.84
1993-20	565	2.083	8	0.96	8.00	10.43	1.99
1993-24	891	2.416	19	0.89	18.20	21.16	2.61
1993-25	8861	650.529	77	0.80	33.38	24.04	3.46
1993-27	2487	8.959	68	0.89	39.98	29.34	3.75
1993-32	948	1.577	26	0.84	21.42	18.65	2.73
1993-35	1080	7.482	47	0.86	29.85	23.31	3.30
1993-38	1552	6.442	59	0.88	37.13	28.14	3.60
1993-39	2905	7.118	75	0.84	38.43	27.43	3.64
1993-40	4122	27.490	77	0.90	44.31	31.57	3.93
1993-41	6500	26.817	54	0.81	32.87	24.20	3.24
1993-44	7868	340.169	77	0.87	40.13	29.05	3.77
1993-47	915	11.832	91	0.83	41.47	25.45	3.76
1993-48	3888	35.869	90	0.84	40.96	28.29	3.76
1993-49	2914	16.855	76	0.82	37.88	26.53	3.56
1993-50	652	7.902	26	0.87	23.75	23.62	2.83
1993-53	149	3.261	27	0.91	26.38	27.74	2.99
1993-54	435	0.652	11	0.85	10.88	13.54	2.03
1993-64	5103	34.162	100	0.79	37.37	26.10	3.64
1993-68	4858	51.813	99	0.80	38.52	26.73	3.66
1993-69	4898	43.538	109	0.81	41.55	28.42	3.82
1993-70	1147	4.090	76	0.80	38.00	26.60	3.47
1993-71	3021	4.754	52	0.67	25.57	18.18	2.65
1995-89	66	2.300	12	0.88	12.00	14.82	2.19
1995-90	474	2.400	34	0.80	23.19	17.95	2.80
1995-91	752	28.100	73	0.81	35.74	24.96	3.47
1995-92	2206	818.800	89	0.71	32.15	21.66	3.17
1995-93	3897	2316.500	120	0.74	37.32	24.66	3.54
1995-94	2040	13.800	37	0.53	17.48	12.29	1.92
1995-95	750	25.200	73	0.81	38.03	25.93	3.46
1995-96	884	44.900	46	0.78	26.43	19.55	2.99
1997-2830	4092	23.848	26	0.85	20.98	18.91	2.77
1997-2831	3454	20.856	47	0.82	28.80	23.93	3.18
1997-2832	440	2.288	6	0.90	6.00	12.37	1.61
1997-2833	88	0.198	2	1.00	2.00	2.00	0.69
1997-2834	704	2.970	7	0.95	7.00	7.92	1.84
1997-2835	440	0.682	8	0.95	8.00	22.49	1.97
1997-2836	550	2.167	11	0.72	10.92	26.49	1.73
1997-2837	946	12.606	20	0.89	18.91	29.80	2.67
1997-2838	704	2.090	10	0.90	9.99	14.76	2.06
1997-2839	119	0.469	6	0.93	6.00	6.00	1.67
1997-2840	704	2.754	6	0.70	6.00	11.04	1.25
1997-2843	264	0.986	4	0.90	4.00	6.50	1.24
1997-2847	132	0.079	2	0.92	2.00	2.33	0.64
1997-2849	30	0.421	2	1.00	2.00	2.50	0.69
1997-2851	220	5.918	4	0.96	4.00	7.60	1.33
1997-2853	572	9.649	9	0.97	9.00	11.86	2.14
1997-2854	836	1.426	10	0.90	9.98	15.76	2.08
1997-2855	484	1.377	9	0.96	9.00	25.97	2.10
1997-2859	704	1.685	16	0.87	15.28	16.58	2.42
1997-2860	308	1.087	5	0.96	5.00	6.93	1.55
1997-2861	440	4.770	4	0.92	4.00	4.45	1.28
1997-2868	83	0.316	2	0.83	2.00	2.00	0.58
2007-5003	2174	48.835	54	0.73	25.29	18.77	2.91
2012-229	12	0.008	2	1.00	2.00	2.00	0.69
2012-241	46	0.411	6	0.93	6.00	12.52	1.66
2012-262	21	0.070	2	0.92	2.00	2.33	0.64
2012-278	209	1.212	12	0.83	11.87	15.06	2.06
2012-326	97	0.147	10	0.92	10.00	13.41	2.12
2012-339	78	0.081	9	0.95	9.00	16.18	2.10
2012-355	20	0.087	3	0.95	3.00	4.50	1.04
2012-368	57	0.071	6	0.88	6.00	11.01	1.58
2012-N5	1168	1.816	29	0.87	23.14	19.62	2.93
2012-N4	1592	2.509	34	0.78	22.07	17.37	2.74
2012-N3	1152	0.971	30	0.84	22.67	19.01	2.86
2012-N2	1008	1.478	27	0.81	21.48	18.08	2.67
2012-N1	1024	3.592	31	0.84	24.75	20.74	2.89
2012-HGIV	984	2.628	27	0.76	20.68	20.41	2.52
2012-HGIVa	928	1.794	29	0.86	23.81	17.14	2.89
2012-S1a	1456	2.380	32	0.82	23.05	18.69	2.86
2012-S1	880	0.866	25	0.81	19.80	16.99	2.62
2012-S2	1064	2.205	37	0.86	27.78	22.89	3.12
2012-S3	1360	4.975	31	0.87	24.64	20.53	2.98
2015-5225	219	1.051	25	0.73	18.32	14.75	2.35
2015-5227	333	2.514	37	0.82	26.00	19.80	2.95
2016-EG1	764	0.452	51	0.82	33.50	24.76	3.24
2016-EGII	384	1.349	40	0.87	31.99	26.30	3.21
2016-EGIII	277	0.924	28	0.85	25.14	22.97	2.84
2016-EGIV	992	1.048	37	0.78	23.68	18.00	2.80
2016-HGI	1450	2.707	58	0.84	33.16	24.59	3.40
2016-HGII	1479	2.358	65	0.80	33.62	23.71	3.33
2016-HGIII	552	0.861	35	0.87	27.94	22.85	3.11
2016-HGIV	756	2.455	29	0.70	19.80	15.27	2.35
2002-AG05	4050	4.950	27	0.70	19.64	15.90	2.30
2002-AL07	675	2.600	14	0.93	13.87	19.47	2.45
2002-AL10	88	0.004	4	0.92	4.00	5.71	1.28
2002-NA05	1792	0.808	35	0.79	23.14	18.26	2.82
2002-NW01	1875	4.325	11	0.56	9.30	8.68	1.35
2002-NW05	1275	0.536	16	0.63	11.38	9.52	1.74
2005-2	2489	27.000	50	0.62	22.36	19.90	2.41
2005-3	833	0.100	18	0.76	16.01	20.06	2.20
2005-4	561	11.200	34	0.88	28.57	13.33	3.12
2005-5	339	2.400	8	0.48	7.60	11.36	1.00
2005-7	67	0.050	8	0.93	8.00	15.59	1.94
2005-8	128	0.050	10	0.90	10.00	14.06	2.07
2005-9	111	0.200	10	0.97	10.00	24.09	2.22
2005-11	239	3.700	17	0.90	16.67	7.43	2.55
2005-12	250	2.000	18	0.79	17.41	18.21	2.27
2005-13	167	1.800	9	0.77	8.98	13.49	1.69
2005-15	606	1.800	14	0.70	12.36	10.85	1.84

Suppl 3 continued

Semiquantitative samples							
Station	Abundance (ind. m^{-2})	Biomass (g ww m^{-2})	Species number	Pielou's evenness	ES(100)	Estimated diversity of 50 individuals	Shannon-Wiener index
1993-50	-	-	27	0.73	17.21	13.52	2.42
2007-4983	-	-	57	0.45	18.94	12.52	1.81
2007-4985	-	-	144	0.48	22.68	14.96	2.37
2007-4987	-	-	48	0.49	16.03	11.24	1.92
2007-4988	-	-	70	0.32	12.29	8.82	1.37
2007-4990	-	-	89	0.67	30.58	19.92	3.02
2007-4996	-	-	31	0.23	9.05	6.27	0.79
2007-4999	-	-	38	0.58	18.47	13.28	2.11
2007-5000	-	-	38	0.57	17.66	13.39	2.08
2007-5003	-	-	99	0.61	27.14	18.29	2.82
2011-5016	-	-	21	0.46	9.50	7.13	1.40
2011-5019	-	-	52	0.32	11.91	8.08	1.27
2011-5020	-	-	76	0.40	16.98	10.58	1.73
2011-5010	-	-	126	0.64	29.36	20.26	3.12
2011-5024	-	-	125	0.54	28.65	17.93	2.61
2011-5026	-	-	73	0.73	31.85	22.03	3.15
2011-5032	-	-	88	0.64	33.24	20.52	2.89
2011-5033	-	-	122	0.69	34.47	23.06	3.31
2011-5034	-	-	88	0.46	19.68	12.56	2.06
2011-5039	-	-	67	0.35	16.48	10.74	1.49
2011-5042	-	-	104	0.72	35.08	22.82	3.33
2011-5051	-	-	103	0.46	16.90	11.37	2.15
2011-5054	-	-	80	0.45	17.29	11.03	1.99
2011-5061	-	-	79	0.43	11.82	9.08	1.86
2012-205	-	-	133	0.71	39.25	24.19	3.48
2012-222	-	-	22	0.48	14.25	10.96	1.49
2012-249	-	-	24	0.52	14.78	11.01	1.64
2012-259	-	-	18	0.60	10.96	8.48	1.73
2012-286	-	-	21	0.54	10.45	7.88	1.64
2012-332	-	-	17	0.55	10.96	8.28	1.55
2012-346	-	-	25	0.31	9.33	6.77	0.99
2012-359	-	-	8	0.98	8.00	24.61	2.04
2013-30	-	-	96	0.52	27.67	16.87	2.39
2013-32	-	-	94	0.48	18.06	12.44	2.16
2013-34	-	-	131	0.57	27.26	17.13	2.76
2015-seep	-	-	199	0.55	28.98	18.79	2.91
2015-5225	-	-	73	0.64	25.92	18.10	2.76

Suppl. 5

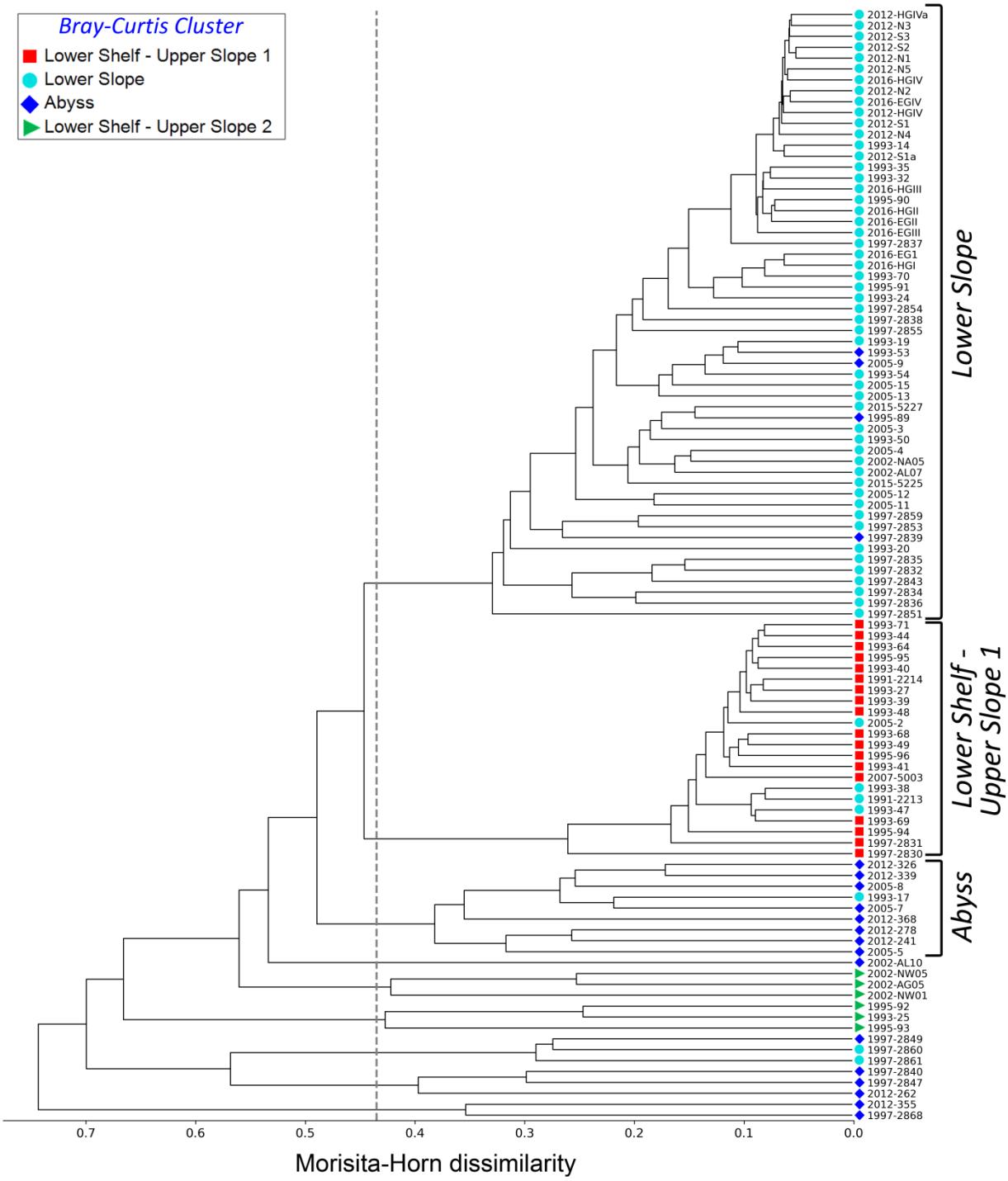

Fig. S-1. Cluster analysis of quantitative stations using Morisita-Horn dissimilarity (square-root transformation). Colour labels for stations are the same as for the Bray-Curtis similarity dendrogram. Dashed line indicates slice at the dissimilarity level of 0.43.

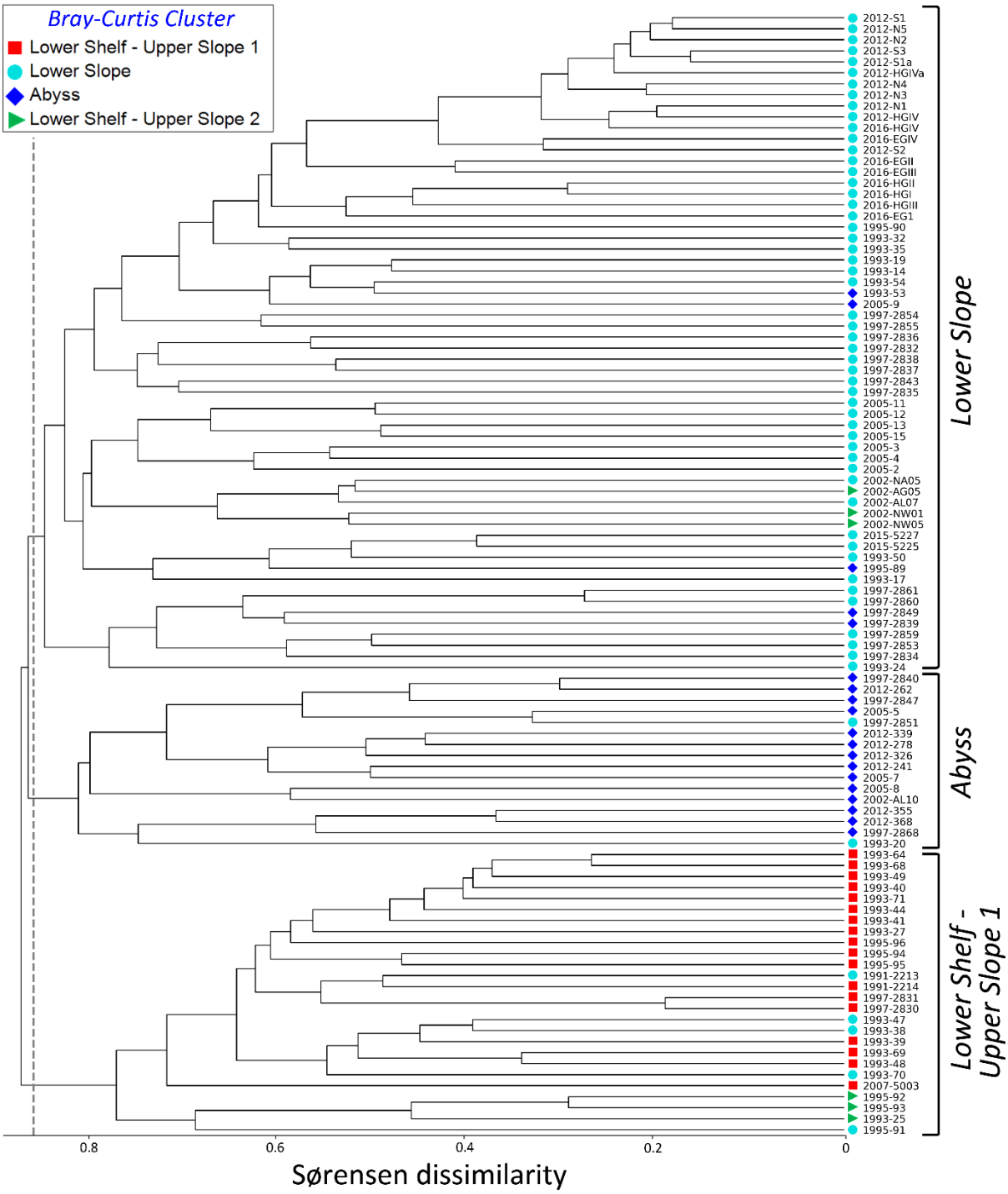

Fig. S-2. Cluster analysis of quantitative stations using quantitative Sørensen dissimilarity (square-root transformation). Colour labels for stations are the same as for the Bray-Curtis similarity dendrogram. Dashed line indicates slice at the dissimilarity level of 0.85.

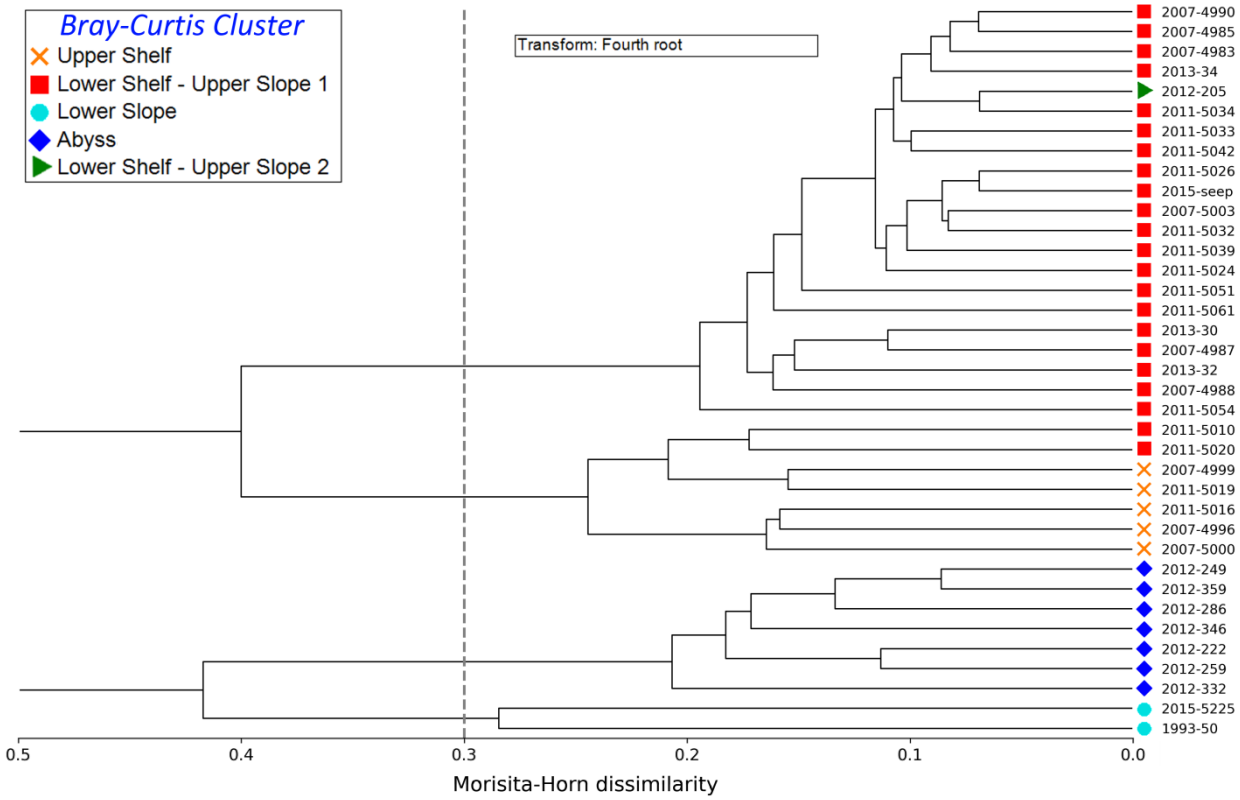

Fig. S-3. Cluster analysis of semi-quantitative stations using Morisita-Horn dissimilarity (4-th root transformation). Colour labels for stations are the same as for the corresponding Bray-Curtis similarity dendrogram. Dashed line indicates slice at the dissimilarity level of 0.3.

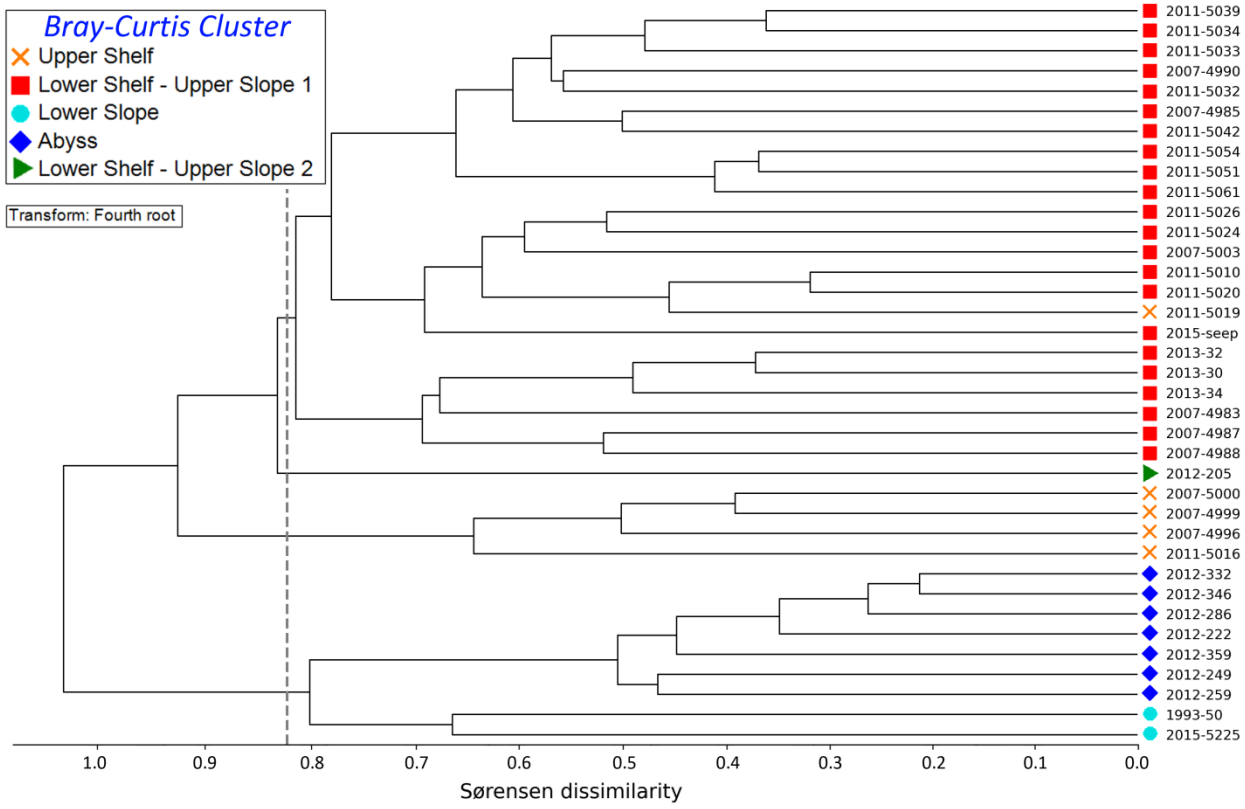

Fig. S-4. Cluster analysis of quantitative stations using quantitative Sørensen dissimilarity (square-root transformation). Colour labels for stations are the same as for the corresponding Bray-Curtis similarity dendrogram. Dashed line indicates slice at the dissimilarity level of 0.83.

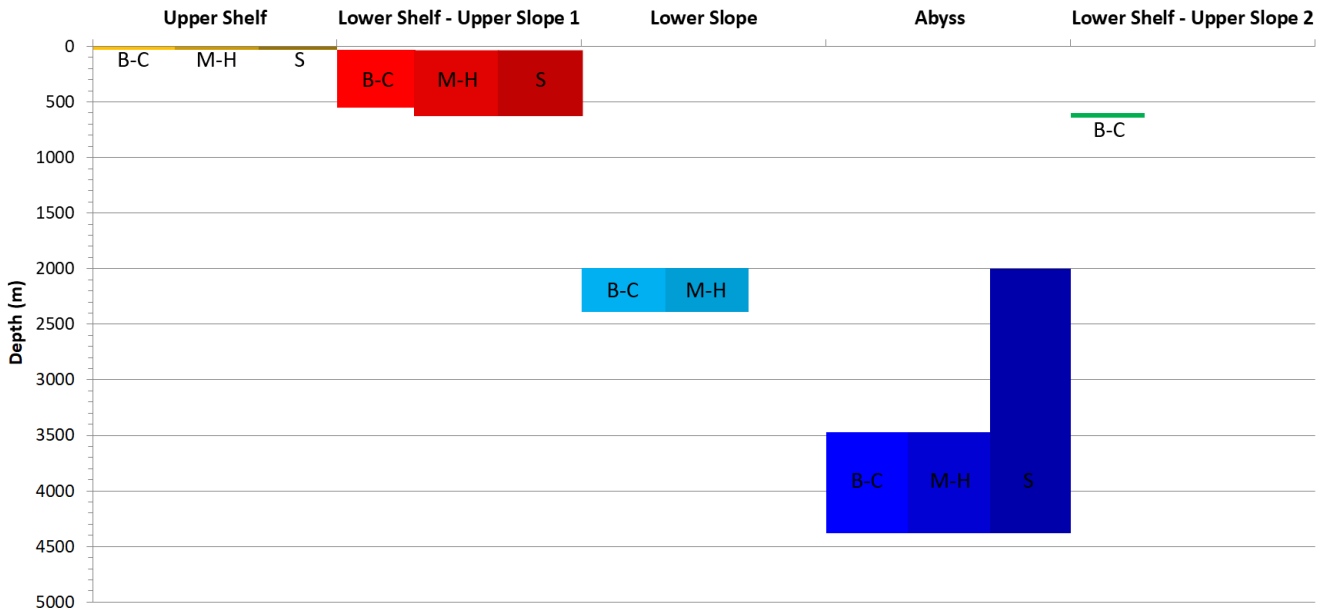

Fig. S-5. Bathymetric distribution of groups of Arctic benthic assemblages based on semi-quantitative samples (three different similarity indices). Colours as in Figs. 8-10. B-C – depth ranges from the Bray-Curtis similarity dendrogram; M-H – depth ranges from the Morisita-Horn similarity dendrogram; S – depth ranges from the quantitative Sørensen similarity dendrogram.

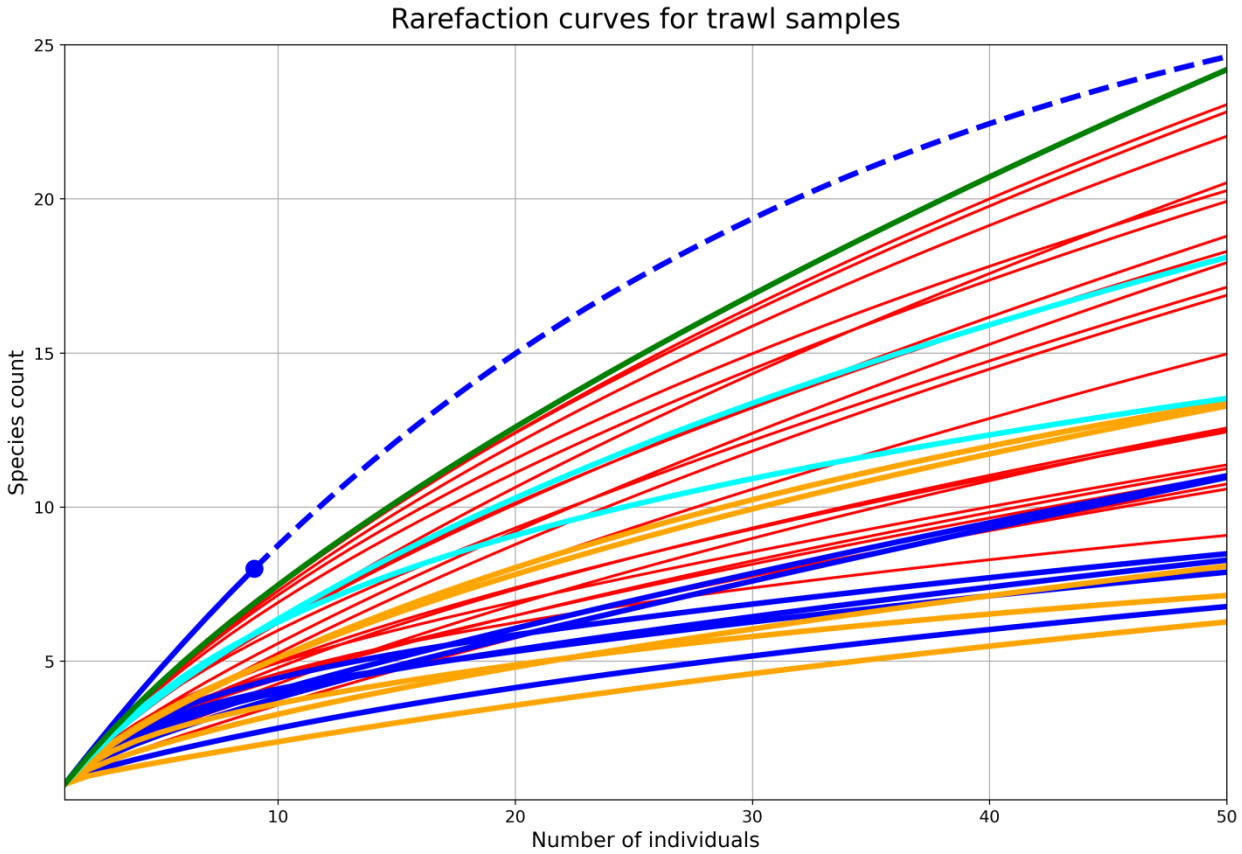

Fig. S-6. Rarefaction curves for the quantitative samples up to 50 individuals with extrapolation based on the Hill numbers (q = 0). Colours as in Figs. 8-10. Continuous lines indicate true (sample-sized) rarefaction; circles indicate the end of sample; dashed lines indicate the extrapolated rarefaction.